

Modeling Traffic Flow Emissions

by

Alessandra Cappiello

Laurea in Environmental Engineering
Politecnico di Milano, 1998

Submitted to the Department of Civil and Environmental Engineering
in partial fulfillment of the requirements for the degree of

Master of Science in Transportation
at the
Massachusetts Institute of Technology

June 2002

© 2002 Massachusetts Institute of Technology
All rights reserved

Author
Department of Civil and Environmental Engineering
May 24, 2002

Certified by
Ismail Chabini
Associate Professor, Civil and Environmental Engineering
Thesis Supervisor

Accepted by
Oral Buyukozturk
Chairman, Departmental Committee on Graduate Studies

Modeling Traffic Flow Emissions

by
Alessandra Cappiello

Submitted to the Department of Civil and Environmental Engineering
on May 24 2002, in partial fulfillment of the requirements for the degree of
Master of Science in Transportation

Abstract

The main topic of this thesis is the development of light-duty vehicle dynamic emission models and their integration with dynamic traffic models. Combined, these models constitute fundamental components to support the development and assessment of traffic management policies, and the optimization of their parameters, to alleviate the negative impacts of road traffic.

We develop and implement a dynamic model of emissions (CO_2 , CO , HC , and NO_x) and fuel consumption for light-duty vehicles. The model is derived from regression-based and load-based emissions modeling approaches, and effectively combines their respective advantages. The model is calibrated for two vehicle categories using FTP as well MEC01 driving cycles data. The US06 driving cycle is used to validate the estimation capabilities of the proposed model. The preliminary results indicate that the model gives reasonable results compared to actual measurements as well to results obtained with CMEM, a well-known load-based dynamic emission model. Furthermore, the results indicate that the model runs fast, and is relatively simple to calibrate.

We propose a framework for the integration of dynamic emission models with non-microscopic dynamic traffic models, that do not estimate vehicle acceleration. A probabilistic model of acceleration is designed and implemented to link the traffic and the emission models. The model provides an experimental distribution of the accelerations for any given speed and road type. The framework is applied to integrate the dynamic emission model developed in this thesis with a mesoscopic dynamic traffic flow model. Using a hypothetical case study, we illustrate the potential of the combined models to estimate the effects of route guidance strategies, which are one of numerous examples of dynamic traffic management strategies, on traffic travel times and traffic emissions. In presence of incidents, it is shown that route guidance can reduce total travel times as well as total emissions.

Thesis Supervisor: Ismail Chabini
Title: Associate Professor, Civil and Environmental Engineering

Acknowledgements

I am grateful to many people who have significantly contributed to make this thesis come true.

Thanks to Ismail Chabini for his guidance, support and encouragement during my two years at MIT. I truly admire his patience and enthusiasm. I am happy for having shared with him the challenges of a new and exciting research topic.

Thanks to Edward Nam from the Ford Scientific Research Laboratory for his continuous support and for teaching me so much about emissions. Thanks to Maya Abou Zeid for helping me so efficiently in several parts of this research. Ed, Maya, working with you was a lot of fun!

Thanks to Ging Ging Liu for sharing with me curiosity and knowledge about many research questions.

Thanks to the ACTS group, especially Nat and Song, for always supporting me.

Thanks to Jon Bottom for helping me so kindly to understand and use his traffic simulator.

Thanks to David Chock for his wise technical counsel.

Thanks to Conan, Tish, and Vida for their precious help and friendship. Without you I wouldn't be here! You are in my heart.

Thanks to Giusi, Paolo, Fran, Judah, Farzan, and Shahram, for helping us in the difficult moments and for celebrating with us the happy moments.

Thanks to all my friends at MIT, including Ging&Billy, Ye&Zhaoyang, Maya, Michael, Derek, Yoosun, Wilson, Seong, Marge, Raimundo, Takeshi, George, Angela, and Cordy, for making these two years a great human experience.

Thanks to my friends in Italy who wrote me during these years and are happy that I am going back. In particular thanks to Fabio, Silvia, Enrico, Clelia, Gió, Laura, Lori, Francy, Susy, Roby, and Vally.

Thanks to Fabrizio, Francesca, Pietro, Clelia, Luca, Valeria, mom and dad for visiting us. I hope you enjoyed Boston as much as we do.

Thanks to all the excellent professors I encountered during my education, including Grazia, prof.ssa Fiocca, Giuseppe Cappiello, Giorgio Guariso, Rodolfo Soncini Sessa, and Moshe Ben-Akiva.

Thanks to Giovanmaria Lechi and Dara Entekhabi for helping me to start my adventure at MIT.

Thanks to Eliot Laniado and Roberto Maja for introducing me to the world of transportation and for believing in me.

Thanks to our wonderful families: m&m, s&r, p&p, b&b, my grandparents, and all the others. Thanks, mom and dad, for being great parents and great people. Thanks, Gaia and Robi, for making our lives cheerful. We love you!

My most heartfelt gratitude is for my smart, generous, and tender Alex. Thanks for sharing everything with me. Without you this thesis wouldn't have been possible. This is Our Thesis.

The research reported upon in this thesis was sponsored by the Ford-MIT Alliance. I would like to thank Ford Motor Company for their financial support, which allowed me to do research on a topic I love.

Contents

1	INTRODUCTION	15
1.1	TRAFFIC CONGESTION AND EMISSIONS	15
1.1.1	<i>Policies</i>	17
1.1.2	<i>Models</i>	18
1.2	GENERAL AREA OF THIS THESIS	20
1.3	THESIS OBJECTIVES AND CONTRIBUTIONS	21
1.4	THESIS ORGANIZATION	22
2	EMISSIONS FROM MOTOR VEHICLES	25
2.1	REGULATION ON AIR QUALITY AND VEHICLE EMISSIONS	25
2.1.1	<i>Driving Cycles</i>	26
2.1.2	<i>Emission Standards</i>	28
2.2	PRINCIPAL VEHICLE EMISSIONS	30
3	LITERATURE REVIEW OF TRAFFIC EMISSION MODELS	35
3.1	VEHICLE EMISSIONS MODELING	35
3.1.1	<i>Factors that Influence Emissions</i>	35
3.1.2	<i>Average Speed-Based Emission Models</i>	36
3.1.3	<i>Dynamic Emission Models</i>	38
3.2	INTEGRATED TRAFFIC AND EMISSION MODELS	46
3.3	CONCLUSIONS	51
4	A STATISTICAL MODEL OF VEHICLE EMISSIONS AND FUEL CONSUMPTION	53
4.1	MODEL STRUCTURE	54
4.2	DATA	55
4.2.1	<i>The NCHRP Database</i>	55
4.2.2	<i>Data Preprocessing</i>	57
4.2.3	<i>Categories Modeled in EMIT</i>	59
4.3	MODEL DEVELOPMENT	60
4.3.1	<i>The Engine-Out Emissions Module</i>	60
4.3.2	<i>The Tailpipe Emissions Module</i>	65
4.4	MODEL CALIBRATION	66
4.4.1	<i>Engine-out Emissions Module</i>	66
4.4.2	<i>Tailpipe Emissions Module</i>	67
4.4.3	<i>Results</i>	69
4.5	MODEL VALIDATION	87
4.6	CONCLUSIONS	94

5	INTEGRATION OF DYNAMIC EMISSION MODELS AND DYNAMIC TRAFFIC MODELS	97
5.1	A PROBABILISTIC APPROACH	98
5.2	PROBABILISTIC ACCELERATION MODEL	100
5.2.1	<i>Model Formulation</i>	101
5.2.2	<i>Data</i>	102
5.2.3	<i>Results</i>	103
5.3	EXPECTED EMISSION RATES FOR A GIVEN SPEED AND ROAD TYPE.....	106
6	A CASE STUDY OF TRAFFIC FLOW EMISSIONS AND FUEL CONSUMPTION ON A SMALL NETWORK	111
6.1	THE MODELING TOOLS	111
6.1.1	<i>Mesoscopic Traffic Model</i>	112
6.1.2	<i>Expected Emission Rates Component</i>	113
6.1.3	<i>Integration Component</i>	114
6.1.4	<i>Scheme of Input and Output Data</i>	115
6.2	THE CASE STUDY DATA	116
6.3	RESULTS	118
7	CONCLUSIONS AND DIRECTIONS FOR FUTURE RESEARCH.....	121
	REFERENCES	125
	APPENDIX A.....	131
	APPENDIX B.....	141
	APPENDIX C.....	153

List of Figures

Figure 1-2: Models system for the estimation of the impact of traffic on air quality.	21
Figure 2-1: A chassis dynamometer.....	26
Figure 2-2: The FTP cycle.	27
Figure 2-3: The US06 cycle.	28
Figure 2-4: The SC03 cycle.	29
Figure 3-1: CMEM structure (from Barth et al., 2000).	45
Figure 4-1: EMIT structure.	55
Figure 4-2: The MEC01 cycle.....	57
Figure 4-3: Category 7 – Engine-out emission rates versus fuel rate. Fuel rate is estimated with Equation 4.1. In Figure b, in addition to CO engine-out, tractive power (in gray) is represented versus fuel rate.	64
Figure 4-4: Category 9 – Engine-out emission rates versus fuel rate. Fuel rate is estimated with Equation 4.1. In Figure b, in addition to CO engine-out, tractive power (in gray) is represented versus fuel rate.	64
Figure 4-5: Categories 7 (left) and 9 (right) – Catalyst pass fractions for CO, HC, and NO _x . The points represent the calibration data; the line represents the modeled CPF.	69
Figure 4-6: Category 7 - FTP bag 2. Second-by-second engine-out (EO) and tailpipe (TP) emission rates of CO ₂ and CO. Thick light line: measurements; dark line: EMIT predictions; thin line: CMEM predictions. The top plot represents the speed trace.	72
Figure 4-7: Category 7 - FTP bag 2. Second-by-second fuel rate (FR) and engine-out (EO) and tailpipe (TP) emission rates of HC and NO _x . Thick light line: measurements; dark line: EMIT predictions; thin line: CMEM predictions.	73
Figure 4-8: Category 7 - FTP bag 3. Second-by-second engine-out (EO) and tailpipe (TP) emission rates of CO ₂ and CO. Thick light line: measurements; dark line: EMIT predictions; thin line: CMEM predictions. The top plot represents the speed trace.	74
Figure 4-9: Category 7 - FTP bag 3. Second-by-second fuel rate (FR) and engine-out (EO) and tailpipe (TP) emission rates of HC and NO _x . Thick light line: measurements; dark line: EMIT predictions; thin line: CMEM predictions.	75
Figure 4-10: Category 7 – MEC01. Second-by-second engine-out (EO) and tailpipe (TP) emission rates of CO ₂ and CO. Thick light line: measurements; dark line: EMIT predictions; thin line: CMEM predictions. The top plot represents the speed trace.	76

Figure 4-11: Category 7 – MEC01. Second-by-second fuel rate (FR) and engine-out (EO) and tailpipe (TP) emission rates of HC and NOx. Thick light line: measurements; dark line: EMIT predictions; thin line: CMEM predictions.	77
Figure 4-12: Category 9 - FTP bag 2. Second-by-second engine-out (EO) and tailpipe (TP) emission rates of CO ₂ and CO. Thick light line: measurements; dark line: EMIT predictions; thin line: CMEM predictions. The top plot represents the speed trace.	78
Figure 4-13: Category 9 - FTP bag 2. Second-by-second fuel rate (FR) and engine-out (EO) and tailpipe (TP) emission rates of HC and NOx. Thick light line: measurements; dark line: EMIT predictions; thin line: CMEM predictions.	79
Figure 4-14: Category 9 - FTP bag 3. Second-by-second engine-out (EO) and tailpipe (TP) emission rates of CO ₂ and CO. Thick light line: measurements; dark line: EMIT predictions; thin line: CMEM predictions. The top plot represents the speed trace.	80
Figure 4-15: Category 9 - FTP bag 3. Second-by-second fuel rate (FR) and engine-out (EO) and tailpipe (TP) emission rates of HC and NOx. Thick light line: measurements; dark line: EMIT predictions; thin line: CMEM predictions.	81
Figure 4-16: Category 9 – MEC01. Second-by-second engine-out (EO) and tailpipe (TP) emission rates of CO ₂ and CO. Thick light line: measurements; dark line: EMIT predictions; thin line: CMEM predictions. The top plot represents the speed trace.	82
Figure 4-17: Category 9 – MEC01. Second-by-second fuel rate (FR) and engine-out (EO) and tailpipe (TP) emission rates of HC and NOx. Thick light line: measurements; dark line: EMIT predictions; thin line: CMEM predictions.	83
Figure 4-18: Category 9 – Tailpipe CO ₂ predicted vs. measured emission rates (a), residuals vs. measured emission rates (b), vs. speed (c), and vs. acceleration (d). In dark EMIT; in gray CMEM.	85
Figure 4-19: Category 9 – Tailpipe CO predicted vs. measured emission rates (a), residuals vs. measured emission rates (b), vs. speed (c), and vs. acceleration (d). In dark EMIT; in gray CMEM.	85
Figure 4-20: Category 9 – Tailpipe HC predicted vs. measured emission rates (a), residuals vs. measured emission rates (b), vs. speed (c), and vs. acceleration (d). In dark EMIT; in gray CMEM.	86
Figure 4-21: Category 9 – Tailpipe NOx predicted vs. measured emission rates (a), residuals vs. measured emission rates (b), vs. speed (c), and vs. acceleration (d). In dark EMIT; in gray CMEM.	86
Figure 4-22: Category 7 – US06. Second-by-second engine-out (EO) and tailpipe (TP) emission rates of CO ₂ and CO. Thick light line: measurements; dark	

line: EMIT predictions; thin line: CMEM predictions. The top plot represents the speed trace.	90
Figure 4-23: Category 7 – US06. Second-by-second fuel rate (FR) and engine-out (EO) and tailpipe (TP) emission rates of HC and NO _x . Thick light line: measurements; dark line: EMIT predictions; thin line: CMEM predictions.	91
Figure 4-24: Category 9 – US06. Second-by-second engine-out (EO) and tailpipe (TP) emission rates of CO ₂ and CO. Thick light line: measurements; dark line: EMIT predictions; thin line: CMEM predictions. The top plot represents the speed trace.	92
Figure 4-25: Category 9 – US06. Second-by-second fuel rate (FR) and engine-out (EO) and tailpipe (TP) emission rates of HC and NO _x . Thick light line: measurements; dark line: EMIT predictions; thin line: CMEM predictions.	93
Figure 5-1: Probabilistic approach for the integration between dynamic emission models and non-microscopic dynamic traffic models.	100
Figure 5-3: Standard deviations of the acceleration distributions for every speed range and road type (from Abou Zeid et al., 2002).	105
Figure 5-4: Standard deviations of the deceleration distributions for every speed range and road type (from Abou Zeid et al., 2002).	105
Figure 5-5: Cumulative relative frequency and cumulative modeled probability of accelerations for the road type arterial and speed range (0-10) km/h (from Abou Zeid et al., 2002).	106
Figure 5-6: Expected emission rates in g/s (on the left) and in g/km (on the right) for road type arterial and vehicle category 9. The expected emission rates in g/km of CO, HC, and NO _x are compared with the facility-specific emission rates from MOBILE6 (thin line).	108
Figure 5-7: Expected emission rates in g/s (on the left) and in g/km (on the right) for road type highway and vehicle category 9. The expected emission rates in g/km of CO, HC, and NO _x are compared with the facility-specific emission rates from MOBILE6 (thin line).	109
Figure 6-1: Set of models used for the prediction of fuel consumption and emissions on a traffic network.	112
Figure 6-2: Example of calculation of the number of vehicles traveling on each link at each time step and their speeds.	115
Figure 6-3: Input and output data of the traffic model and the integration component.	116
Figure 6-4: Network configuration of the case study.	117
Figure 6-5: Total fuel consumption, tailpipe emissions and travel time (tt) aggregated on all network links and over time for every scenario modeled.	120
Figure B-1: Link travel times for scenario 0.	142

Figure B-2: Link volumes for the scenario 0.....	143
Figure B-3: Link travel times for the scenario 1.....	144
Figure B-4: Link volumes for scenario 1.....	145
Figure B-5: Link travel times for scenario 2.....	146
Figure B-6: Link volumes for scenario 2.....	147
Figure B-7: Link travel times for scenario 3.....	148
Figure B-8: Link volumes for scenario 3.....	149
Figure B-9: Link travel times for scenario 4.....	150
Figure B-10: Link volumes for scenario 4.....	151
Figure C-1: Total fuel consumption, tailpipe emissions, and travel time (tt) on link 0 for every scenario modeled.	153
Figure C-2: Total fuel consumption, tailpipe emissions, flow, and travel time (tt) on links 1, 2, and 3 for every scenario modeled.	154
Figure C-3: Total fuel consumption, tailpipe emissions, flow, and travel time (tt) on links 4, 5, and 6 for every scenario modeled.	155
Figure C-4: Total fuel consumption, tailpipe emissions, flow, and travel time (tt) on links 8, 9, and 10 for every scenario modeled.	156
Figure C-5: Total fuel consumption, tailpipe emissions, flow, and travel time (tt) on links 11, 12, and 13 for every scenario modeled.....	157

List of Tables

Table 2.1: Tier 1 emission standards (g/mi) for light-duty vehicles	29
Table 4.1: Number of vehicles for each vehicle/technology category.	58
Table 4.2: Vehicles used for the category 7 composite vehicle.	60
Table 4.3: Vehicles used for the category 9 composite vehicle.	60
Table 4.4: Category 7 – Calibrated parameters for the engine-out emissions module (Equations 4.7, 4.8, and 4.9). The t-statistics are reported in parentheses.	67
Table 4.5: Category 9 – Calibrated parameters for the engine-out emissions module (Equations 4.7, 4.8, and 4.9). The t-statistics are reported in parentheses.	67
Table 4.6: Categories 7 and 9 – Calibrated parameters for the tailpipe CO ₂ emissions module (Equation 4.11). The t-statistics are reported in parentheses.	68
Table 4.7: Category 7 – Calibrated parameters of the catalyst pass fraction functions (Equation 4.12).	68
Table 4.8: Category 9 – Calibrated parameters of the catalyst pass fraction functions (Equation 4.12).	68
Table 4.9: Category 7 – Calibration statistics for the engine-out module.	71
Table 4.10: Category 7 – Calibration statistics for the tailpipe module.	71
Table 4.11: Category 9 – Calibration statistics for the engine-out module.	71
Table 4.12: Category 9 – Calibration statistics for the tailpipe module.	71
Table 4.13: Category 7 – Validation statistics for the engine-out module.	87
Table 4.14: Category 7 – Validation statistics for the tailpipe module.	87
Table 4.15: Category 9 – Validation statistics for the engine-out module.	87
Table 4.16: Category 9 – Validation statistics for the tailpipe module.	87
Table 5.1: Standard deviation of acceleration and deceleration as a function of speed range and road type.	104
Table 5.2: Number of observations of acceleration and deceleration for every speed range and road type.	104
Table 6.1: Total fuel consumption, tailpipe emissions, and travel time (tt) aggregated on all network links and over time for every scenario modeled.	120

Chapter 1

Introduction

This thesis is concerned with the modeling of traffic flow emissions. This chapter introduces the context in which traffic emission models are used, and presents the objectives, the contributions, and the organization of the thesis.

1.1 Traffic Congestion and Emissions

Road transportation has an essential economic and social role. However, it is one of the major contributors to energy consumption, air pollution, and emission of greenhouse gases (WBCSD, 2001). Moreover, it is at the origin of various other externalities, such as congestion, incidents, and noise pollution. Air quality, fuel consumption, and the production of greenhouse gases are major topics of national and local regulations and of international agreements. To comply with these regulations and improve the quality of the environment where we live, it is necessary to implement adequate policies. Hence, there is need to develop methods for the assessment of the impacts on environment and mobility of these policies, and for the optimization of the associated parameters.

Benefits on emissions and fuel consumption are generally believed to be strictly linked to reduction in congestion. Congestion corresponds to increases in the density of traffic as well as in the frequency of accelerations and stop-and-go transients, during which more emissions are generated. However, improvements in congestion may not always correspond to improved total emissions. For example, high free flow speeds generally represent favorable traffic conditions, but can generate high emissions, and lower travel times may encourage vehicle drivers to make more and longer trips (Dowling Associates, 2000). Moreover, the spatial distribution of emissions can be affected in a negative way by measures that improve congestion. For example, the use of traffic signals and ramp

metering can prevent the formation of congestion, but their introduction leads to higher concentration of emissions in the proximity of the signals.

As a consequence, it is necessary to consider both congestion and emissions in the problem of policies development, assessment and optimization. Moreover, other criteria, such as safety and equity, can be considered (Button and Verhoef, 1999). Therefore, the problem can benefit from multi-criteria analysis methods, a review of which can be found in Gal et al. (1999).

Mathematical models of traffic flow and vehicle emissions are useful tools to support the policies development, assessment and optimization process (Barratt, 2001). Often, especially in environmental problems, the decision processes are characterized by a high degree of complexity, uncertainty, and subjectivity (Colorni et al., 1999). Therefore, models should be used in the context of Decision Support Systems (DSS) to provide the analyst and the decision maker with quantitative estimates, trends, and insight on the policies simulated (Guariso and Werthner, 1989). Figure 1-1 shows a DSS framework that can be designed to manage traffic congestion and emissions. The framework includes a model-based traffic emission laboratory and a policy generation module. The model-based laboratory receives data and actions from the policy generation module, simulates the policy, and sends back indicators of congestion and emissions, which are used to evaluate the policy.

The following sections present an overview on the policies and the models that can be applied in this framework.

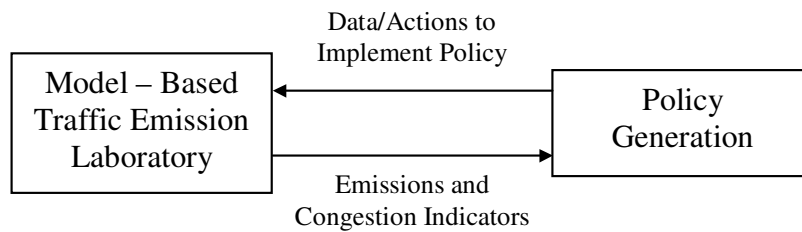


Figure 1-1: DSS framework for traffic and emissions control.

1.1.1 Policies

The policies for traffic and emissions control can be classified as follows¹:

- Vehicle technology measures, aimed at reducing engine-out emissions (e.g. use of cleaner fuel or exhaust gas recirculation), and/or tailpipe emissions (e.g. more effective catalytic converters).
- Traditional transportation measures, such as the construction of new road infrastructure, and the introduction of additional public transportation services.
- Innovative measures, relying on the application of information, communication and processing technologies to transportation systems. This concept is generally referred to in the literature as Intelligent Transportation Systems (ITS).

Now we analyze the principal strengths and limitations of these three classes of policies.

Using vehicle technology measures, criteria pollutant emissions per unit of length traveled (g/km of CO , HC , NO_x) have been significantly reduced during the last decades. Today's sophisticated emissions control devices keep emissions at a minimum with the help of optimal engine operation conditions. As a result, without a shift in the powertrain system (e.g. fuel cells), further technological improvements for internal combustion engine driven vehicles can only be marginal. On the other hand, vehicles can become high emitters if their emission control devices do not work correctly or if drivers tamper with them. It is estimated that 10% of the vehicles on the road contribute to half of the mobile emissions inventory (Wenzel and Ross, 1996). Therefore it is very important to minimize the emissions during the entire vehicle life. This can be accomplished with effective inspection and maintenance and on-board diagnostic (Degobert, 1995). Moreover, the positive effects of technological improvements require time to take effect, due to the gradual fleet substitution rate (WBCSD, 2001). It is estimated, for example, that in Europe, given the rate of new vehicle registration, the general use of new pollution control systems on vehicles is liable to take approximately a decade (Degobert, 1995).

With respect to traditional transportation measures, the construction of new road infrastructures is becoming increasingly limited by economic, spatial and environmental constraints, especially in urban areas (WBCSD, 2001). The introduction of traditional

¹ An alternative way to classify policies for traffic and emissions control is to distinguish between demand-oriented (for instance, move transportation demand from individual vehicles to public transportation using road pricing) and supply-oriented (for instance, increase the capacity of a road network). It is important to remember, though, that there are interactions and feedback effects to be taken into account when designing and evaluating a policy. For example, in the medium and long term, supply-oriented policies can lead to an increase in demand, with a consequent deterioration of the level of service.

public transportation services is desirable in dense urban areas, but is not practically feasible in situations of urban sprawl, as is the case in major urban areas of the United States.

ITS applications require time before they can be broadly implemented, but some technologies are already available and have the potential of being effective methods to minimize traffic negative impacts, including congestion and emissions. In particular, the following innovative technologies are becoming available (Sussman, 2000):

- Advanced Traffic Management Systems (traffic light control, incident management, ramp metering, electronic toll collection, etc.), which can support Travel Demand Management (TDM) measures and prevent congestion;
- Advanced Traveler Information Systems, including pre-trip information and on-trip dynamic information, which can optimize the users' choices (route, time, and mode);
- Advanced Vehicle Control Systems, such as cruise control, which can directly reduce fuel consumption and emissions by controlling the vehicle operating conditions, and also reduce congestion by reducing the likelihood of accidents.

1.1.2 Models

The interactions between transportation demand and supply determine the traffic flows on the road network. Vehicles consume fuel and produce emissions that, diffused from these mobile sources, determine the concentration of the pollutants in the air. The models needed in a traffic emissions laboratory to simulate these phenomena are represented in Figure 1-2.

Models can represent networks at various spatial scales, from a regional area to a single intersection. With respect to the temporal dimension, models can be static, if they assume a steady-state equilibrium condition, or otherwise time-dependent (or dynamic). These various modeling approaches require different efforts in terms of model development and calibration, input data, and computational effort. The choice of the modeling approach depends on the objective (from regional transportation planning to local traffic management measures) and on the constraints in terms of data availability and computational time. For example, applications that involve real-time data collection and information processing typically need to operate much faster than real time.

A typical model-based traffic emission laboratory is composed of a system of sub-models. The most sophisticated systems are composed of:

- *Demand models*: trip generation, trip distribution, modal choice, and possibly other models. These are generally econometric models that estimate the transportation demand from demographic and land use information. Trip generation, trip distribution,

mode choice, together with traffic assignment, constitute the classical four-steps modeling approach. Alternatively, activity based or trip-chain based approaches can be used (Ben-Akiva and Bowman, 1998). Main outputs of demand models are Origin-Destination (O/D) demand matrices by transportation mode. In the following, we consider only the road transportation mode. In static models the O/D demand is constant, while in dynamic models it is time-dependent, where the time index refers to the departure time from the origin. Note that, in addition to within-day dynamic models, there are day-to-day dynamic models, that can represent, for example, the time-dependence of the demand in terms of day of the week.

- *Supply models*, which simulate the performances resulting from users' demand, and the technical and organizational aspects of the physical transportation supply. The system includes the network configuration, the network loading or flow propagation model (that defines the relationship among path and link flows), the link performance model (that defines the relationships between link performances (such as travel time and cost) and flow of vehicles), and the path performance model (that defines the relationships between the performances of the single links and those of a whole path between any origin-destination pair).
- *Traffic assignment models*, which represent the interaction between demand and supply. A variety of traffic flow models exist, and differ in the way traffic flow is represented and moved across a network. Microscopic and mesoscopic models represent flows at a vehicle level, while macroscopic models represent flows as a real number quantity. In microscopic models, vehicles are moved according to car following and lane changing models, while in macroscopic and mesoscopic models flows are moved using relationships between aggregated traffic flow variables (speed, density, and flow). Microscopic models' outputs are position, speed, and acceleration of each vehicle at each time step. Macroscopic models' outputs are link flows and link travel times. The output is constant if the model is static and time-dependent if the model is dynamic. Mesoscopic models' outputs are link flows and link traversal times for each vehicle, or time-dependent speed for each vehicle.

Microscopic models allow for a detailed representation of traffic networks and are usually appropriate for a local area only, as, at a larger scale, they can be time-consuming from a computational and development standpoints, and difficult to calibrate. Non-microscopic models possess better computational speed and are relatively easier to calibrate. They do not allow for detailed representation of traffic as micro-simulation models do, but they are applicable to larger scale traffic networks. They are then typically more appropriate for regional modeling.

Moreover, each type of traffic model can be used alone, or integrated to other types of traffic models. For example, a macroscopic model can be used to model a large network, while a microscopic model can be used to generate more detailed information on single intersections considered individually.

- *Emission models*, which calculate emissions produced by the vehicles as a function of their characteristics and of their operating conditions (i.e. speed and acceleration).
- *Dispersion and photochemical models* (called also air quality models), which estimate how the pollutants emitted react with other components of the air, how they are dispersed and how ultimately they impact air quality in terms of concentrations of pollutant. While macroscopic dispersion models are relatively simple, microscopic dispersion models require detailed information about the external environment such as urban morphology (e.g. road width, buildings height, etc.), and micro-climate conditions (Barratt, 2001).

For an overview on demand, supply, and traffic models, the reader is referred to Cascetta (2001). Emission models and their integration with traffic models are discussed in more details in Chapter 3. An overview on dispersion and photochemical models can be found in Barratt (2001).

1.2 General Area of this Thesis

Within the context described in the previous section, we are interested in the area of dynamic emission models and their integration with dynamic traffic models.

In the area of dynamic emission models, we note the following. Some models represent the physical phenomena that generate emissions. These models are sophisticated as they require extensive data for their calibration, and can involve high computational time requirements. Other models are simpler to calibrate and require lower computational time, but they use explanatory variables that are not derived from a physical basis, and therefore can give non-desirable results if applied to situations not covered by the calibration data.

In the area of traffic and emission models integration, we note the following. Microscopic traffic models can be integrated directly with dynamic emission models and examples of this integration have been reported upon in the literature. On the contrary, there are fewer examples of integration involving non-microscopic traffic models and dynamic emission models. However, as discussed previously, non-microscopic traffic models have some advantages (such as better computational speeds and easier calibration) that make them more suitable for large-scale applications.

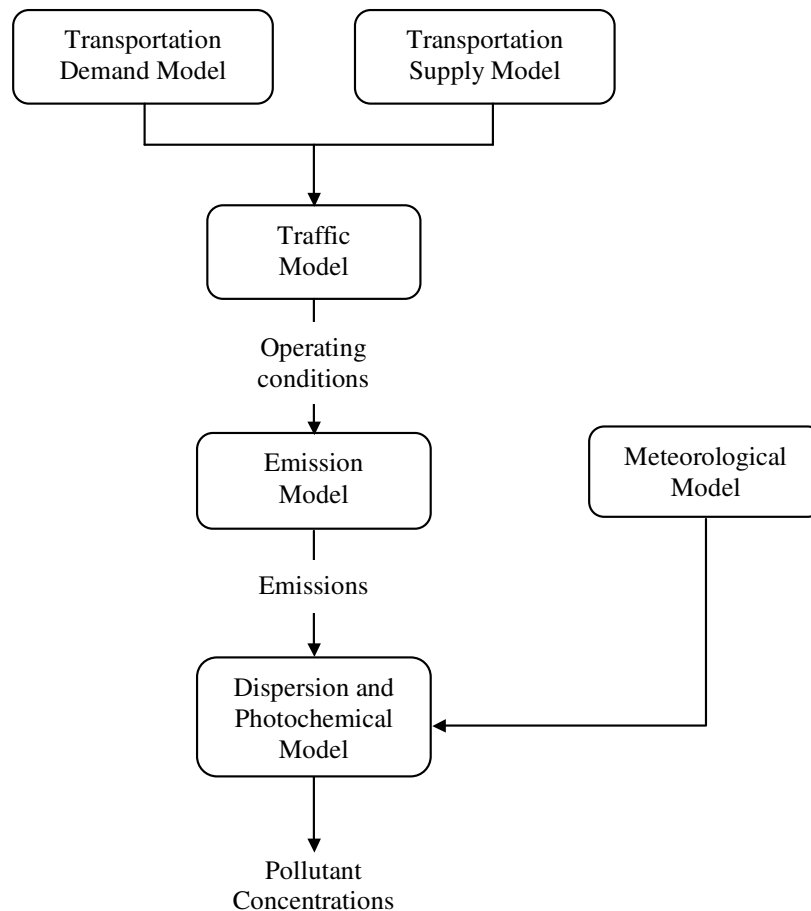


Figure 1-2: Models system for the estimation of the impact of traffic on air quality. The scheme represents a simplification, in the sense that in real world there are feedbacks that complicate the system, such as the influence of transportation supply on land use, or the effect of traffic flows on travel demand in case of congestion.

1.3 Thesis Objectives and Contributions

This thesis has the following main objectives:

- Identify the main strengths and limitations of existing approaches to traffic emissions modeling.
- Develop a new dynamic emission model, that is simple to calibrate in various situations, gives reasonably accurate results and can run fast. Such model would build on existing approaches, and combine some of their advantages.
- Develop a methodology for the integration of dynamic emission models with non-microscopic dynamic traffic models.

- Implement a combined dynamic traffic and emission model using the above developments, and explore, by modeling a small network, the potential of the combined model to assess the impacts of traffic management policies on congestion and emissions.

This thesis provides answers to the above objectives. Its main contributions are the following.

- An extensive literature review on emission models and their integration with traffic models was carried out. Strengths and weaknesses of different emissions modeling approaches have been identified. The principal approaches for dynamic emissions modeling are the emission maps, the regression-based approach, and the load-based approach.
- We designed EMIT, an emission model of instantaneous emissions and fuel consumption for light-duty vehicles. The model is designed based on an effective combination of the regression-based and the load-based approaches. EMIT was calibrated and validated for two vehicle categories. The model gives results with good accuracy for fuel consumption and carbon dioxide, reasonable accuracy for carbon monoxide and nitrogen oxides, and less desirable accuracy for hydrocarbons. The model runs fast, and is relatively easy to calibrate.
- We proposed a probabilistic approach to model accelerations for given road types and speed ranges, and an approach to integrate dynamic emission models and non-microscopic dynamic traffic models.
- The approach to integrate dynamic emission models with non-microscopic dynamic traffic models was used to assess the impacts of traffic management strategies on travel times, emissions, and fuel consumption.
- In the course of this thesis a number of future research questions have been identified.

1.4 Thesis Organization

This thesis is organized as follows. Chapter 2 provides a background on the principal motor vehicle emissions in order to understand their characteristics and the mechanisms of their generation, and introduces the related US regulations. Chapter 3 presents the literature review on available vehicle emission models and their integration with traffic models. Chapter 4 describes the development, calibration and validation of the emission model EMIT. Chapter 5 proposes the probabilistic approach to integrate dynamic emission models and non-microscopic dynamic traffic models, and describes how the expected emission and fuel consumption rates are calculated. Chapter 6 describes the application of the combined

model to assess the impact of dynamic traffic management strategies. Finally, Chapter 7 concludes the thesis and gives suggestions for future research.

Chapter 2

Emissions from Motor Vehicles

In Chapter 1 we generically introduced the problem of traffic emissions. We now provide more detailed information on this topic and define terminology that is used in the sequel of this thesis. In particular, we provide a summary of the US regulation on air quality and vehicle emissions and a description of the principal vehicle emissions. For more information about the emission standards, the reader is referred to the website of the US Environmental Protection Agency (EPA)'s Office of Transportation and Air Quality (www.epa.gov/otaq). For more detailed information about vehicle emissions, the reader is referred to Degobert (1995) and Heywood (1988).

This chapter is organized as follows. Section 2.1 summarizes the US regulations on air quality and vehicle emissions. Section 2.2 describes the principal vehicle emissions, their generation processes in motor vehicles, and their effects on health and environment.

2.1 Regulation on Air Quality and Vehicle Emissions

The Clean Air Act of 1970 first allowed for the regulation of automobile emissions in the United States. The next twenty years saw great advancements in emissions control and after-treatment technologies, however more was needed since the air quality in cities was still poor. The Clean Air Act Amendments of 1990 (CAAA90) mandate that every area in the United States meet air quality standards for six pollutants: ozone (O_3), sulfur dioxide (SO_2), carbon monoxide (CO), nitrogen dioxide (NO_2), lead (Pb), and particulate matter with an aerodynamic diameter less than 10 microns (PM_{10}). The standards are defined in terms of concentration of the pollutant in the air using various temporal aggregations. Short-term (24 hours or less) averages are designed for CO and O_3 , to protect against acute, or short-term, health effects; long-term averages (i.e. annual average) are designed for the other pollutants to protect against chronic health effects.

While SO_2 and Pb are presently emitted principally by stationary fuel combustion and industrial processes respectively, for the other four pollutants transportation represents a significant source. The CAAA90 regulate motor vehicles emissions by gradually phasing in more stringent standards for light duty vehicles. The emission standards, called Tier 1 (and later Tier 2) control total HC (THC), non-methane HC ($NMHC$), CO , NO_x and PM . Heavy-duty vehicles are regulated separately and are not considered in this study. The standards fix the maximum tailpipe emission rates for a vehicle taking account of its type and mileage. The emission rates must be measured on standard driving cycles using the Federal Test Procedure and calculated in g/mile using the official EPA method. The following two sections present the driving cycles and the emission standards defined by the EPA.

2.1.1 Driving Cycles

The official protocol for testing vehicles compliance with the emissions standards requires laboratory measurements. Light-duty vehicles are tested on chassis dynamometers (Figure 2-1), which allow the wheels to spin and use inertial weights at various horsepower settings to simulate real world conditions. A hose is attached to the tailpipe to collect the exhaust gases and direct them into a sampler.



Figure 2-1: A chassis dynamometer
(from http://www.otl.doe.gov/otu/field_ops/emis_tour/dynam.html)

Once the non-kinematic variables (such as different types of resistances, air temperature, and engine temperature) are reproduced on the chassis dynamometer, the movement of the vehicle is simulated using a speed-time curve, called 'driving cycle'. The driver follows the

driving cycle shown on a computer monitor, by accelerating and breaking the vehicle. The driver function can also be performed using a robot. A more detailed description of chassis dynamometers can be found in Degobert (1995).

We present the driving cycles regulated by the EPA in the US. In Chapter 4 of this thesis we present another driving cycle, used for the development of emission models. For each driving cycle, we report the speed-time curve and some statistics that summarize the characteristics of the driving cycles: total time, distance driven, average speed, highest speed, and maximum specific power. Specific power is two times the product of vehicle speed and acceleration ($2 \cdot v \cdot a$).

In the US, the standard cycle is the Federal Test Procedure (FTP) cycle (Figure 2-2). Originally developed in the 70's, it was intended to reflect the actual driving conditions both on arterial roads and highways. This cycle has three separate phases: a cold-start (505 seconds) phase, a hot-transient (870 seconds) phase, and a hot-start (505 seconds) phase. The three phases are referred to as bag 1, bag 2, and bag 3 because exhaust samples are collected in three separate bags during each phase. Between the end of the second phase and the start of the third phase, the engine is turned off for 10 minutes, which are called soak time. The 505-second driving curves for the first and third phase are identical. The total test time for the FTP is 2,457 seconds (40.95 minutes), the top speed is 56.7 mph (92.3 km/h), the average speed is 21.4 mph (34.2 km/h). The distance driven is approximately 11 miles (17.6 km) and the maximum specific power is 192 (mph)²/s (491 (km/h)²/s).

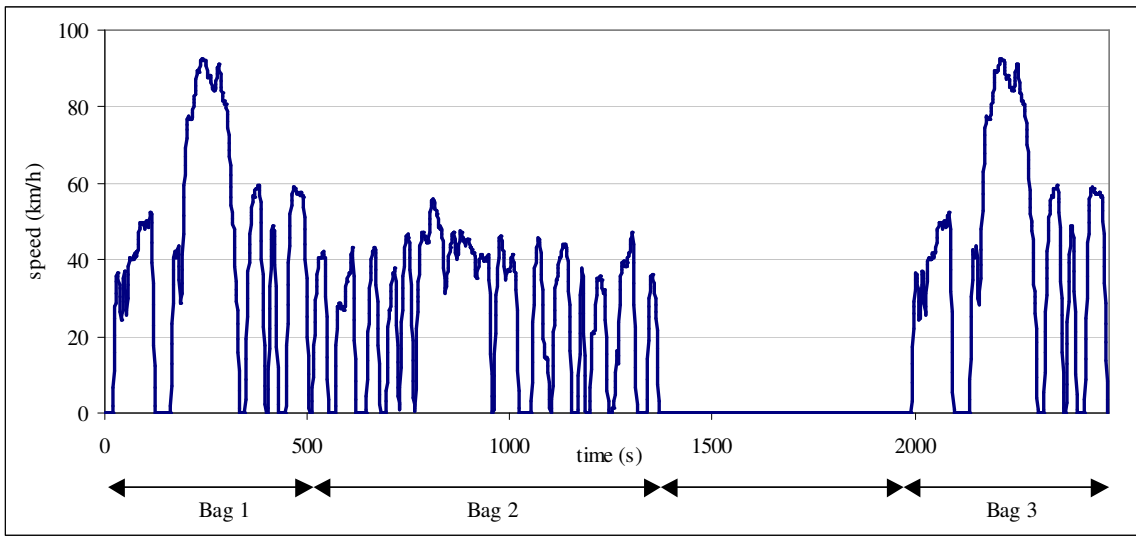


Figure 2-2: The FTP cycle.

It has been recognized that the FTP cycle does not accurately characterize today's real-world driving conditions; for example it does not include aggressive high power driving (Goodwin, 1996). A Supplemental Federal Test Procedure (SFTP) has been introduced progressively starting in year 2000 and will be effective for all light-duty vehicles in year 2004. The SFTP includes two additional cycles: the US06 to represent aggressive highway driving, and the SC03 to measure the increased emissions due to air conditioning.

The US06 (Figure 2-3) is a hot-start cycle representing driving conditions with higher speeds and harder accelerations. The total time for the US06 test is 600 seconds (10 minutes), the highest speed is 80.3 mph (128.5 km/h), the average speed is approximately 48 mph (76.8 km/h), and the maximum specific power is 480 (mph)²/s (1223 (km/h)²/s). The distance driven is 8 miles (12.8 km).

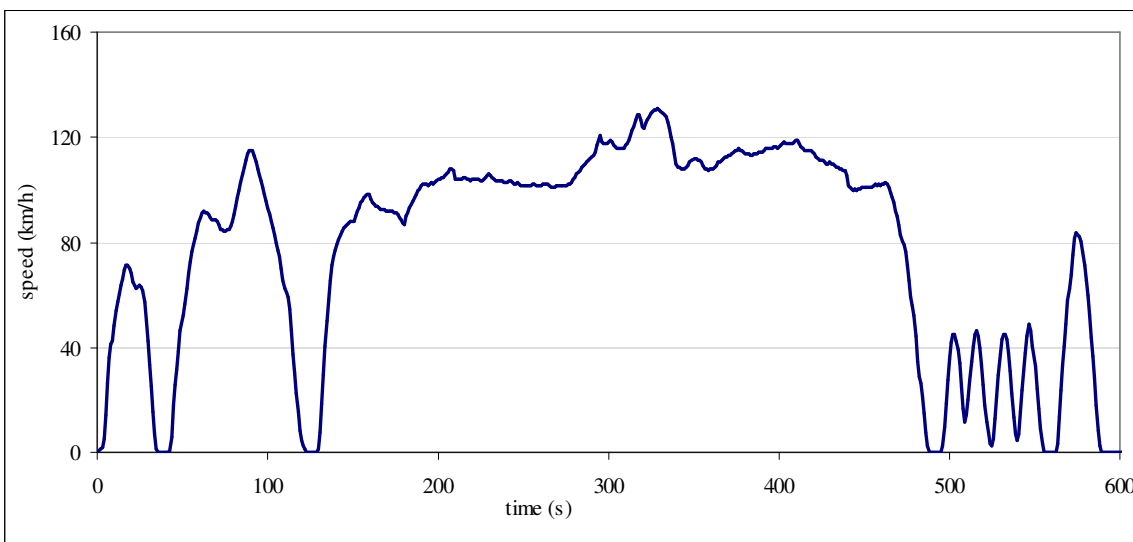


Figure 2-3: The US06 cycle.

The SC03 (Figure 2-4) driving cycle is similar to the FTP bag 3, but with slightly higher accelerations and excludes the 10 minutes soak.

2.1.2 Emission Standards

Emission standards for light duty vehicles are checked from chassis dynamometers tests measuring the total tailpipe emissions generated during each phase.

The Tier 1 standards (see Table 2.1) were phased-in progressively between 1994 and 1997. They are defined for light-duty vehicles at two vehicle ages: 50,000 miles (or 5 years) and at 100,000 miles (or 10 years). Light-duty vehicles are divided into the following principal vehicle categories: passenger cars, light light-duty trucks (LLDT), with a gross

vehicle weight rating (GVWR) below 6000 lb, and heavy light-duty trucks (HLDT), with a GVWR above 6000 lb. Diesel and gasoline vehicles have different NO_x standards.

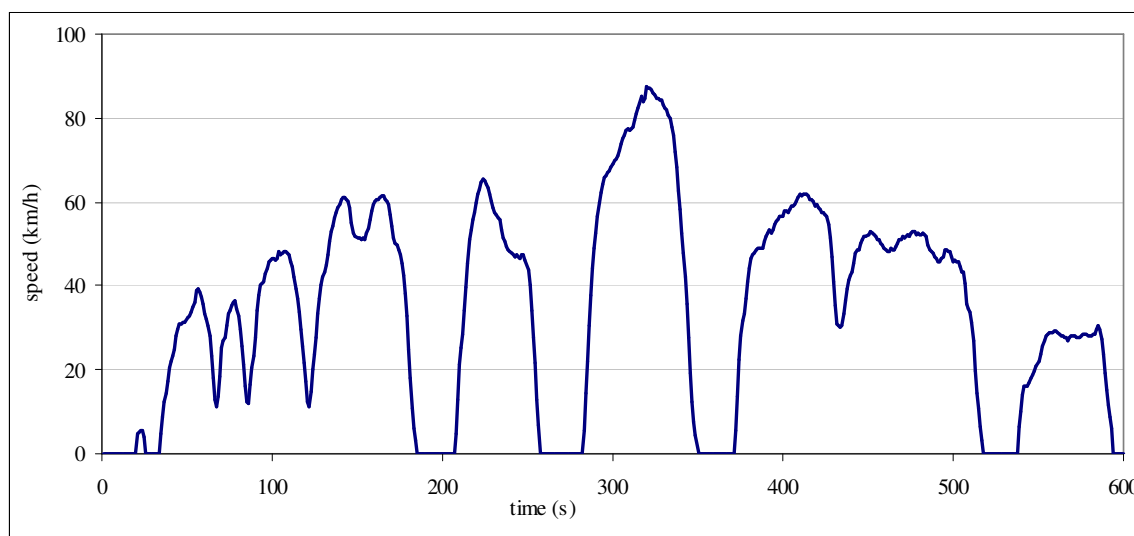


Figure 2-4: The SC03 cycle.

Table 2.1: Tier 1 emission standards (g/mi) for light-duty vehicles

Vehicle category	50,000 miles / 5 years					
	THC	NMHC	CO	NOx diesel	NOx gasoline	PM
Passenger cars	0.41	0.25	3.4	1.0	0.4	0.08
LLDT, LVW <3,750 lbs	-	0.25	3.4	1.0	0.4	0.08
LLDT, LVW >3,750 lbs	-	0.32	4.4	-	0.7	0.08
HLDT, LVW <5,750 lbs	0.32	-	4.4	-	0.7	-
HLDT, ALVW >5,750 lbs	0.39	-	5.0	-	1.1	-

Vehicle category	100,000 miles / 10 years ²					
	THC	NMHC	CO	NOx diesel	NOx gasoline	PM
Passenger cars	-	0.31	4.2	1.25	0.6	0.10
LLDT, LVW <3,750 lbs	0.80	0.31	4.2	1.25	0.6	0.10
LLDT, LVW >3,750 lbs	0.80	0.40	5.5	0.97	0.97	0.10
HLDT, LVW <5,750 lbs	0.80	0.46	6.4	0.98	0.98	0.10
HLDT, ALVW >5,750 lbs	0.80	0.56	7.3	1.53	1.53	0.12

Notes:

THC denotes total hydrocarbons; NMHC denotes non-methane hydrocarbons; NOx diesel denotes NOx for diesel vehicles; NOx gasoline denotes NOx for gasoline vehicles.

LLDT denotes light light-duty trucks; HLDT denotes heavy light-duty trucks; LVW denotes loaded vehicle weight (unloaded weight + 300 lbs); ALVW denotes adjusted LVW, equal to (gross vehicle weight + loaded weight)/2.

(from <http://www.dieselnet.com/standards/us/light.html>)

² Useful life 120,000 miles / 11 years for all HLDT standards and for THC LDT standards.

The Tier 2 standards are planned to be phased in between 2004 and 2009. These standards fix a reduction of the amount of sulfur in fuels and define more stringent emission limits regardless of the fuel used and the vehicle weight. As a consequence, vehicles with larger engines will need to improve the emission control technology more than smaller vehicles to meet the standards. The standards are defined at 50,000 miles and at 120,000 miles and are structured into 8 certification levels (called bins). Manufacturers will have to certify every vehicle model to any of the 8 bins. Moreover, the average NO_x emissions of the entire fleet produced by every manufacturer will have to meet the fixed standard of 0.07 g/mi.

Although the introduction of emission standards caused a major decrease in emissions, there are factors that limit this positive effect. First, vehicle miles traveled have considerably increased. In fact, total passenger km by light-duty vehicles in North America increased by 240% from 1960 to 1990 (Schafer, 1998). In addition, it is estimated that the average on-road vehicle exceeds the standards. This is due to factors such as the presence of high emitters (i.e. vehicles with malfunctioning emission control devices), and the frequency of cold starts and high power driving events that are not represented in the FTP cycle (Goodwin, 1996).

2.2 Principal Vehicle Emissions

In the previous section we introduced the four vehicle emission species regulated by the EPA (CO , HC , NO_x , and PM). In this section, we describe the main characteristics, the mechanisms of generations, and the effects on health and environment of these emissions. In addition, we describe ozone (O_3), which is a byproduct of NO_x and HC , and carbon dioxide (CO_2), which is a greenhouse gas.

In order to understand the principles of emissions generation in a motor vehicle, it is useful to introduce the variable “air-to-fuel mass ratio”. The stoichiometric ratio (~14.5) corresponds to the mass of air needed to oxidize completely a mass of fuel.

Under high power conditions, engines are typically designed to operate with a mixture rich in fuel, in order to prevent the catalyst from overheating. This is called enrichment. Enrichment also often occurs during cold starts to heat faster the engine and the exhaust so that the catalyst can light-off sooner. Enrichment can have a significant effect on emissions.

Alternatively, during long deceleration events, the mixture can go lean because engines are often designed to shut off the fuel since power is not required. Though less significant than enrichment, enleanment conditions can also affect emissions.

2.2.1.1 Carbon Monoxide

Carbon monoxide (CO) is a byproduct of incomplete combustion. The principal chemical reactions that happen during a combustion are:



The first reaction is much faster (~10 times) than the second. Therefore, CO can be either an intermediate product, or a final product, when there is insufficient O_2 to adequately mix with the fuel. Under enrichment conditions, due to the lack of oxygen, much of the carbon present in the excess fuel is partially oxidized to CO instead of CO_2 . Note that CO is also generated under stoichiometric conditions due to possible partial oxidation of HC .

CO is colorless, odorless, but poisonous. It reacts with the hemoglobin present in the blood to form carboxyhemoglobin, causing a reduction in the oxygen transported from the lungs to the body cells. High concentrations of CO can increase the risk of cardiovascular problems and impede the psychomotor functions. Infants, elderly, and people with cardiovascular diseases and respiratory problems are more at risk. Also, CO indirectly contributes to the buildup of ground-level ozone and methane.

The EPA estimates that 51% of CO emissions in the US come from on-road mobile sources, and in cities the proportion can be much higher (EPA, 2001c).

2.2.1.2 Hydrocarbons

Hydrocarbon emissions (HC) result from incomplete combustion or from fuel evaporation. The incomplete combustion in motor vehicles can be due to several causes. For example, for a lack of O_2 , or because fuel can collect in the crevices of the cylinder, or because some fuel species burn at a higher temperature, thus do not completely combust. In stoichiometric and enrichment conditions, HC emissions are usually proportional to fuel rate consumption. HC puffs can be emitted under enleanment conditions, which can occur during long deceleration events (An et al., 1998) and transients (Nam, 1999). During decelerations, the dramatic drop in fuel results in a cessation of combustion, and hence virtually all of the remaining fuel (what little is left) is emitted unburned. However this fuel excess is typically oxidized in the catalyst. This is an example of a history effect.

Evaporative emissions related to motor vehicles can be: (a) diurnal emissions, caused by the diurnal temperature while the vehicle is not being driven; (b) hot-soak emissions, occurring for about one hour after the end of the trip due to the high temperature of the fuel system; (c) running losses, occurring during the trip due to the higher temperature and

pressure of the fuel system; (d) resting losses of gasoline vapor through faulty connections, gas tanks, etc.; (e) refueling emissions.

Hydrocarbons react in the presence of NO_x and sunlight to form ground-level ozone and contribute to the formation of smog, which has deleterious health and greenhouse effects. A number of aromatic hydrocarbons, such as benzene, are carcinogens (Degobert, 1995).

The EPA estimates that on-road mobile sources contribute 29% of the total HC emitted in the US (EPA, 2001c).

2.2.1.3 Nitrogen Oxides

Nitrogen oxides (NO_x) is the generic term for a group of highly reactive gases. They form when fuel is burned at high pressure and temperature conditions, which induce the dissociation and subsequent recombination of atmospheric N_2 and O_2 that generate NO_x . Many of the nitrogen oxides are colorless and odorless. However, nitrogen dioxide (NO_2) can be seen in the air as a reddish-brown layer over many urban areas.

The primary sources of NO_x are motor vehicles and other industrial, commercial, and residential sources that burn fuels. The combustion in motor vehicle engines causes the production of primarily NO but also NO_2 , as shown by the following chemical reactions:



When the fuel consumption rate is low, very little NO_x is emitted. Under enleanment conditions, more NO_x tends to be formed due to the excess oxygen. During stoichiometric conditions, NO_x emissions tends to increase as more fuel is burned, due to the increased combustion temperature.

NO_x is a precursor to the formation of ground level ozone. It reacts with ammonia, moisture, and other compounds to form nitric acid that may cause serious respiratory problems. It also contributes with SO_2 to the formation of acid rain and of particulate matter. It also causes eutrophication (nutrient overload in water bodies) and contributes to the formation of smog.

The EPA estimates that on-road mobile sources contribute 34% of the total NO_x emitted in the US. 42% of this is produced by diesel vehicles (EPA, 2001c). This is since diesels engines operate lean and haul heavy loads.

2.2.1.4 Ozone

Ozone (O_3) is a gas not usually emitted directly into the air, but created at ground level by quite complex photochemical reactions that involve principally nitrogen oxides, oxygen, and

hydrocarbons, in the presence of sunlight (NRC, 1991). As a result, its concentration in the air is usually higher during summertime. Ozone is beneficial in the upper atmosphere, where it protects the Earth by filtering out ultraviolet radiation; at ground level, it can cause health problems, such as eye inflammation, short term decrease in lung functions, and long term damage to the lungs and chronic respiratory illness. Moreover, it causes damage to plants and ecosystems. Many urban areas tend to have high levels of ozone, but even rural areas are subject to increased ozone levels because wind can carry ozone and its precursors over long distances. Therefore, managing ozone pollution is most effective if done from a regional rather than local perspective.

2.2.1.5 Particulate Matter

Particulate matter (PM) is a generic term for all the particles suspended in the air, including resuspended road dust, smoke, and liquid droplets. Some particles are emitted directly into the air from a variety of sources such as motor vehicles (from brakes and tires), factories, and construction sites. Other particles are formed when gases from burning fuels (such as NO_x , SO_2 , and ammonia) react with water vapor in the atmosphere. They are usually classified based on their size, which varies from visible to microscopic. The CAAA90 set a standard for particulate with an aerodynamic diameter less than 10 microns (PM_{10}). The EPA has only recently begun to monitor $PM_{2.5}$. Breathing small size PM can cause respiratory health problems, including lung cancer. Moreover, PM harms the environment by changing the nutrient and chemical balance in water bodies, it causes erosion and staining of structures and monuments, and is the major cause of reduced visibility in many parts of the US.

The EPA estimates that on-road mobile sources contribute 10% of the total $PM_{2.5}$ emitted in the US. 72% of this is produced by diesel vehicles (EPA, 2001c).

2.2.1.6 Carbon Dioxide

Carbon dioxide (CO_2) is the principal product of complete combustion (see Equation 2.1). Although it is naturally present in the atmosphere and it is not considered a pollutant, CO_2 is a greenhouse gas that contributes to the potential for global warming. The EPA reports that CO_2 represents about the 80% of the greenhouse gas emissions in the US (EPA, 2001b) and that motor vehicles contribute 30% to the total emissions of CO_2 from fossil fuel combustion. Since greenhouse gases control is a global problem, it requires long-term efforts and international agreements, as proposed for example in the United Nations Framework Convention on Climate Change (see <http://unfccc.int>).

Chapter 3

Literature Review of Traffic Emission Models

In Chapter 2 we summarized the characteristics and the mechanisms of generations of the principal vehicle emissions. In this chapter we describe various approaches present in the literature to model vehicle emissions. Strengths and weaknesses of these modeling approaches are identified and examples of emission models are presented. We also present some examples of how emission models have been integrated with traffic models in the literature.

Other reviews exist in the literature. For example, NRC (2000) gives an overview of models used in the US, and Joumard (1999) reviews models used in Europe.

This chapter is organized as follows. In Section 3.1 we present the literature review of vehicle emission models. First, we introduce the variables and parameters that influence emissions and that can be represented in emission models. Then, we classify models in static and dynamic models, and we divide dynamic models into three subclasses. For each class of models, we give examples. In Section 3.2 we present examples of integration between emission and traffic models. Section 3.3 concludes the chapter pointing out some research needs in the area of traffic emissions modeling.

3.1 Vehicle Emissions Modeling

3.1.1 Factors that Influence Emissions

Variables and parameters that influence emissions can be grouped in the following categories: vehicle technology specifications, vehicle status, vehicle operating conditions, and external environment conditions.

- Vehicle technology specifications include general vehicle design characteristics (weight, aerodynamic efficiency, etc.), propulsion characteristics (Otto or Diesel cycle), type of fuel, emission control devices (i.e. catalyst converter), and engine power.
- Vehicle status includes mileage, age, and mechanical status.
- Vehicle operating conditions include engine dynamics (engine speed, power demand, etc.), air-to-fuel mass ratio, vehicle kinematic variables (speed and acceleration), and temperature of the catalyst. These variables can in turn depend on the vagaries of individual driver behavior.
- External environment conditions include air conditions (ambient temperature, atmospheric pressure, relative air humidity), and road characteristics (longitudinal grade, curves, and pavement quality).

Given the strong influence of vehicle technology specifications and status on the emissions generation process, emission models are usually calibrated separately for every vehicle make and model, or for homogeneous vehicle categories. Vehicle operating conditions are generally the principal input to the models, while external environment conditions can be introduced as secondary inputs.

There are a variety of approaches for vehicle emissions modeling, each with its strengths, its weaknesses and its limitations. There are technology-based engineering models that are very detailed and are usually in practice developed for a specific vehicle or engine (Heywood, 1988). These models are needed for technology development, calibration and regulation purposes. However, integrated traffic emissions modeling requires a simpler and more general approach that takes account of vehicles diversity grouping them in homogeneous categories.

Emission models are usually calibrated using chassis (or engine) dynamometer measurements (see Section 2.1.1). During a dynamometer test, emissions can be measured (a) as total generated during the cycle or during single bags, or (b) continuously (typically second-by-second). These approaches correspond to two different ways of modeling emissions, which in this thesis are called average speed-based modeling (or static modeling, using the correspondent traffic models taxonomy) and dynamic modeling respectively.

3.1.2 Average Speed-Based Emission Models

Let E_i denote the total emissions of a species i or the total fuel consumption, for a given time period (i.e. hour, day, year) and a given area (region, city, or generic network). These models, referred to in the literature as static models or emission inventory models, calculate E_i as:

$$E_i = \sum_c \sum_l VKT_l \cdot f_c \cdot BER_i(\bar{s}_l, c)$$

where:

c is the vehicle category;

l is the index of a sub-network (e.g. a single link or a set of links) characterized by an average speed \bar{s}_l ;

VKT_l are the vehicle-kilometers traveled (or vehicle-miles traveled VMT_l) in the given time period in sub-network l ;

f_c is the fraction of vehicles of category c ;

$BER_i(\bar{s}_l, c)$ is the base emission rate per kilometer (or mile) for a species i . $BER_i(\bar{s}_l, c)$ is determined from standard driving cycles at a particular average speed \bar{s}_l , for each vehicle category c . For this reason, base emissions are also called cycle emissions, and non-base emissions are called off-cycle emissions. The BERs can be corrected at different speeds with the use of speed correction factors (SCFs). Correction factors can also be used to take account of different conditions, such as cold-start and facility-specific modes of operation.

Average speed-based models are generally fed with output from macroscopic static traffic models or with forecasts of total VKT (or VMT). These models cannot be used to generate estimates of instantaneous emissions, since they determine the emissions in a time interval as a function of the average speed of a cycle. They should therefore be used in steady state conditions. Applications of these models typically include large-scale analyses and cases when the average speed adequately characterizes the vehicle flow (i.e. uninterrupted flow in highways).

However, in most applications, it is necessary to predict traffic emissions with a higher spatial and temporal resolution. Moreover, in many cases the same average speed can correspond to significantly different driving conditions. Thus, average speed-based models may significantly misestimate the emissions. For example, these models can underestimate the emissions in highly dynamic driving conditions, for the same average speed of a given cycle.

Internationally used inventory emission models are:

- the MOBILE6 model, developed by the EPA, which is used in all US States except California;
- the Motor Vehicle Emission Inventory (MVEI) Models developed by the California Air Resources Board (CARB, 1996);

- the COmputer Programme to calculate Emissions from Road Transport (COPERT) III model (Ntziachristos and Samaras, 2000). COPERT III is a part of the CORINAIR programme, sponsored by the European Environmental Agency, that develops sets of software tools to support European countries in compiling annual air emission inventories.

In the rest of this section we give an overview of MOBILE6.

MOBILE6

MOBILE6 (EPA, 2002) is the latest in a series of MOBILE models, the first version of which dates back to 1978. MOBILE6 calculates average fleet emissions for:

- HC , CO , and NO_x ;
- evaporative emissions;
- gasoline, diesel, and natural gas-fueled cars, trucks, buses, and motorcycles;
- years from 1952 to 2050.

Compared with the previous versions, MOBILE6 has a new modeling methodology that uses facility-specific (i.e. freeways, arterial/collectors, freeway ramps, and local roadways with different levels of congestion) driving cycles, developed in Sierra Research (1997), to calculate facility-specific speed correction factors (EPA, 2001a).

The EPA is currently designing a new generation model (called MOVES), which will probably be a modal model. It would cover HC , CO , NO_x , PM , air toxics, and greenhouse gases emissions (see <http://www.emc.mcnc.org/projects/ngm/>).

3.1.3 Dynamic Emission Models

In the dynamic approach, emissions are measured continuously during chassis dynamometer tests and stored for particular time intervals (usually every second). The operational conditions of the vehicle at a given time, defined commonly by the speed value, are recorded simultaneously with the emissions. The accelerations are then calculated from the speed-time curve. More comprehensive measurements can include quantities such as engine speed, throttle position, mass air flow, air conditioning use, and transmission gear.

Instantaneous measurements allow both instantaneous and modal analysis and modeling, based respectively on instantaneous vehicle kinematic variables, such as speed and acceleration, or on more aggregated modal variables, such as time spent in acceleration mode, in cruise mode, and in idle mode.

Let $E_i(t)$ denote the emissions of species i (or the fuel consumption) generated at time t in a given area (i.e. region, city, or generic network). $E_i(t)$ may be calculated as follows³:

$$E_i(t) = \sum_j e_i(c_j, x_j(t))$$

where:

j is the vehicle ID;

c_j is the category of vehicle j ;

$x_j(t)$ denotes instantaneous or modal variables of vehicle j at time t . Some models use also history variables (such as past values of speed, and time elapsed since the beginning of the trip).

$e_i(c_j, x_j(t))$ denotes the emission of species i for vehicle j at time t .

In the rest of this thesis, unless otherwise indicated, when calculating the emissions at time t , all kinematic variables will refer to the same time t .

Due to the large amount of information needed and to the computational requirements, the dynamic approach was used until recently to model only the emissions of a single vehicle, single links or single intersections, instead of a network containing multiple vehicles. Due to new developments in data availability and improved computational power, the dynamic approach is increasingly applicable to larger networks.

The dynamic emission models in the literature can be classified into three principal groups: emission maps, regression-based models, and load-based models.

3.1.3.1 Emission Maps

Emission maps, called also velocity-acceleration (VA) lookup tables, have the form of matrices, where one dimension represents speed ranges, and the other acceleration or specific power ranges. For each emission species and for each vehicle category, the instantaneous emission measurements are assigned to one cell of the emission matrix, according to vehicle speed and acceleration measured at that instant of time. Then, for each cell the mean of all emission measurements is calculated.

Although easy to generate and use, emission maps have several limitations. They can be sparse and sensitive to the driving cycle used to populate them (Sturm et al., 1998). Moreover, they are usually not flexible enough to account for such factors as road grade,

³ Similarly, dynamic models allow calculating the emissions of a single vehicle trip, summing over time the emissions generated by the single vehicle.

accessory use, or history effects. Some of these factors can be represented building a library of emission maps by defining the conditions under which a matrix is populated or introducing multiplicative factors to apply after the matrix is used.

Due to their simplicity, emissions maps are widely used, especially in Europe. For a detailed review of emission maps, and for a discussion on their limitations and applicability, see Hickman et al. (1999) and Sturm et al. (1998). Sturm et al. (1998) investigate the requirements that driving cycles should satisfy to obtain satisfactory maps, the influence of data aggregation and data interpolation methods, and the need of additional parameters to account for dynamics of driving behavior.

MODEM

The MODEM microscopic emission database was developed as a part of the European Commission's DRIVE II research program (Jost et al., 1992). The database derives from tests on 150 vehicles sampled from the vehicle population of different European Union countries. The vehicles were tested on 14 cycles based on a large-scale survey of the operating conditions of vehicles in urban areas across Europe.

The emissions of HC , CO , CO_2 , and NO_x are calculated using emission maps for 12 different vehicle types. The speed ranges between 0 km/h and 90 km/h, and the product of acceleration and speed ranges between -15 and $+15$ (m^2/s^3).

3.1.3.2 Regression-Based Models

Regression-based models are usually linear regressions that employ functions of instantaneous vehicle speed and acceleration, or modal variables, as explanatory variables. These models overcome the sparseness and discretization problems of the emission maps. However, they can lack a clear physical interpretation, and can also overfit the calibration data when using a large number of explanatory variables. Therefore these models can give non-desirable results if applied to situations not covered by the calibration data.

In the following paragraphs, some examples of statistical models from the recent literature are described.

Georgia Institute of Technology Model

This model was developed within the framework of MEASURE (see Section 3.2) for the metropolitan region of Atlanta, Georgia. It is a statistical aggregate trip-based model, designed for the application to measured or forecasted trip-based traffic activity. This

means that the model predicts not instantaneous emissions, but average emission rates per second relative to an entire trip or driving cycle.

The model consists of least squares regressions on driving cycle data (Fomunung et al., 1999). The estimated variable is the emission rate (for CO , HC , and NO_x) normalized to the mean FTP bag 2 emission rate. The explanatory variables are selected, using a hierarchical tree-based regression technique, among the following sets of variables⁴:

- modal variables such as average speed and percentage of cycle exceeding various thresholds of positive kinetic energy, power, and acceleration;
- interaction dummy variables obtained combining vehicle characteristics, such as odometer readings, fuel injection type, catalytic converter type, and high/normal emitter status.

The model is calibrated using a very large database containing more than 13,000 vehicle tests, which enhances its statistical significance, although only few recent model year vehicles are represented. For the calibration, the data were weighted to reflect the model year distribution of the Atlanta fleet.

Unlike the other models described in this chapter, the Georgia Institute of Technology model is not calibrated separately for different vehicle technology categories. Rather, it represents explicitly, within the regressions, vehicle technology specifications and status. Thus, it is somehow more compact.

Despite its qualities listed above, the Georgia Institute of Technology model has some limitations. First, to adapt it to another urban area, it is complex to design and calibrate, since many derived variables have to be calculated and offered to the model. Second, the model does not predict instantaneous emission rates, but only trip based emission rates, which prevents its applicability to microscale studies. Third, the model is place-specific, because the model year distribution is incorporated in the calibration coefficients.

The model has been validated for the Atlanta metropolitan region and compared with MOBILE5a (Fomunung et al., 2000).

⁴ As an example, for NO_x the significant explanatory variables are: (1) average speed of cycle, (2) percent of cycle time spent with inertial power surrogate greater than 120 mph^2/s , (3) percent of cycle time spent accelerating at rates greater than 6 mph/s , (4) percent of cycle time spent with deceleration rate greater than 2 mph/s , (5) an interaction variable between fuel injection type 'carburetor' and odometer reading less than 25,000 miles, (6) a variable representing vehicles that have carburetors with odometer reading between 25,000 and 50,000 miles, (7) a variable for vehicles that have 'oxidation only' type catalyst and odometer reading is between 50,000 and 100,000 miles, (8) a variable for vehicles that have '3-way catalyst' type converter and mileage between 25,000 and 50,000 miles, (9) a variable for vehicles with 3-way catalyst type converter and mileage between 50,000 and 100,000 miles, (10) a variable with fuel injection type 'port' with odometer reading between 50,000 and 100,000 miles, and is also a high emitter, (11) a variable with 'throttle body' fuel injector type and odometer reading 50,000-100,000 miles, and is also a high emitter.

POLY

POLY was developed by researchers at the Polytechnic University of New York and the Texas Southern University. This model adopts linear least squares regressions that take into account, in addition to instantaneous speed and acceleration, also past accelerations and road grade (Teng et al., 2002). The model formulation is as follows:

$$e_i(c,t) = \beta_0 + \beta_1 v(t) + \beta_2 v^2(t) + \beta_3 v^3(t) + \beta_{T'} T'(t) + \beta_{T''} T''(t) + \beta_{A_t} A(t) + \dots + \beta_{A_{t-9}} A(t-9) + \beta_w W(t)$$

where:

$e_i(c,t)$ denotes the emission rate for species i , that depends on vehicle category c and time t ;

$v(t)$ is the speed at time t ;

$T'(t)$ is the duration of acceleration since its inception up to the current time t ;

$T''(t)$ is the duration of deceleration since its inception up to the current time t ;

$A(t-\bar{t})$ is the combined acceleration or deceleration at time $t-\bar{t}$ ($t=0,\dots,9$), calculated from the acceleration $a(t)$ and the grade $g(t)$ (in %) as follows:

$$A(t-\bar{t}) = a(t-\bar{t}) + 9.81 \cdot \left(\frac{g(t-\bar{t})}{\sqrt{1+g(t-\bar{t})}} \right);$$

$W(t)$ is the product of $v(t)$ and $A(t)$

β s are the parameters calibrated for each vehicle category c .

The model uses the NCHRP vehicle emissions database, described in Section 3.1.3.3. For its calibration, the model uses the FTP data, while for its validation it uses both the MEC01 and the US06 data. The results obtained for some individual vehicles have been compared with the results obtained with CMEM (see Section 3.1.3.3) and with the Virginia Polytechnic Institute model (see next paragraph).

Virginia Polytechnic Institute Model

It is a statistical instantaneous model that predicts CO , HC , and NO_x , consisting in a set of linear least squares regressions (Dion et al., 1999). So far it has been developed using a limited database derived from 8 vehicles tested at the Oak Ridge National Laboratory. The data were aggregated into a composite vehicle lookup table. The vehicle speed ranges from 0 to 121 km/h and the vehicle acceleration ranges from -1.5 to 3.7 m/s².

The explanatory variables are the set of combinations of speed and acceleration that obtained the best fit among many combinations. The model estimates the logarithm of the

emission (or fuel consumption) rate, in order to prevent the prediction of negative emission rates. The model is given by the following equations:

$$\text{Log}(e_i) = \begin{cases} \sum_{m=0}^3 \sum_{n=0}^3 (\alpha_{m,n}^i \cdot v^m \cdot a^n) & \text{for } a \geq 0 \\ \sum_{m=0}^3 \sum_{n=0}^3 (\beta_{m,n}^i \cdot v^m \cdot a^n) & \text{for } a < 0 \end{cases}$$

where:

e_i is the emission (or fuel consumption) rate;

v is the vehicle speed;

a is the vehicle acceleration.

Ahn et al. (2002) validated the model, using one vehicle from EPA data. The model is planned to be recalibrated using the NCHRP vehicle emissions database (described in Section 3.1.3.3).

The model has been integrated both with the traffic microsimulation model INTEGRATION, and with a mesoscopic model that calculates the average profile of speed along the network links, given average speed, number of stops, and duration of stops (Dion et al., 1999).

Although POLY and the Virginia Polytechnic Institute model were validated with reasonable results, these models, due to the large number of explanatory variables, may overfit the data. Therefore they may give non-desirable results if applied to situations not covered by the calibration data. In Chapter 4 of this thesis, we show that using a significantly smaller number of variables it is possible to obtain a model with good estimation capabilities.

3.1.3.3 Load-Based Models

Load-based models represent the physical and chemical phenomena that generate emissions. These models are usually composed of modules that simulate single steps of the process, each calibrated with laboratory measurements as well vehicle specifications data.

The model developed in Chapter 4 of this thesis is derived from the load-based approach. In this section we present the principles of the approach. Chapter 4 describes in greater detail the relationships used by load-based models. Readers interested in a more comprehensive description are referred to Barth et al. (2000), Goodwin (1996), Thomas and Ross (1997), An et al. (1998), and Nam (1999).

The primary variable of these models is the fuel consumption rate FR . When the engine power is zero, the fuel rate equals a small constant value. Otherwise, fuel consumption is mainly dependent on engine speed, engine power, and air-to-fuel ratio. Engine power is calculated as the sum of total tractive power requirement at the wheels and engine power requirement for accessories, such as air conditioning. Tractive power is given by the sum of an inertial driving term, a rolling resistance term, and an air drag resistance term. These terms depend on vehicle characteristics and on vehicle speed and acceleration.

Once the fuel rate FR is calculated, the engine-out emission rates for a species i (EO_i) are modeled as function of FR and air-to-fuel ratio. The tailpipe emission rates for a species i (TP_i) are modeled as the fraction of the engine-out emission rates that leave the catalytic converter: $TP_i = EO_i \cdot CPF_i$, where CPF_i is the catalyst pass fraction. Hot-stabilized catalyst pass fractions are modeled in the literature in various ways as a function of the air-to-fuel ratio, the fuel rate, and/or the engine-out emissions. Catalyst pass fractions corresponding to cold-starts are modeled taking account also of the cumulative fuel consumption (as a surrogate for catalyst temperature) and the time elapsed since the beginning of the trip.

Alternatively to fuel rate, vehicle specific power (VSP) can be used as the principal variable in the load-based approach. VSP is equal to the tractive power divided by the vehicle mass. This is a variable generally used to evaluate and compare emissions from different measurement sources such as remote sensing, tunnel studies, chassis dynamometer, and on-board sensors (Jimenez et al., 1999). The EPA may use VSP (instead of FR) in its new generation model.

Theoretically, load-based models are adaptable to any vehicle with similar technologies and to any operating mode or vehicle condition, by adjusting their parameters. They have a detailed and flexible physical basis, which define the variables and parameters that should be included when modeling emissions. Moreover, they can take into account history effects and road grade. However, these models require knowledge of various vehicle specifications and a relatively complex modeling of the processes involved. Moreover, when applied to the entire flow of vehicles in a network over a period of time, the computational effort can be high.

In the rest of this section we give an overview of CMEM, a load-based model, which is gaining in popularity.

CMEM

CMEM (Comprehensive Modal Emissions Model) is a model developed at the University of California at Riverside and at the University of Michigan (Barth et al., 2000). The model has been calibrated using the National Cooperative Highway Research Program (NCHRP) vehicle emissions database, which was developed at UC Riverside (Barth et al., 2000). The database includes chassis dynamometer measurements of second-by-second speed, and engine-out and tailpipe emission rates of CO_2 , CO , HC and NO_x on three driving cycles: the FTP cycle, the US06 cycle, and an engineered cycle, called Modal Emission Cycle (MEC01). The chassis dynamometer tests were conducted on more than 300 automobiles and light trucks divided in 26 vehicle/technology categories. A more detailed description of the database is presented Section 4.2.1.

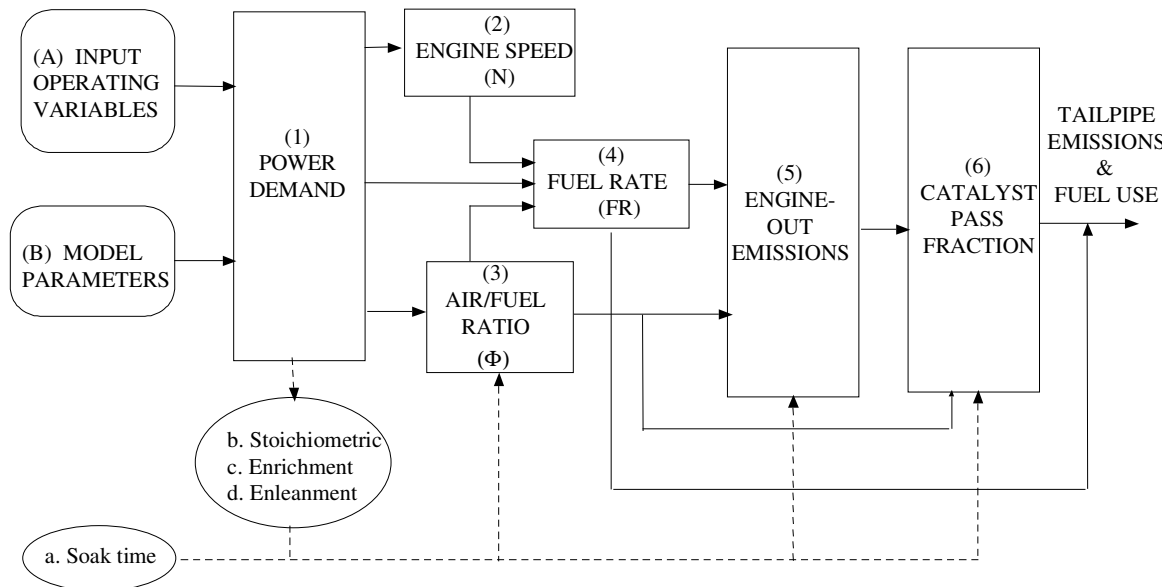


Figure 3-1: CMEM structure (from Barth et al., 2000).

As shown in Figure 3-1, CMEM is composed of six modules (depicted in square boxes): (1) power demand, (2) engine speed, (3) air/fuel ratio, (4) fuel rate, (5) engine-out emissions, and (6) catalyst pass fraction. The user specifies the composition of the vehicle fleet and, for each vehicle, its category and second-by-second speed trajectory. Optionally, soak time, acceleration, road grade, and accessory use can be specified. CMEM estimates second-by-second fuel consumption and tailpipe emission rates of CO , HC , NO_x , and CO_2 . The model represents stoichiometric, cold-start, enrichment, and enleanment conditions. At a

given moment, the model determines which of these conditions the vehicle is operating in, by comparing the vehicle power demand with thresholds. The model represents also cold and intermediate soak time starts.

CMEM was calibrated for the 26 vehicle/technology categories, using FTP bag 1 and bag 2 and MEC01 data. It was validated using FTP bag 3 and US06 data (Barth et al., 2000; Schultz et al., 2001).

3.2 Integrated Traffic and Emission Models

In this section, we give an introduction on the topic of integration between traffic and emission models, and we report some examples from the recent literature.

In the literature there are varieties of traffic models and emission models.

As discussed in Section 1.1.2, traffic models can be static or dynamic. The latter models can differ from the traffic representation standpoint, and have different limitations on the spatial and temporal scales that can be represented.

As discussed in Section 3.1, vehicle emission models can be more aggregate (average speed-based or static models) or more detailed (dynamic models). The latter models can use instantaneous or modal variables.

The integration between traffic and emission models can be done at various levels. Spatial aggregation, temporal scale, and vehicle aggregation characterize the integration. The choice of the level of detail depends on the objective behind the use of the models (i.e. regional transportation planning vs. design of local traffic control measures), and on other constraints such as data availability and computational time requirement.

Average speed-based emission models are usually combined with static traffic models. Sometimes, for large-scale inventory analysis applications, no traffic model is used, and *VKT* (or *VMT*) determined from driver surveys are used as input to the emission model. Although these models cannot provide a disaggregate and accurate output, they are commonly used for transportation planning purposes due to their relative simplicity. To represent time variability, the same combination of models can be applied on a time of the day basis.

Recently research efforts have been made to integrate models that use time-dependent speeds and accelerations.

Dynamic macroscopic (or mesoscopic) traffic models can be used to generate time-dependent link flows and speeds. In order to feed the emission model with vehicle speeds and accelerations, various approaches can be used. It is possible for example to apply a

spatial distribution of speeds and/or accelerations, consisting of facility-based driving cycles or statistical distributions.

When the needed input data are available and the scale of the application is not such that the computational effort becomes excessive, a traffic microsimulator can be integrated with an instantaneous emission model in a straightforward fashion. The traffic model generates time-dependent speeds and accelerations for each vehicle, which constitute the input to the emission model.

In the following paragraphs, we briefly describe some examples of efforts to integrate dynamic traffic and emission models.

Models in the DIANA project

The aim of the DIANA (Development of integrated air pollution modeling systems for urban planning) project is to create a comprehensive traffic emissions modeling system. In (Niittymaki et al., 2001) the traffic microsimulation model HUTSIM and its emission calculation sub-program, both developed by the Helsinki University of Technology (Kosonen, 1999), are integrated with an atmospheric street dispersion model developed by the Finnish Meteorological Institute (Berkowicz, 1997). The emission sub-module calculates fuel consumption and emissions of NO_x , NO_2 , and CO using a VA lookup table for cars and vans (length < 8m), and a lookup table for buses and trucks.

CMEM and the ITEM framework

Researchers at the University of California at Riverside developed various applications of their emission model CMEM. They proposed ITEM (Integrated Transportation/Emissions Model), a modeling framework designed to integrate CMEM with a hybrid macroscopic/microscopic architecture of traffic models (Barth, 1998). By combining a macroscopic traffic assignment model with a set of microscopic simulation models (organized by roadway facility type), both regional and local emission inventories are estimated. The primary component of ITEM is a macroscopic traffic assignment model that can dynamically determine link densities and speeds for a regional network. This component provides input into microscopic simulation sub-models that incorporate detailed emissions data for the particular case they simulate. The macroscopic and microscopic components are set up to run in parallel.

An integration of CMEM with a microscopic traffic model, PARAMICS, is presented in (Malcom et al., 2001). The integrated modeling tool was validated with real-world traffic

and emissions data from existing tunnel studies. The average predicted speeds and NO_x emissions were slightly higher than the field measurements. Results for CO and HC emissions, and fuel consumption were still being analyzed at the time of the study.

Another application of CMEM is presented in Barth et al. (1999b) and in Barth et al. (2000). As mentioned in Section 3.1.2, a set of facility-specific driving cycles was developed by the EPA to reproduce the driving characteristics of a wide range of roadway types and congestions levels (Sierra Research, 1997). CMEM was applied to these cycles to obtain facility-specific emission factors for every vehicle category. These factors could be applied to traffic models that predict traffic flow and congestion conditions for the network links.

MEASURE

MEASURE (Mobile Emissions Assessment System for Urban and Regional Evaluations), developed by the researchers of the Georgia Institute of Technology, is an aggregated traffic emission model that uses large databases and the GIS technology (Bachman et al., 2000). The model has been implemented for the metropolitan area of Atlanta.

MEASURE does not include a proper traffic simulation model, in the sense that vehicles are not tracked through the network. Instead, empirical statistical distributions of vehicle activity by facility type are used. The modules presented in Bachman et al. (2000) are based on statistical analysis of real-world data, and are integrated on an hour of the day basis. More details follow.

Fleet composition and vehicle activity in terms of modal variables are generated for the principal network and for the local roads. Modal variables distributions are defined as a function of road type, level of service, and other Highway Capacity Manual parameters with the following method. Congestion level is estimated from traffic volume and road capacity. Then the model uses speed and acceleration distribution tables (available for interstate highways, ramps, arterials, and signalized intersections) to estimate the modal activities.

At this point, emissions for each link and sub-zone are estimated. For example, the total emissions of a single link are calculated using the expression:

$$E_i = \sum_{c \in C_i} (TG_c \cdot B_c \cdot I_c) \cdot F_i \cdot T$$

where: C_i denotes the vehicle categories defined for the species i , TG_c is the fraction of registered vehicles on the road in category c , B_c is the mean FTP bag 2 emission rate in g/s for category c , F_i is the normalized emission factor for species i derived with the emission model described in the Section 3.1.3.2 (or with other models), I_c denotes the interaction

factor for category c and the estimated modal conditions, and T is the total travel time for that road link.

In addition, engine start emissions are estimated using aggregate zonal information.

Finally, the GIS support is loaded with the estimated emissions that can be used as input to air quality models.

Integration of emission models with VISSIM

PTV is a German company that offers software for transportation modeling. In Fellendorf (1999) the following set of models has been integrated. (1) A traffic demand model (VISEM) that includes: traffic generation, traffic distribution, and mode choice. The output is the set of individual trip chains within one day in the study area. (2) A microscopic traffic model (VISSIM), in which the individual vehicles are moved according to a car following model for longitudinal vehicle movements and a rule-based algorithm for lateral movements, plus special driving maneuvers. (3) A dynamic traffic assignment model to represent route choice. The traffic assignment algorithm applies iteratively the microscopic traffic model. (4) Emission maps of CO , HC , and NO_x emissions for passenger cars and heavy trucks. To improve the accuracy of the emission maps in hot-stabilized operating conditions, 'dynamic correction factors' are applied to the emission maps. These factors depend on kinematic variables such as the number of changes from positive to negative accelerations, idling portions, and mean acceleration values. For cold-start conditions, two approaches, one developed by the TÜV Rheinland and one developed by the Volkswagen Group Research Department, are discussed and compared. To the best of our knowledge, these emission models are not publicly available.

The microscopic model VISSIM has been integrated with other emission models.

In Young Park et al. (2001) VISSIM was combined with MODEM (described in Section 3.1.3.1), and with a simple Gaussian dispersion model. Pollutant concentrations were calculated with this combined model for a real local network using data from the SCOOT urban traffic control system (Hunt et al., 1991). The results were compared with on-road measurements and macroscopic estimates obtained with the UK Design Manual for Road and Bridges model (UKDOT, 1995). The two models gave similar results but showed significant errors from the field measurements.

The integration of VISSIM with a load-based model is presented in Nam et al. (2002). The emission model is derived from CMEM, with the introduction of an air conditioning module. The integrated model was validated by comparing its output in a modeled network

with the emissions measured on-board a vehicle driving through the real-world network. Larger scale comparisons are still under development.

TRANSIMS

TRANSIMS (TRansportation ANalysis and SIMulation System), developed by Los Alamos National Laboratory, is an integrated system of models (Los Alamos National Laboratory, 2002). It is part of the Travel Model Improvement Program sponsored by the US Department of Transportation, the Environmental Protection Agency, and the Department of Energy. The model has been implemented for the city of Portland, Oregon.

TRANSIMS defines a framework and provides some tools that can be directly used by analysts. The framework includes the following modules: population synthesizer, household and commercial activity generator, route planner, traffic simulator, emissions estimator, and output visualizer.

In Williams et al. (1999) the integration between the traffic and the emissions modules is explained. In the traffic simulation module, the transportation network is discretized into 7.5 meters long cells (cellular automata). The model can be viewed as a hybrid between a mesoscopic and a microscopic model. Due to the spatial discretization, the speed is defined in 16 mph ranges. Since the emission module requires a finer resolution, the vehicle trajectories are smoothed using frequency distributions of the product speed times acceleration ($v \cdot a$) using the so-called 'three-cities data' (EPA, 1993). This results in speed and acceleration values, which are clustered in bins, for all vehicles.

The emission module has three sub-modules: an evaporative module, a light-duty tailpipe module, and a heavy-duty tailpipe module.

The light-duty tailpipe module uses CMEM (see Section 3.1.3.3) to populate emission maps with bins of 2 mph for the speed, and 1.5 foot per second squared for the acceleration. Tailpipe emissions of CO_2 , CO , HC , and NO_x , and fuel consumption on 30 meters long road segments for 15 minutes time periods are calculated using the traffic model, the distribution of accelerations, and the emission maps.

The emission module can be combined with the EPA's MODELS-3 (<http://www.epa.gov/asmdnerl/models3/>) to produce three-dimensional hourly gridded emissions over the metropolitan area. MODELS-3 includes a meteorology model and an air-chemistry and dispersion model.

3.3 Conclusions

Although not exhaustive, our review reveals that traffic emissions modeling constitutes a challenging and multifaceted area of research.

As regards emissions modeling, it has been recognized that average speed-based models are too simple and aggregate. In the last decade, research efforts have focused on dynamic emissions modeling, which is based on instantaneous or modal vehicle variables, such as speed and acceleration. The principal approaches for dynamic emissions modeling are the emission maps, the regression-based approach, and the load-based approach.

Although easy to build and use, emission maps have several limitations. They can be sparse and sensitive to the driving cycle used to populate them. Moreover, they are usually not flexible enough to account for such factors as road grade, accessory use, or history effects.

Regression-based models are relatively easy to calibrate, and typically run fast. However, they can lack a physical interpretation, when using explanatory variables that are not derived from a physical basis. Moreover, in some cases the number of explanatory variable is excessive, causing the risk of over-fitting the calibration data. Therefore these models can give non-desirable results if applied to situations not covered by the calibration data.

Load-based models have a detailed and flexible physical basis and can take into account history effects and road grade. However, these models require knowledge of various vehicle specifications and a relatively complex modeling of the processes involved. Moreover, they require higher computational times.

We conclude that there is need of models that are simultaneously simple to calibrate in various situations, give reasonably accurate results and can run fast. Based on these objectives, in Chapter 4 of this thesis we develop a model that combines the regression-based and load-based approaches and captures some of their respective advantages.

We presented examples of integration of dynamic emission models with both microscopic and non-microscopic dynamic traffic models. Microscopic traffic models can be integrated directly with dynamic emission models and examples of this integration are well represented in the literature. On the contrary, to the best of our knowledge, there are few examples of integration involving non-microscopic traffic models. As discussed in Chapter 1, non-microscopic traffic models have some advantages (such as better computational speeds and easier calibration) that make them more suitable for large-scale applications. Therefore, we

believe that it is valuable to investigate further the integration of emission models with non-microscopic traffic models.

The few examples found in the literature include TRANSIMS, the approach presented in Dion et al. (1999), and ITEM, introduced in Barth (1998). While the approaches used in those cases are valuable for particular applications, they do not generally allow for the integration of dynamic emission models with any non-microscopic dynamic traffic model. In Chapter 5 of this thesis, we propose a probabilistic approach for the integration of dynamic emission models and any type of non-microscopic dynamic traffic models. The proposed approach can be adopted in applications where non-microscopic models are typically used, such as the analysis of large-scale networks and the solution of non-operational (such as planning) application problems.

Chapter 4

A Statistical Model of Vehicle Emissions and Fuel Consumption

From the literature review of emission models described in Chapter 3, it is possible to draw the following observations. First, emission maps are not satisfactory because they can be cycle dependent, sparse, and not flexible enough to account for history effects, accessory usage and road grade. Second, regression-based models often lack a clear physical interpretation and tend to overfit the calibration data using arbitrary numbers and combinations of explanatory variables. Third, load-based models have a detailed and flexible physical basis, but are more complex to design and calibrate, and can be computationally intensive.

Consequently, we believe, it is valuable to design a simple model that, in addition of giving results with reasonable accuracy, can run fast and is easy to calibrate in various situations. The latter property is useful as emission models are more likely to be recalibrated as fleet compositions differ in real world. For instance, vehicle fleet compositions vary from city to city and country to country, as well as over time.

This chapter presents a new model for instantaneous emissions and fuel consumption of light-duty vehicles, referred to here as EMIT⁵.

The chapter is organized as follows. Section 4.1 presents the structure of the model. Section 4.2 describes the analysis and the preprocessing of the data used for the model development. The description of the data precedes the description of the model because the data is used to verify some assumptions during the development of the model. Section 4.3 presents the derivation from the load-based approach and the development of the model (notation, rationale, simplifying assumptions, and formulation). The model was calibrated

⁵ The preliminary results of the model are published in Cappiello et al. (2002).

and validated for two vehicle/technology categories. Sections 4.4 and 4.5 present respectively the calibration and the validation results. Section 4.6 gives conclusions and outlines directions for future research.

4.1 Model Structure

We have developed an emission model referred to here as EMIT (EMISSIONS from Traffic). It is a simple statistical model (with a basis in the physical system) for instantaneous emissions and fuel consumption of light-duty composite vehicles. In order to realistically reproduce the behavior of the emissions, the explanatory variables in EMIT have been derived from the load-based approach, using some simplifying assumptions. The model, due to its simple structure, is relatively easy to calibrate and is expected to require less computational time than load-based models.

Figure 4-1 depicts a block diagram of the structure of EMIT. EMIT is composed of two main modules: the engine-out emissions module and the tailpipe emissions module. Although implementing two modules adds a level of complexity to the model, this allows EMIT to predict not only tailpipe, but also its precursor engine-out emissions. This property of the model is useful in practice. For instance, it allows for the modeling of engine and catalyst technology improvements, vehicle degradation, as well the implications of effectiveness of inspection and maintenance programs. Moreover, it allows for modular and incremental modeling, by identifying model parts that would require improvements, and thus further research.

Given a vehicle category and its second-by-second speed and acceleration, the first module predicts the corresponding second-by-second fuel consumption and engine-out emission rates. These, in turn, are the inputs for the next module that predicts second-by-second tailpipe emission rates. Although the present thesis considers only the modeling of fuel consumption and emissions of CO_2 , CO , HC , and NO_x for gasoline light-duty vehicles, we note that the methodology developed can be applied to the study of other pollutants, such as PM , and diesel vehicles.

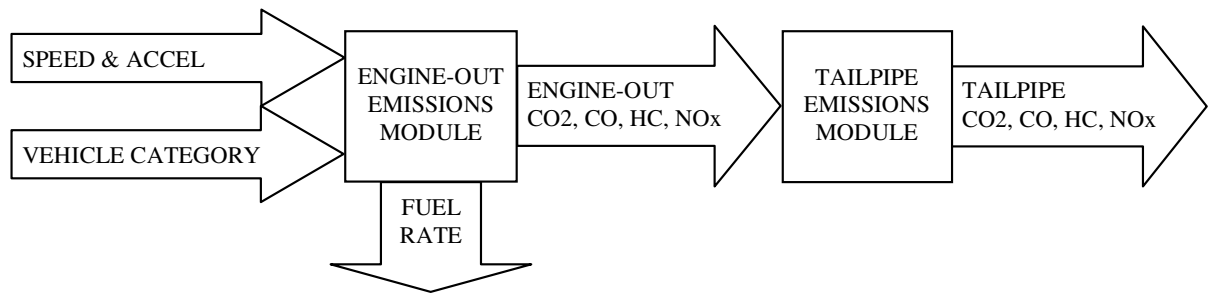


Figure 4-1: EMIT structure.

4.2 Data

4.2.1 The NCHRP Database

The data used for the development, calibration and validation of EMIT is the National Cooperative Highway Research Program (NCHRP) vehicle emissions database, which consists of data relative to chassis dynamometer tests conducted at the College of Environmental Research and Technology, University of California at Riverside, between 1996 and 1999. The NCHRP database was used in the development of CMEM and of other emission models (see Section 3.1.3). The purpose of this section is to provide the principal information on the database. A complete description of the database and the dynamometer testing procedure can be found in Barth et al. (2000).

The database includes measurements of second-by-second speed and engine-out and tailpipe emission rates of CO_2 , CO , HC , and NO_x for 344 light-duty vehicles (202 cars and 142 light trucks). For a limited number of vehicles the measurements of engine speed, throttle position, mass air flow, emission control temperature, gear, and other quantities are also included. Only speed and emissions data are needed in the development of EMIT.

For the development of the NCHRP database, a total of 26 vehicle/technology categories were defined in terms of fuel and emission control technology, accumulated mileage, power-to-weight ratio, emission certification level, and, finally, by normal or high emitter status. In the sequel of this thesis, we use the simplifying terminology of vehicle category to refer to a vehicle/technology category. The vehicles were randomly recruited, principally in California. For each vehicle category, the sample size was determined based on the approximate percentage contribution of that category to the emissions inventory. The vehicles were tested on chassis dynamometer using three driving cycles: the standard FTP cycle, the high-speed aggressive US06 cycle, and the Modal Emission Cycle (MEC01), an engineered aggressive cycle. The FTP and the US06 are cycles prescribed by the EPA for

regulation purposes, and are described in Section 2.1.1. The MEC01 cycle was designed at UC Riverside for the development of the NCHRP database and the CMEM model. We describe the MEC01 cycle in the following paragraph.

The MEC01 cycle was designed with the purpose of covering the speed, acceleration, and specific power ranges typical of most light-duty vehicles. The cycle was designed in three successive versions, labeled version 5, 6, and 7. Version 5, which is significantly different from the successive versions, was used for the first 43 vehicles tested. The remaining vehicles were tested on version 6 or 7, which differ only after the first 900 seconds. Version 7 is depicted in Figure 4-2. It consists of five different sections: stoichiometric cruise, constant power, constant acceleration, scrambled cruise⁶, and air conditioning⁷. The total time of the test is 1,920 seconds (32 minutes), the highest speed is 80 mph (128 km/h), the average speed is approximately 43 mph (69 km/h), and the maximum specific power is 400 (mph)²/s (1,024 (km/h)²/s). The cycle represents driving conditions with higher speeds and harder accelerations than the FTP cycle, but its maximum specific power is less than that achieved by the US06 cycle.

The database does not contain the results of all tests. It contains only the data of tests that were successfully completed, since there were cases of vehicle failure. The most common reasons of failure were engine overheating or brake problems. Appendix A contains information about the vehicles contained in the database, including vehicle characteristics (e.g. vehicle name, model year, mass, odometer reading, etc.) and availability of test data. FTP data are available for all vehicles, MEC01 data are available for most vehicles, and US06 data are available for most cars and for a limited number of light trucks. Appendix A does not coincide with the vehicle testing summary reported in Barth et al. (2000). First, we corrected the information about the data availability based on the data actually present in the database distributed by UC Riverside. Second, we revised the vehicle classification, as described in Section 4.2.2.

⁶ The scrambled cruise section has the same cruise events as the stoichiometric cruise section (except the 50 mph event). The order of the cruise events is scrambled, so that each cruise event follows an opposite acceleration or deceleration event from the original stoichiometric cruise section.

⁷ The air conditioning section repeats the stoichiometric cruise section with the air conditioner on if the vehicle is equipped.

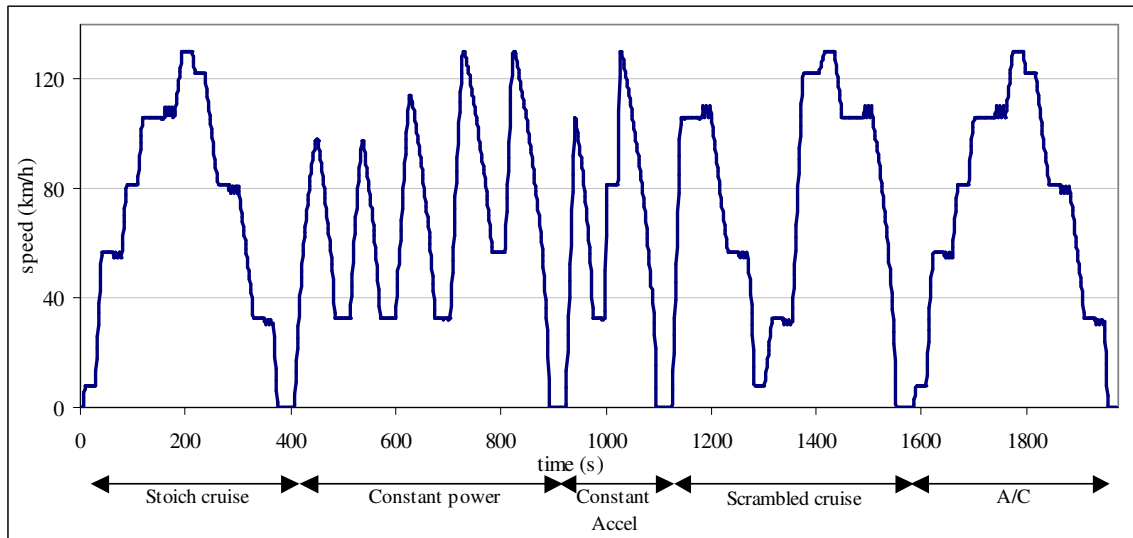


Figure 4-2: The MEC01 cycle.

4.2.2 Data Preprocessing⁸

The primary objective of EMIT is to predict emissions from average vehicles, each representative of a vehicle category, rather than from specific makes and models. Thus, for each category, the data were aggregated into composite vehicles data. A compositing procedure similar to that used in Barth et al. (2000) was implemented. The vehicle classification identified in Barth et al. (2000) was adopted with some minor modification. The original Category 22 (bad catalyst) includes both cars and trucks. We divided it into two separate categories, given the availability of a large number of vehicles. The other high emitters categories include both cars and trucks, as in the original classification. The classification of individual vehicles was partly revised, with particular attention to high emitters, which we considered misclassified in a number of cases. The revised classification is shown in Appendix A.

Only the vehicles for which both the FTP cycle and the MEC01 cycle (version 6 or 7) are available were considered. Table 4.1 shows for each category the number of vehicles based on the revised classification, and the number of vehicles used to obtain the composite vehicle data.

The compositing procedure is conducted as follows. For each vehicle category and for each driving cycle, the vehicle tests data are time-aligned by maximizing the R-square among the speed traces. This is performed by time shifting the data and/or cutting few

⁸ This work was done in collaboration with Edward Nam and Maya Abou Zeid.

seconds of data. Then, the average second-by-second speed and emission rates are calculated to create the composite vehicle data. Only the first 900 seconds of the MEC01 cycle (stoichiometric cruise and constant power sections) are averaged because, as mentioned above, versions 6 and 7 are different after the first 900 seconds.

Table 4.1: Number of vehicles for each vehicle/technology category.

Vehicle/Technology Category	Number of vehicles in the NCHRP database based on the revised classification	Number of vehicles used for the compositing procedure
<i>Normal Emitting Cars</i>		
1. No Catalyst	8	6
2. 2-way Catalyst	12	7
3. 3-way Catalyst, Carbureted	6	3
4. 3-way Catalyst, FI, >50K miles, low power/weight	25	15
5. 3-way Catalyst, FI, >50K miles, high power/weight	18	12
6. 3-way Catalyst, FI, <50K miles, low power/weight	16	11
7. 3-way Catalyst, FI, <50K miles, high power/weight	9	7
8. Tier 1, >50K miles, low power/weight	12	9
9. Tier 1, >50K miles, high power/weight	11	9
10. Tier 1, <50K miles, low power/weight	16	10
11. Tier 1, <50K miles, high power/weight	19	11
24. Tier 1, >100K miles	9	8
<i>Normal Emitting Trucks</i>		
12. Pre-1979 (<=8500 GVW)	6	4
13. 1979 to 1983 (<=8500 GVW)	8	4
14. 1984 to 1987 (<=8500 GVW)	11	8
15. 1988 to 1993, <=3750 LVW	24	20
16. 1988 to 1993, >3750 LVW	11	10
17. Tier 1 LDT2/3 (3751-5750 LVW or Alt. LVW)	17	13
18. Tier 1 LDT4 (6001-8500 GVW, >5750 Alt. LVW)	14	12
25. Gasoline-powered, LDT (> 8500 GVW)	9	8
40. Diesel-powered, LDT (> 8500 GVW)	10	9
<i>High Emitting Vehicles</i>		
19. Runs lean	11	8
20. Runs rich	7	6
21. Misfire	5	4
22car. Bad catalyst	21	16
22truck. Bad catalyst	19	14
23. Runs very rich	10	10
Total	344	254

Notes:

FI denotes fuel injection; GVW denotes gross vehicle weight; LVW denotes loaded vehicle weight.

Acceleration and fuel rate are two variables required in the development of the model, but not reported in the database.

We calculate acceleration as the variation between two consecutive second-by-second speeds.

We calculate fuel rate using the following carbon balance formula:

$$FR = [CO_2 / 44 + CO / 28] \cdot [12 + 1 \cdot 1.85] + HC \quad (4.1)$$

where numbers 44, 28, 12 and 1 are the molecular weights of CO_2 , CO , C , and H respectively, number 1.85 is the approximate number of moles of hydrogen per mole of carbon in the fuel, and CO_2 , CO , and HC are the measured engine-out emission rates. Basically, this formula derives the equivalent mass of hydrocarbon from the carbon balance of the emissions measurements (Goodwin, 1996; Hickman et al., 1999).

Other data used in the model are the following composite vehicle specification parameters: mass, rolling resistance coefficients, and air drag coefficient. These parameters were derived in Barth et al. (2000), by averaging the parameters of the single vehicles in each category.

In summary, the composite vehicle data used for the development of EMIT are: (1) second-by-second data from the dynamometer tests: speed, engine-out emission rate, tailpipe emission rate, and fuel rate (estimated from Equation 4.1), and (2) the following composite vehicle specific data: mass, rolling resistance coefficients, and air drag coefficient.

4.2.3 Categories Modeled in EMIT

At the time of writing this thesis, EMIT has been calibrated for the following two vehicle categories:

- category 7 (3-way Catalyst (“Tier 0” emission standard), fuel injection, less than 50,000 miles accumulated, and high power/weight ratio),
- category 9 (Tier 1 emission standard, more than 50,000 miles accumulated, and high power/weight ratio).

The characteristics of the vehicles used for the compositing procedure for vehicle categories 7 and 9 are presented in Tables 4.2 and 4.3.

Because fuel-to-air ratio is not modeled explicitly, EMIT is calibrated using data that cover a large spectrum of operating conditions, including stoichiometric, enrichment and enleanment conditions, in order to capture the emissions variability. The following set of hot-stabilized composite data are used for the calibration (see Section 4.4): (a) FTP bag 2,

(b) FTP bag 3, excluding the first 100 seconds (to account for the catalyst light-off time), and (c) first 900 seconds of the MEC01 cycle. The US06 cycle is used to validate the model (Section 4.5). Cold-start conditions are not modeled but can be easily added in a future development, as discussed in Section 4.6.

Table 4.2: Vehicles used for the category 7 composite vehicle.

Vehicle ID	Model name	Model year	Mass (lb)	Odometer (miles)
126	Suzuki Swift	92	2,125	48,461
136	Nissan 240SX	93	3,125	43,009
147	Mazda Protege	94	2,875	40,201
169	Mercury Tracer	81	2,500	6,025
248	Saturn SL2	93	2,500	42,264
257	Nissan Altima	93	3,250	32,058
259	Honda Accord LX	95	3,000	49,764

Table 4.3: Vehicles used for the category 9 composite vehicle.

Vehicle ID	Model name	Model year	Mass (lb)	Odometer (miles)
187	Toyota Paseo	95	2,375	56,213
191	Saturn SL2	93	2,625	63,125
192	Honda Civic DX	94	2,375	57,742
199	Dodge Spirit	94	3,000	57,407
201	Dodge Spirit	94	3,000	56,338
229	Honda Civic LX	93	2,625	61,032
242	Saturn_SL2	94	2,625	64,967
260	Toyota Camry LE	95	4,000	51,286
281	Honda Accord EX	93	3,250	72,804

4.3 Model Development

In this section the engine-out and tailpipe emissions modules are derived from the load-based approach (which is introduced in Section 3.1.3.3).

4.3.1 The Engine-Out Emissions Module

Let i denote the generic emission species (i.e. $i = CO_2, CO, HC, NO_x$). Let EO_i denote the engine-out emission rate of species i in g/s, and EI_i the emission index for species i , which is the mass of emission per mass unit of fuel consumed. By definition of EI_i , engine-out emission rates are given by:

$$EO_i = EI_i \cdot FR \quad (4.2)$$

where FR denotes the fuel consumption rate (g/s).

The following paragraphs describe how FR and EI_i are modeled in a typical load-based formulation.

When the engine power is zero, the fuel rate is equal to a typically small constant value. Otherwise, fuel consumption is mainly dependent on the engine speed and the engine power. This is modeled as follows:

$$FR = \begin{cases} \phi \cdot \left(K \cdot N \cdot V + \frac{P}{\eta} \right) & \text{if } P > 0 \\ K_{idle} \cdot N_{idle} \cdot V & \text{if } P = 0 \end{cases} \quad (4.3)$$

where:

ϕ : fuel-to-air equivalence ratio, which is the ratio of the actual fuel-to-air mass ratio to the stoichiometric fuel-to-air mass ratio. When $\phi \cong 1$, the mixture is stoichiometric. When $\phi > 1$, the mixture is rich. When $\phi < 1$, the mixture is lean.

K : engine friction factor (kJ/rev/liter),

N : engine speed (rev/s),

V : engine displacement (liters),

η : engine indicated efficiency,

K_{idle} : constant idle engine friction factor (kJ/rev/liter),

N_{idle} : constant idle engine speed (rev/s),

P : engine power output (kW).

The fuel-to-air equivalence ratio ϕ can be modeled for enleanment, stoichiometric, and enrichment conditions. When engine power is equal to zero, the mixture becomes lean, due to fuel shut-off. Since emissions are not very sensitive to the level of enleanment (except for a fraction of the high emitters), in enleanment conditions it is reasonable to approximate ϕ by a constant. In enrichment conditions, ϕ is a function of engine power and acceleration, but is usually modeled in terms of engine power (or torque) only. When engine power (or torque) is greater than an enrichment threshold, the mixture goes rich. Such a threshold can be modeled in terms of specific power and vehicle parameters. Above the threshold, ϕ can be modeled as a linear function of engine power. When engine power (or torque) is positive but less than the enrichment threshold, the mixture is considered stoichiometric. More details of a model of the fuel-to-air equivalence ratio are described in Barth et al. (2000).

To link the engine speed N to the wheel speed v , a transmission model is necessary. This can be modeled in a limited fashion as function of vehicle speed, gear shift schedule, gear ratio, and engine peak torque (Thomas and Ross, 1997; Barth et al., 2000).

The engine friction factor K can then be modeled as function of engine speed (Barth et al., 2000).

Engine power is modeled as:

$$P = \frac{P_{tract}}{\varepsilon} + P_{acc} \quad (4.4)$$

where:

P_{tract} : total tractive power requirement at the wheels (kW),

ε : vehicle drivetrain efficiency,

P_{acc} : engine power requirement for accessories, such as air conditioning.

The drivetrain efficiency ε depends on engine speed and engine torque. It can be approximated as a function of vehicle speed and specific power, as discussed in Barth et al. (2000).

When positive, the tractive power is given by:

$$P_{tract} = A \cdot v + B \cdot v^2 + C \cdot v^3 + M \cdot a \cdot v + M \cdot g \cdot \sin \vartheta \cdot v \quad (4.5)$$

where:

v : vehicle speed (m/s),

a : vehicle acceleration (m/s²),

A : rolling resistance coefficient (kW/m/s),

B : speed correction to rolling resistance coefficient (kW/(m/s)²),

C : air drag resistance coefficient (kW/(m/s)³),

M : vehicle mass (kg),

g : gravitational constant (9.81 m/s²),

ϑ : road grade (degrees).

When the right hand side of Equation 4.5 is non-positive, P_{tract} is set equal to zero. All parameters (A , B , C , and M) are known and readily available for each vehicle.

In conclusion, FR can be modeled as function of v , a , ϑ , P_{acc} , and known vehicle parameters, since all other variables in Equations 4.3, 4.4, and 4.5 (ϕ , K , N , P , and ε) can be expressed in terms of v , a , ϑ , and P_{acc} , and vehicle parameters. The vehicle parameters are available from vehicle manufacturers or can be calibrated.

Emission indices EI_i are modeled in the literature in various ways as a function of ϕ (Thomas and Ross, 1997; Barth et al., 2000), or ϕ and FR (Goodwin, 1996). However, generally, as more fuel is burned, more emissions are formed. As a result, to first approximation EO_i is a linear function of FR :

$$EO_i = \lambda + \mu \cdot FR \quad (4.6)$$

Figures 4-3 and 4-4 show the trends of engine-out emission rates versus fuel rate for the vehicle categories modeled in EMIT. With the exception of *CO*, the trend is approximately linear, though sometimes somewhat scattered. *CO* presents a linear trend for low to medium values of *FR*, and increases more rapidly for larger values of *FR* corresponding to the enrichment conditions.

EMIT has been developed and calibrated for hot-stabilized conditions with zero road grade ($\vartheta = 0$), and without accessory usage ($P_{acc} = 0$). The model does not represent history effects, such as cold-start emissions and hydrocarbon enrichment puffs (see Section 2.2 for a description of these phenomena). These factors can be included in future developments, as discussed in Section 4.6. Nevertheless, considering only hot-stabilized conditions is not a critical limitation for highway applications, since most vehicles are hot by the time they reach the highways. Moreover, the hydrocarbons puffs do not significantly affect tailpipe emissions in normal emitting vehicles, since the catalytic converter is usually effective under enrichment conditions (An et al., 1998).

The following are assumptions adopted in the development of EMIT:

- Although, as discussed, ϕ , K , N , and ε can be expressed in various functional forms of v and a , their effects on fuel rate can be aggregated into the effects of v , v^2 , v^3 , and $a \cdot v$, which are the independent variables in Equation 4.5.
- Since emission rates can be approximated as a linear function of fuel rate (Equation 4.6), the variables that govern emission rates are the same variables that govern fuel rate.
- Since in this thesis we do not consider accessory usage ($P_{acc} = 0$), P_{tract} is used as a surrogate for P to test if the vehicle is in idle mode.

Given the previous assumptions, combining Equations 4.3, 4.4, and 4.5, we have:

$$FR = \begin{cases} \alpha_{FR} + \beta_{FR}v + \gamma_{FR}v^2 + \delta_{FR}v^3 + \zeta_{FR}av & \text{if } P_{tract} > 0 \\ \alpha'_{FR} & \text{if } P_{tract} = 0 \end{cases} \quad (4.7a)$$

$$(4.7b)$$

and, from Equation 4.6:

$$EO_i = \begin{cases} \alpha_i + \beta_i v + \gamma_i v^2 + \delta_i v^3 + \zeta_i av & \text{if } P_{tract} > 0 \\ \alpha'_i & \text{if } P_{tract} = 0 \end{cases} \quad (4.8a)$$

$$(4.8b)$$

where P_{tract} is calculated with Equation 4.5, using A , B , C , and M from Barth et al. (2000).

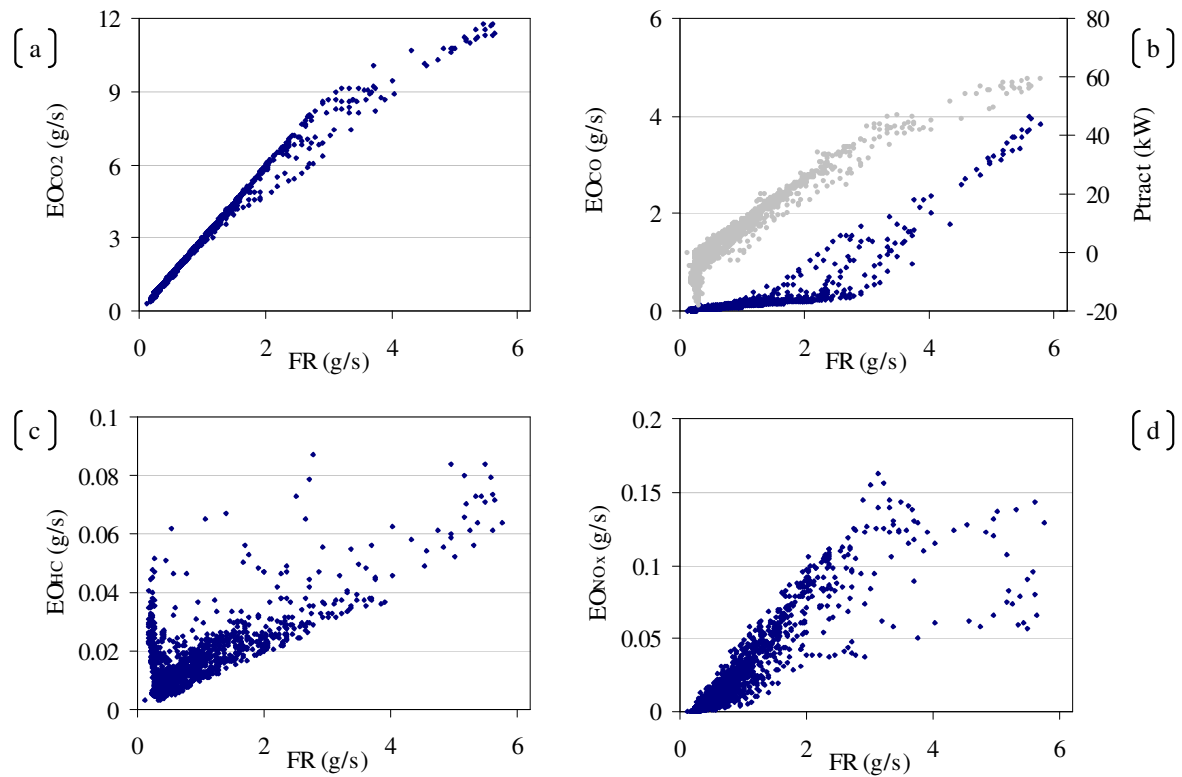


Figure 4-3: Category 7 – Engine-out emission rates versus fuel rate. Fuel rate is estimated with Equation 4.1. In Figure b, in addition to CO engine-out, tractive power (in gray) is represented versus fuel rate.

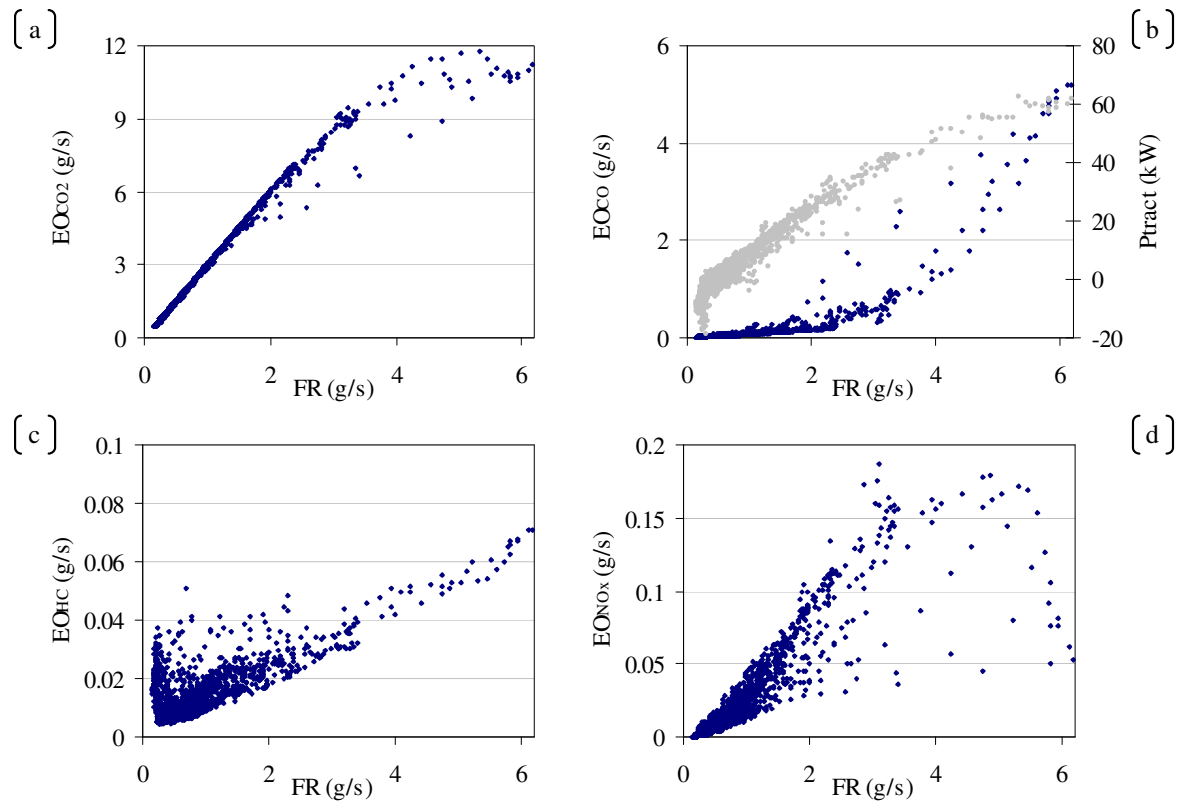


Figure 4-4: Category 9 – Engine-out emission rates versus fuel rate. Fuel rate is estimated with Equation 4.1. In Figure b, in addition to CO engine-out, tractive power (in gray) is represented versus fuel rate.

For CO , the effect of enrichment is too distinct to be incorporated in the same equation, as seen in Figures 4-3b and 4-4b. For enrichment conditions the emissions are modeled as a linear function of the corresponding stoichiometric emissions:

$$EO_{CO} = \begin{cases} EO_{CO}^{stoich} = \alpha_{CO} + \beta_{CO}v + \delta_{CO}v^3 + \zeta_{CO}av & \text{if } 0 < P_{tract} \leq P_{tract}^{enrich} & (4.9a) \\ \kappa + \chi \cdot EO_{CO}^{stoich} & \text{if } P_{tract} > P_{tract}^{enrich} & (4.9b) \\ \alpha'_{CO} & \text{if } P_{tract} = 0 & (4.9c) \end{cases}$$

The enrichment threshold P_{tract}^{enrich} is determined empirically based on the cut-point in the trend of EO_{CO} versus FR (see Figures 4-3b and 4-4b).

Equations 4.7, 4.8 and 4.9 are calibrated for each vehicle category using least square linear regressions.

4.3.2 The Tailpipe Emissions Module

Tailpipe emission rates TP_i (g/s) are modeled as the fraction of the engine-out emission rates that leave the catalytic converter:

$$TP_i = EO_i \cdot CPF_i \quad (4.10)$$

where CPF_i denotes the catalyst pass fraction for species i .

Catalyst efficiency is difficult to predict accurately, and varies greatly from hot-stabilized to cold-start conditions. As stated previously, at this time cold-start conditions are not considered.

Hot-stabilized catalyst pass fractions are modeled in the literature in various ways as a function of ϕ , FR , and/or engine-out emissions (Barth et al., 2000; Goodwin, 1996). Since the physical and chemical phenomena that control catalyst efficiency are challenging to capture, often these functions are purely empirical.

EMIT calculates:

- The tailpipe CO_2 (which is not much different from engine-out CO_2), directly using the equations:

$$TP_{CO_2} = \begin{cases} \alpha_{CO_2} + \beta_{CO_2}v + \gamma_{CO_2}v^2 + \delta_{CO_2}v^3 + \zeta_{CO_2}av & \text{if } P_{tract} > 0 & (4.11a) \\ \alpha'_{CO_2} & \text{if } P_{tract} = 0 & (4.11b) \end{cases}$$

- The tailpipe CO , HC and NO_x with Equation 4.10. The catalyst pass fractions are modeled empirically as piecewise linear functions of engine-out emission rates under different operating regimes. The most general function is composed of three pieces:

$$CPF_i = \begin{cases} m'_i \cdot EO_i + q'_i & \text{if } 0 \leq EO_i < z'_i \\ m''_i \cdot EO_i + q''_i & \text{if } z'_i \leq EO_i < z''_i \\ m'''_i \cdot EO_i + q'''_i & \text{if } EO_i \geq z''_i \end{cases} \quad (4.12)$$

4.4 Model Calibration

4.4.1 Engine-out Emissions Module

Previous calibration of Equation 4.7a indicates that the coefficient of v^2 is negative, which is counterintuitive, but not statistically significant. This second order speed term is expected to be small, since it mainly represents a higher order correction to the rolling resistance term. The term in v^2 is then dropped in the calibration process. Dropping it, the goodness of fit of the regression is practically unaffected (adjusted R-squared~0.96) and all coefficients are positive and statistically significant.

All regressions of Equations 4.8 give satisfactory results in terms of statistical significance as well as adjusted R-squared. For Equation 4.9a, it is necessary to employ a more ‘robust’ calibration, by removing a few outliers (~3% of the data) from the calibration data. For HC , the emissions puffs are omitted in the calculation of α' .

The calibrated parameters are shown in Tables 4.4 and 4.5. Engine-out emission rates (EO_i) are expressed in g/s, vehicle speed (v) is expressed in km/h, speed times acceleration (av) is expressed in m^2/s^3 , and power is expressed in kW.

We note the following:

- All coefficients have a high t-statistics, except for β_{HC} in both categories, and β_{CO} in category 9, which have been dropped.
- All coefficients are, as expected, positive, except for α_{NOx} in both categories and β_{CO} in category 7. The negative sign of α_{NOx} is consistent with the negative intercept of the trend of NO_x shown in Figures 4-3d and 4-4d.

Table 4.4: Category 7 – Calibrated parameters for the engine-out emissions module (Equations 4.7, 4.8, and 4.9). The t-statistics are reported in parentheses.

	CO ₂	CO	HC	NO _x	FR
α	.907 (42.9)	.0633 (21.2)	.0108 (23.1)	-.00522 (-5.2)	.326 (26.3)
β	.0136 (24.4)	-3.43 e-04 (-4.2)	(dropped)	.00038 (14.4)	.00228 (6.9)
δ	1.86e-06 (53.8)	1.73 e-07 (30.9)	1.20e-08 (15.6)	1.64e-08 (10.8)	9.42e-07 (46.2)
ζ	.231 (216.3)	.00977 (43.5)	.00124 (52.3)	.00282 (55.9)	.0957 (152.4)
α'	.862	.0369	.00552	.00326	.300
κ		-3.66 (-11.2)			
χ		12.5 (16.4)			
P_{tract}^{enrich}		30			

Table 4.5: Category 9 – Calibrated parameters for the engine-out emissions module (Equations 4.7, 4.8, and 4.9). The t-statistics are reported in parentheses.

	CO ₂	CO	HC	NO _x	FR
α	1.02 (40.8)	.0316 (22.8)	.00916 (58.1)	-.00391 (-3.7)	.365 (26.1)
β	.0118 (20.7)	(dropped)	(dropped)	.000305 (11.4)	.00114 (6.5)
δ	1.92e-06 (48.4)	1.09e-07 (49.9)	7.55e-09 (33.3)	2.27e-08 (14.0)	9.65e-07 (44.0)
ζ	.224 (195.5)	.00883 (43.0)	.00111 (60.5)	.00307 (64.9)	.0943 (150.3)
α'	.877	.0261	.00528	.00323	.299
κ		-6.10 (-14.3)			
χ		21.8 (18.9)			
P_{tract}^{enrich}		34			

4.4.2 Tailpipe Emissions Module

Equation 4.11 is calibrated for each vehicle category using least square linear regressions. The calibrated parameters are shown in Table 4.6. Engine-out emission rates (EO_i) are expressed in g/s, vehicle speed (v) is expressed in km/h, speed times acceleration (av) is expressed in m^2/s^3 , and power is expressed in kW.

Equation 4.12 is calibrated for CO , HC and NO_x by minimizing the sum of the squared differences between the predicted and measured tailpipe emission rates. The predicted tailpipe emission rates are obtained as the product of the modeled catalyst pass

fraction and the measured engine-out emission rates (to minimize error propagation). The catalyst pass fraction functions are represented in Figure 4-5. The calibrated coefficients are reported in Tables 4.7 and 4.8.

Table 4.6: Categories 7 and 9 – Calibrated parameters for the tailpipe CO₂ emissions module (Equation 4.11). The t-statistics are reported in parentheses.

	Category 7	Category 9
α	1.01 (41.49)	1.11 (47.0)
β	0.0162 (25.22)	0.0134 (19.3)
δ	1.90e-06 (47.62)	1.98e-06 (47.0)
ζ	0.252 (205.18)	0.241 (42.0)
α'	0.985	0.973

Table 4.7: Category 7 – Calibrated parameters of the catalyst pass fraction functions (Equation 4.12).

m'_{CO}	0.927	q'_{CO}	0.048	z'_{CO}	0.816
m''_{CO}	0.0538	q''_{CO}	0.749		
m'_{HC}	0	q'_{HC}	0.045	z'_{HC}	0.022
m''_{HC}	9.16	q''_{HC}	-0.152		
m'_{NOx}	0.127	q'_{NOx}	0.110		

Table 4.8: Category 9 – Calibrated parameters of the catalyst pass fraction functions (Equation 4.12).

m'_{CO}	0	q'_{CO}	0	z'_{CO}	0.005
m''_{CO}	1.15	q''_{CO}	-0.006	z''_{CO}	0.705
m'''_{CO}	0.045	q'''_{CO}	0.746		
m'_{HC}	0	q'_{HC}	0.011	z'_{HC}	0.011
m''_{HC}	3.69	q''_{HC}	-0.031	z''_{HC}	0.047
m'''_{HC}	23.39	q'''_{HC}	-0.977		
m'_{NOx}	0.124	q'_{NOx}	0.067		

CPF_{HC} and CPF_{NOx} are challenging to model (Goodwin, 1996; Nam, 1999). CPF_{HC} is scattered especially for medium levels of engine-out emissions, where the highest values are related to high power episodes. CPF_{NOx} is especially noisy for very low engine-out emissions, with values ranging from nearly zero to ~ 0.95 in category 9 and more than 1 in category 7.

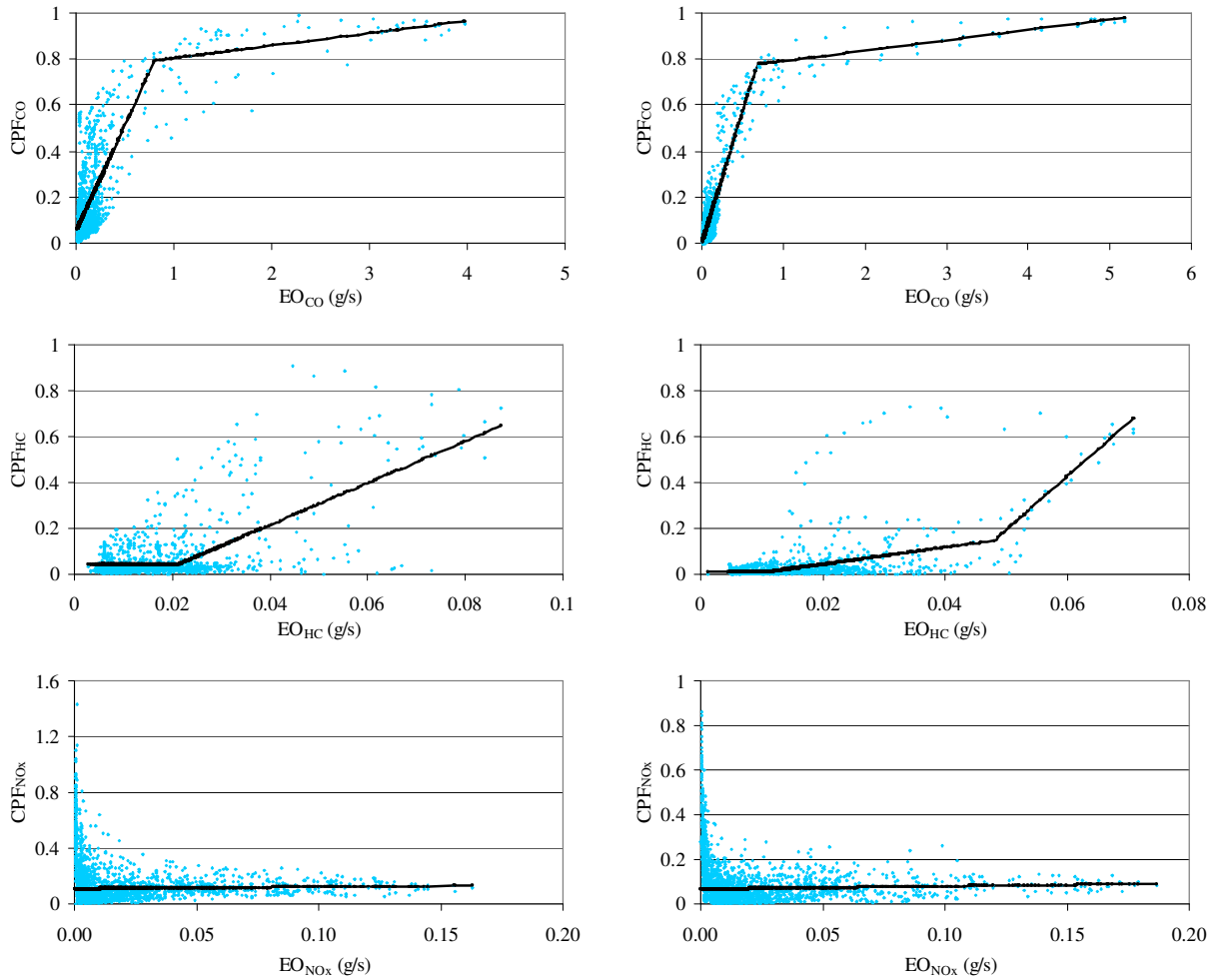


Figure 4-5: Categories 7 (left) and 9 (right) – Catalyst pass fractions for CO, HC, and NO_x. The points represent the calibration data; the line represents the modeled CPF.

4.4.3 Results

The quality of the calibrated model is assessed using a variety of statistics and graphical analyses.

Let TME denote the total measured emission (in grams) of a given species (or fuel consumption) over the cycle. Let TPE denote total predicted emission (or fuel consumption) over the cycle. We calculate the following statistics for each emission species (or fuel consumption):

- Average error (g/s), which is the difference between TME and TPE , divided by the duration of the cycle (in seconds).
- Relative average error, which is the ratio between the average error and the measured average emission (or fuel consumption) rate.
- Correlation coefficient ρ , which is the ratio between the covariance of the predicted and measured emission (or fuel consumption) rates and the product of their standard deviations.
- R-square (R^2) between the measured and the predicted emission (or fuel consumption) rates.

Furthermore, we look at the following graphical representations:

- Graphical analysis of predicted versus measured emission (or fuel consumption) rates.
- Graphical analysis of the residuals (second-by-second differences between the predicted and measured emission rates).
- Graphical comparison between the predicted and the measured second-by-second emission (or fuel consumption) rates over time.

Tables 4.9 through 4.12 show, for the engine-out and the tailpipe modules of both vehicle categories, measured average emission (or fuel consumption) rates, average error, relative average error, ρ , and R^2 .

Figures 4-6 through 4-17 show how the EMIT outputs fit the measured second-by-second emission (or fuel) rates used for the calibration. The plots show also that the EMIT outputs are comparable with those obtained with the load-based model CMEM Version 2.01 (Barth et al., 1999a) (see Section 3.1.3.3) for the same vehicle categories⁹. A comparison between Figures 4-6, 4-7, 4-12, and 4-13 (FTP bag 2) and Figures 4-10, 4-11, 4-16, and 4-17 (MEC01) shows that the model can capture the emissions variability in a wide range of magnitudes.

⁹ EMIT and CMEM are calibrated using very similar sets of data. From the documentation (Barth et al., 2000), it can be inferred that for category 7 CMEM is calibrated using the data relative to the same 7 vehicles used by EMIT, while for category 9 CMEM is calibrated using the same 9 vehicles used by EMIT, plus one more.

Table 4.9: Category 7 – Calibration statistics for the engine-out module.

	CO ₂	CO	HC	NO _x	FR
Measured average rate (g/s)	2.26	0.157	0.0147	0.0208	0.806
Average error (g/s)	-0.00111	-0.00551	-0.00170	0.000244	0.0000522
Relative average error (%)	0.0	-3.5	-11.7	1.2	0.0
ρ	0.99	0.93	0.76	0.93	0.98
R ²	0.98	0.87	0.58	0.86	0.97

Table 4.10: Category 7 – Calibration statistics for the tailpipe module.

	CO ₂	CO	HC	NO _x
Measured average rate (g/s)	2.52	0.0780	0.00130	0.00241
Average error (g/s)	-0.000667	-0.00602	-0.000158	0.0000404
Relative average error (%)	0.0	-7.7	-12.1	1.7
ρ	0.99	0.92	0.73	0.89
R ²	0.98	0.84	0.53	0.79

Table 4.11: Category 9 – Calibration statistics for the engine-out module.

	CO ₂	CO	HC	NO _x	FR
Measured average rate (g/s)	2.30	0.124	0.0133	0.0211	0.797
Average error (g/s)	0.000130	-0.00308	-0.00165	0.000181	-0.0000695
Relative average error (%)	0.0	-2.5	-12.3	0.9	0.0
ρ	0.99	0.95	0.79	0.93	0.98
R ²	0.97	0.90	0.63	0.87	0.97

Table 4.12: Category 9 – Calibration statistics for the tailpipe module.

	CO ₂	CO	HC	NO _x
Measured average rate (g/s)	2.49	0.0629	0.000682	0.00160
Average error (g/s)	-0.0000401	-0.00402	-0.000161	-0.0000219
Relative average error (%)	0.0	-6.4	-23.6	-1.4
ρ	0.99	0.94	0.76	0.82
R ²	0.97	0.88	0.58	0.67

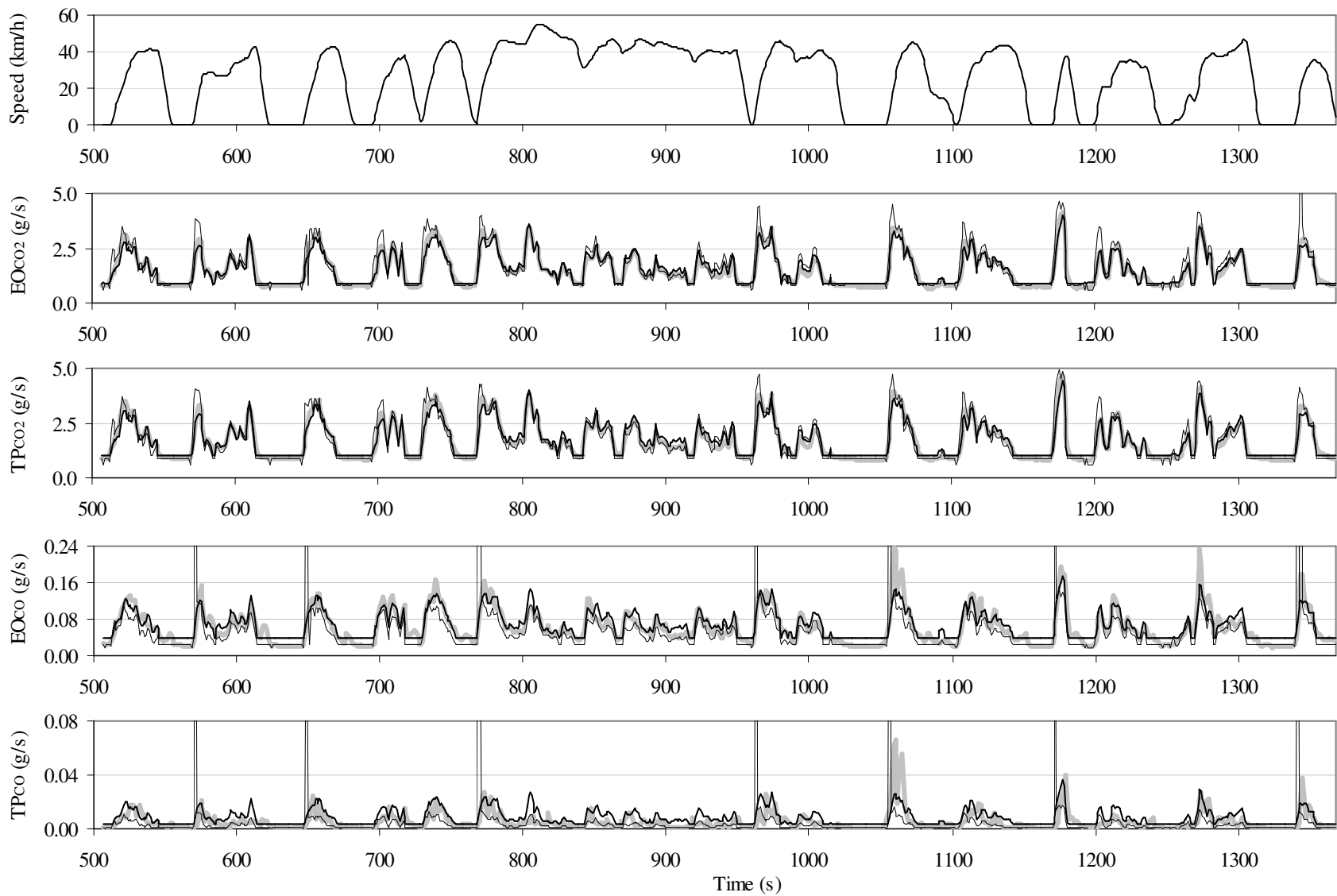


Figure 4-6: **Category 7 - FTP bag 2.** Second-by-second engine-out (EO) and tailpipe (TP) emission rates of CO₂ and CO. Thick light line: measurements; dark line: EMIT predictions; thin line: CMEM predictions. The top plot represents the speed trace.

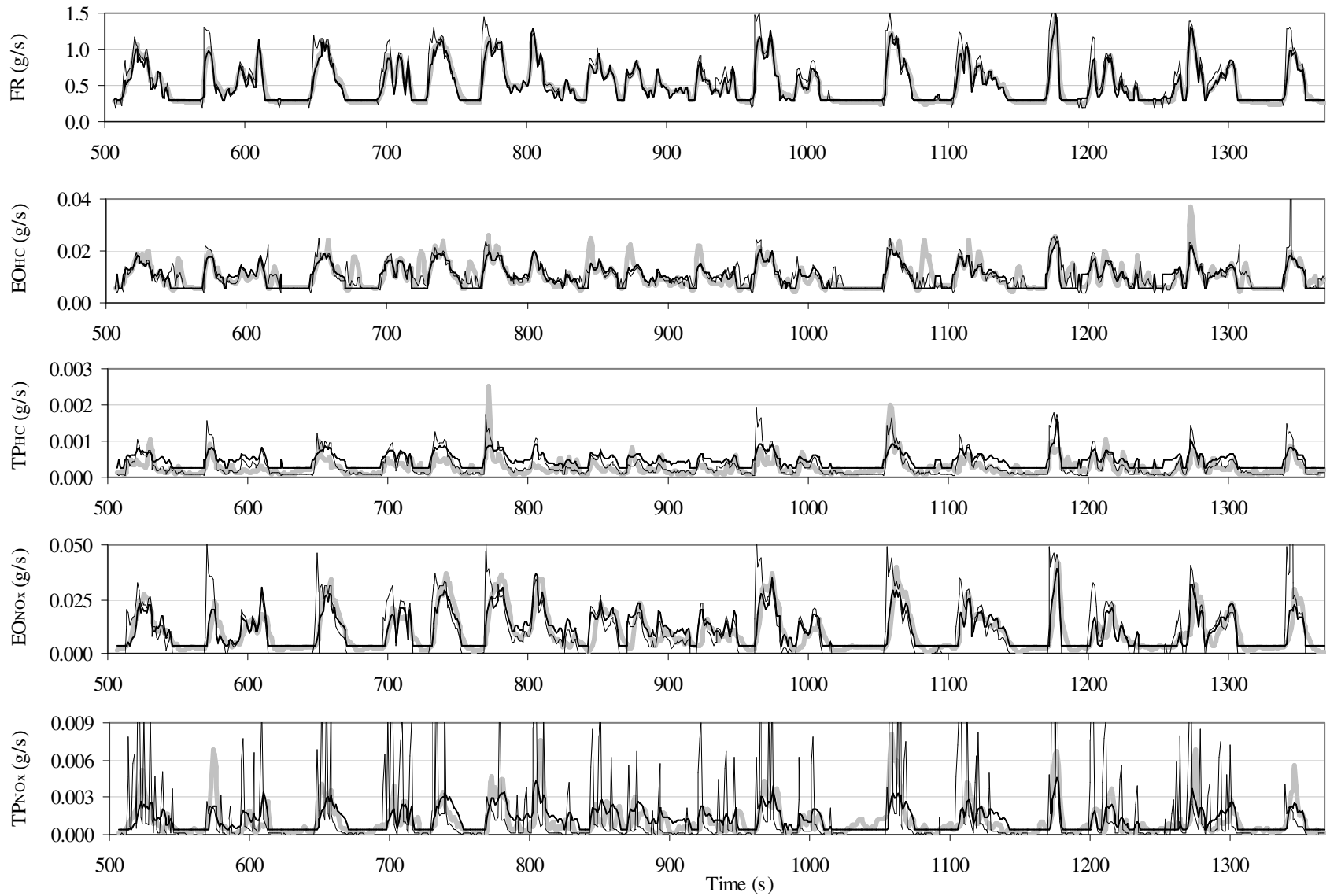


Figure 4-7: **Category 7 - FTP bag 2.** Second-by-second fuel rate (FR) and engine-out (EO) and tailpipe (TP) emission rates of HC and NOx. Thick light line: measurements; dark line: EMIT predictions; thin line: CMEM predictions.

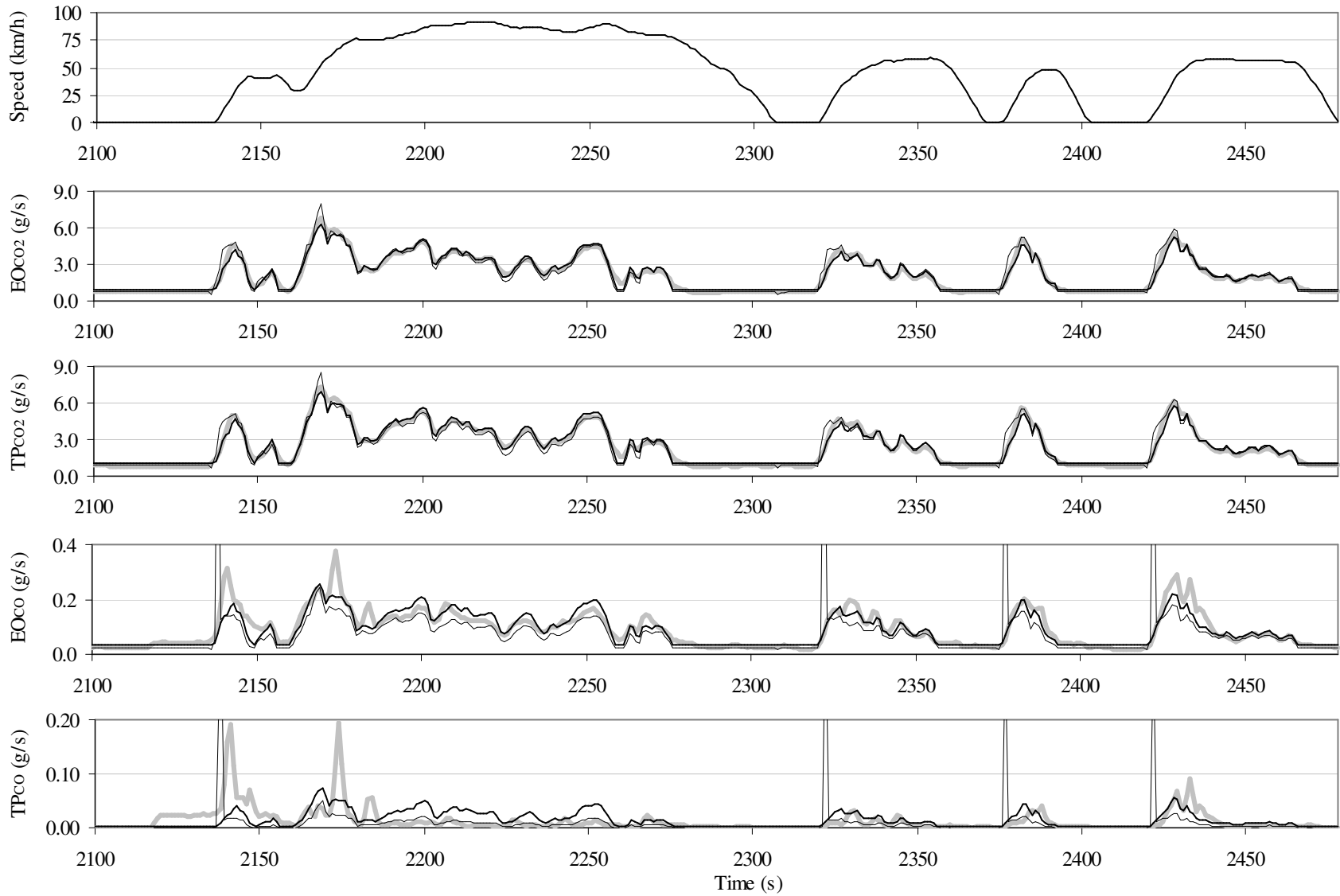


Figure 4-8: **Category 7 - FTP bag 3.** Second-by-second engine-out (EO) and tailpipe (TP) emission rates of CO₂ and CO. Thick light line: measurements; dark line: EMIT predictions; thin line: CMEM predictions. The top plot represents the speed trace.

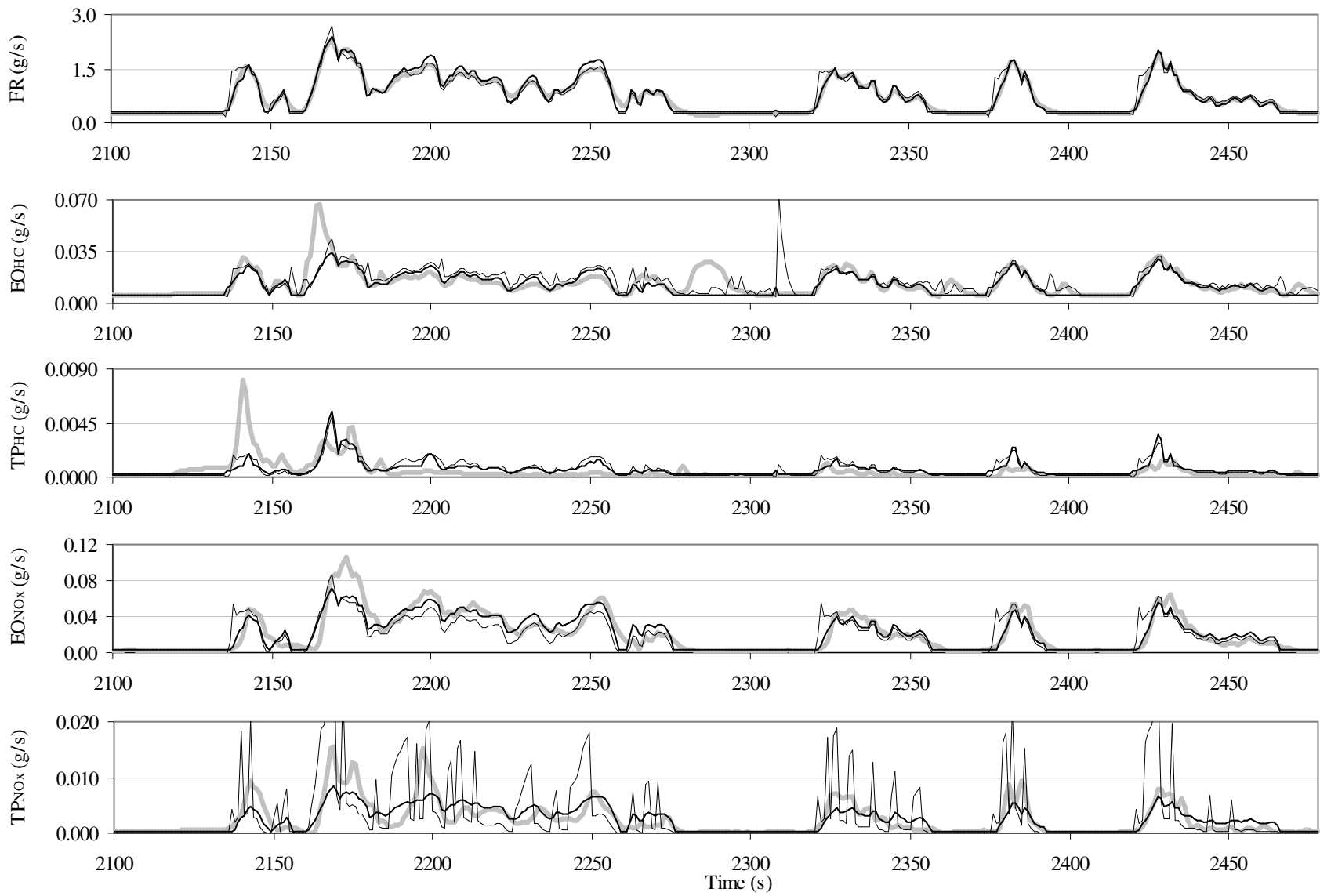


Figure 4-9: **Category 7 - FTP bag 3.** Second-by-second fuel rate (FR) and engine-out (EO) and tailpipe (TP) emission rates of HC and NOx. Thick light line: measurements; dark line: EMIT predictions; thin line: CMEM predictions.

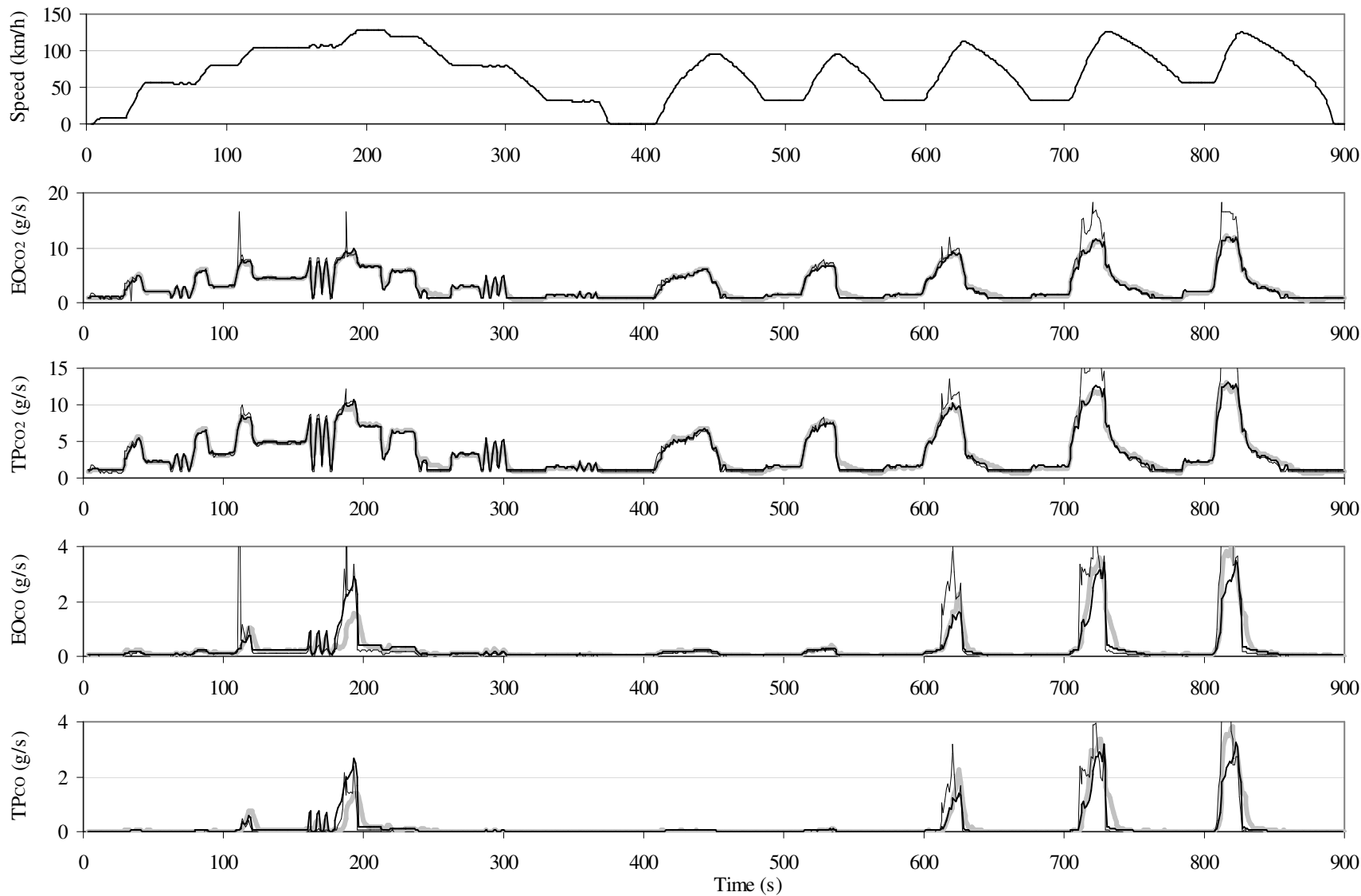


Figure 4-10: **Category 7 – MEC01**. Second-by-second engine-out (EO) and tailpipe (TP) emission rates of CO₂ and CO. Thick light line: measurements; dark line: EMIT predictions; thin line: CMEM predictions. The top plot represents the speed trace.

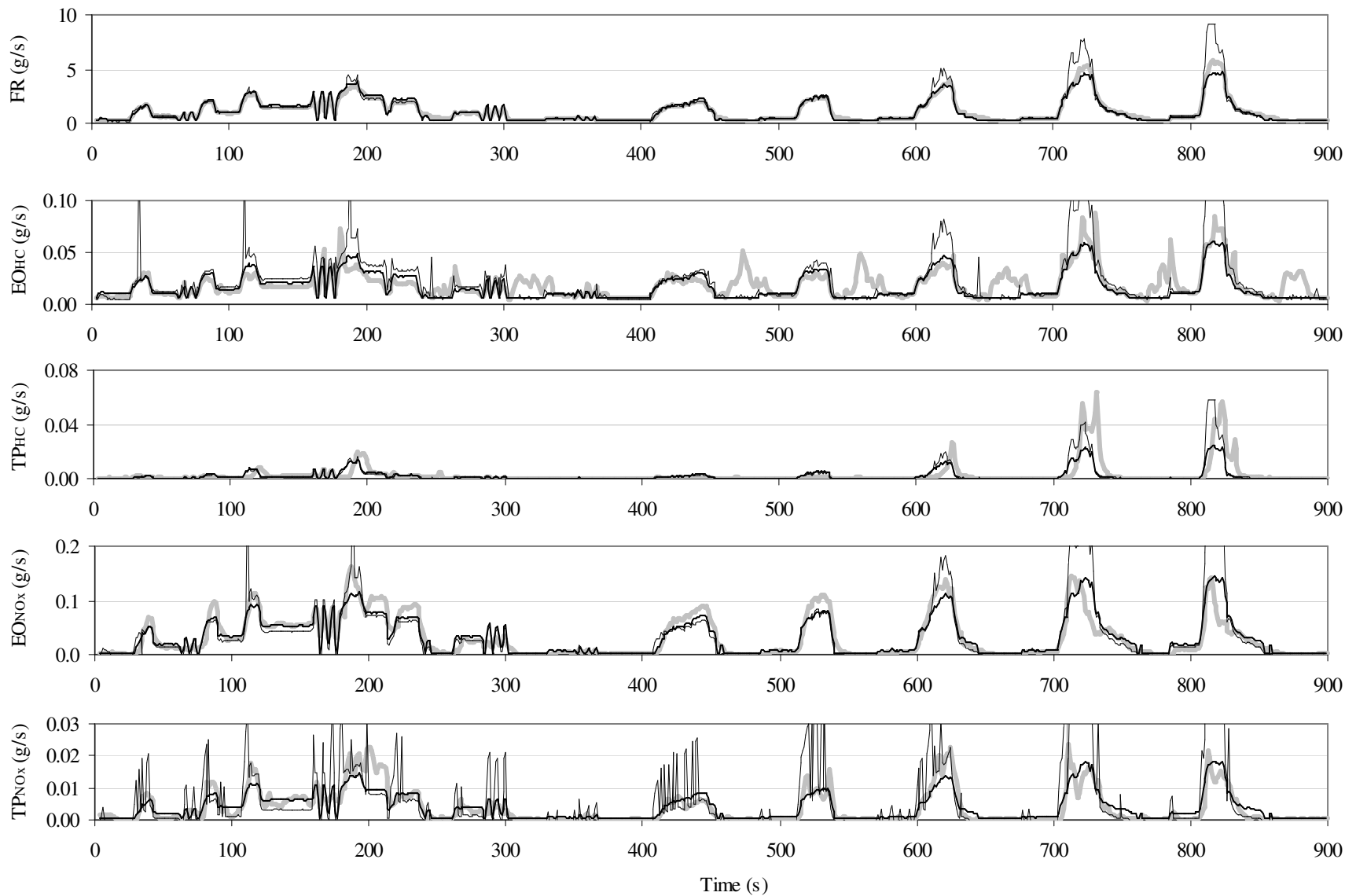


Figure 4-11: **Category 7 – MEC01.** Second-by-second fuel rate (FR) and engine-out (EO) and tailpipe (TP) emission rates of HC and NOx. Thick light line: measurements; dark line: EMIT predictions; thin line: CMEM predictions.

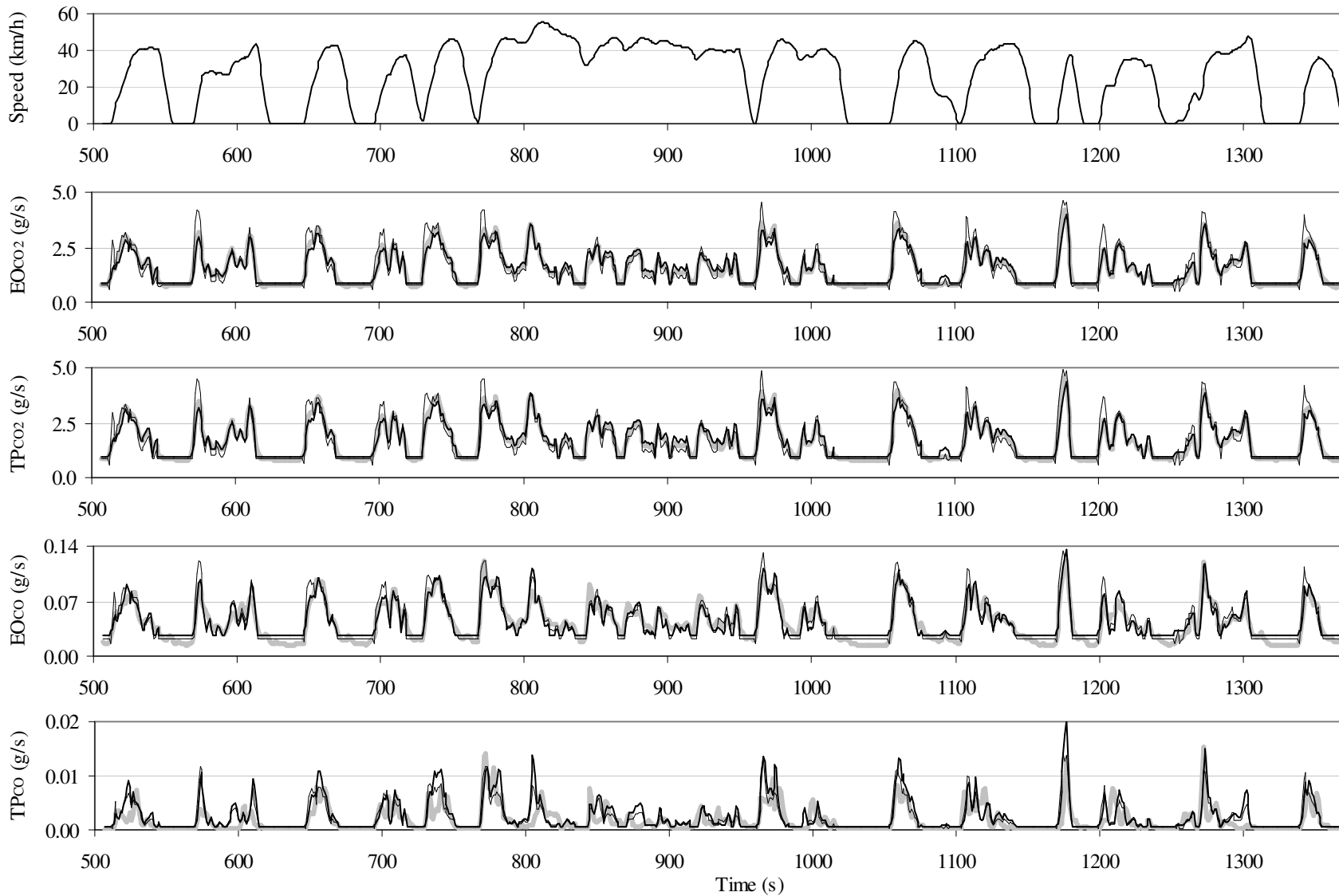


Figure 4-12: **Category 9 - FTP bag 2.** Second-by-second engine-out (EO) and tailpipe (TP) emission rates of CO₂ and CO. Thick light line: measurements; dark line: EMIT predictions; thin line: CMEM predictions. The top plot represents the speed trace.

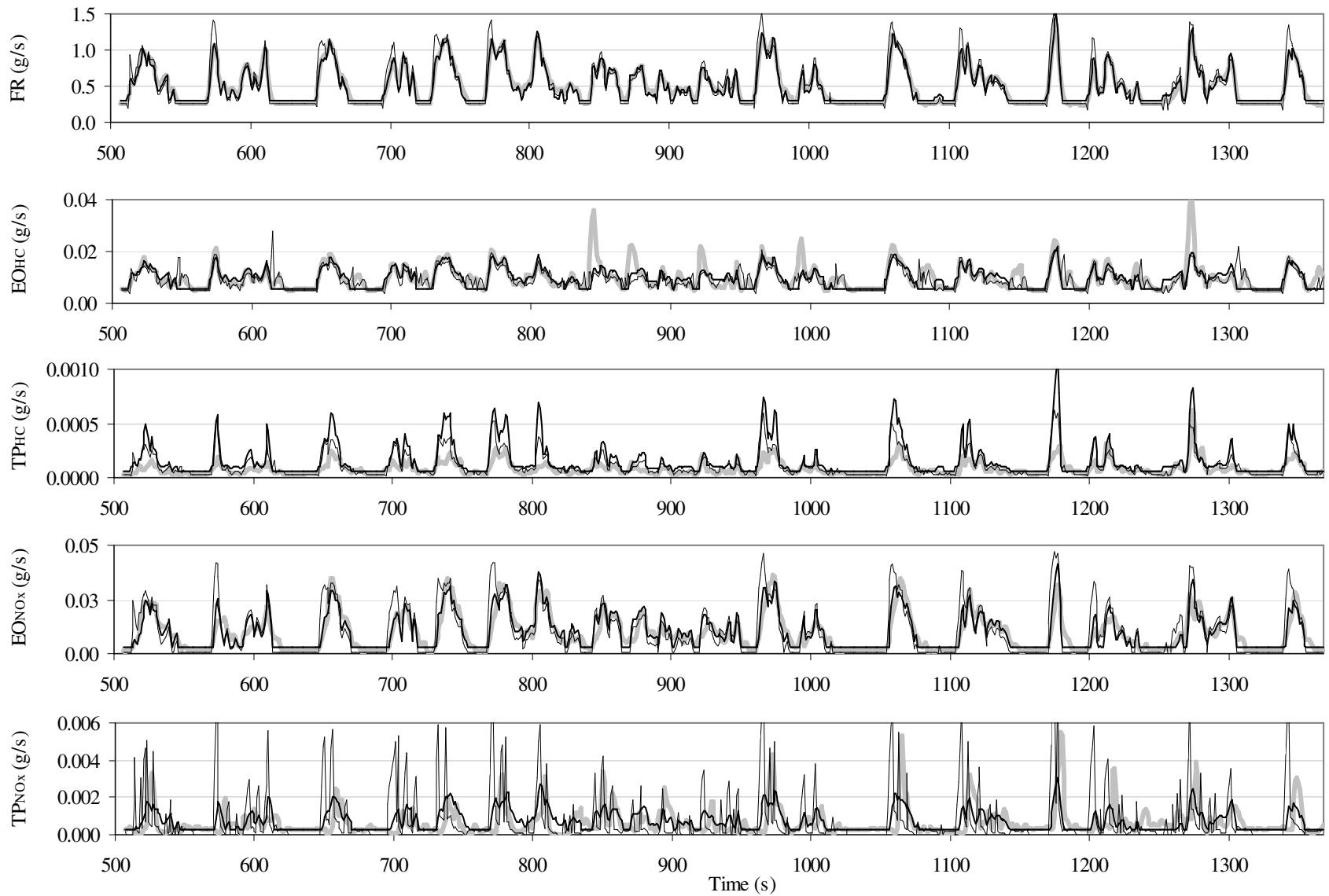


Figure 4-13: **Category 9 - FTP bag 2.** Second-by-second fuel rate (FR) and engine-out (EO) and tailpipe (TP) emission rates of HC and NO_x. Thick light line: measurements; dark line: EMIT predictions; thin line: CMEM predictions.

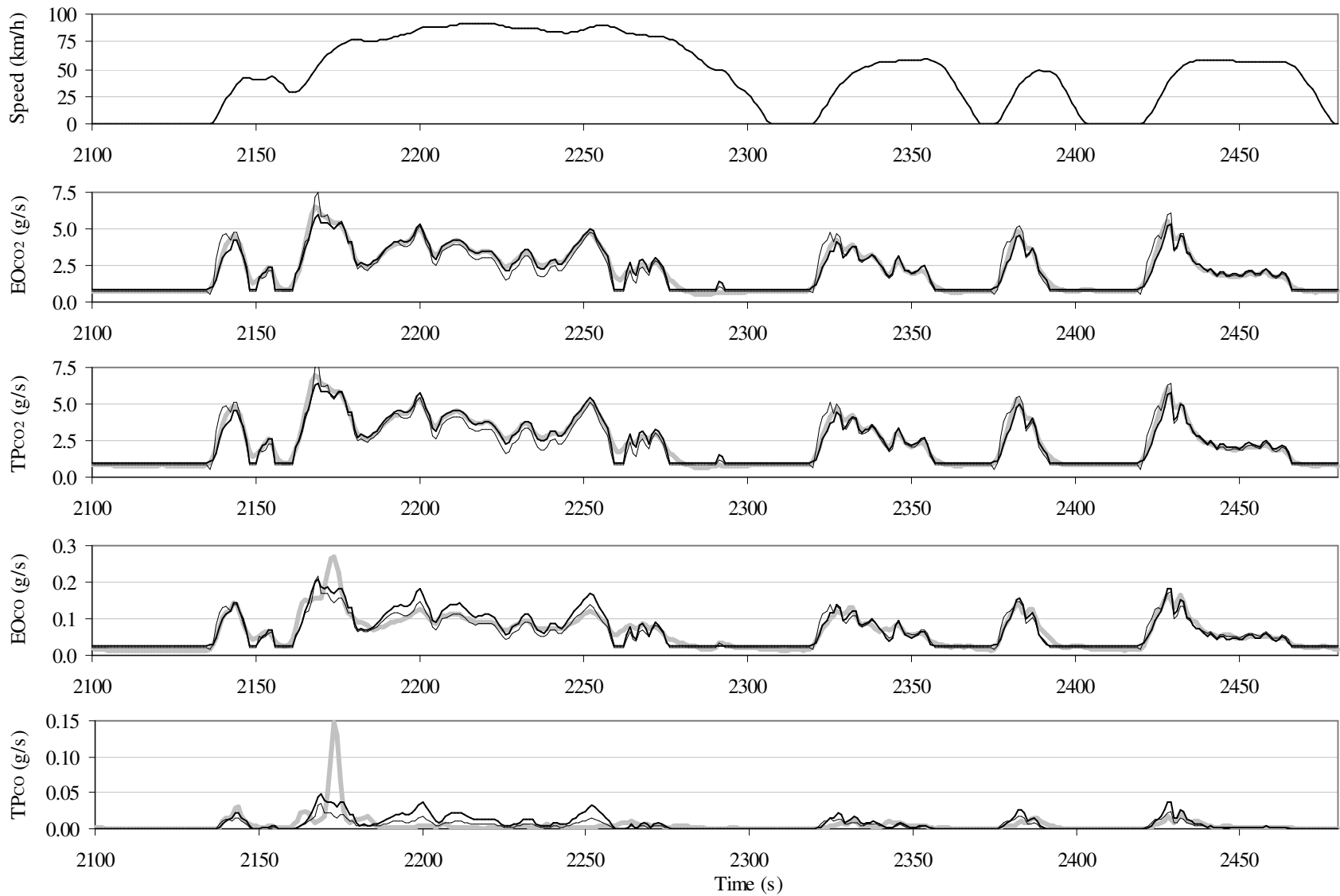


Figure 4-14: **Category 9 - FTP bag 3.** Second-by-second engine-out (EO) and tailpipe (TP) emission rates of CO₂ and CO. Thick light line: measurements; dark line: EMIT predictions; thin line: CMEM predictions. The top plot represents the speed trace.

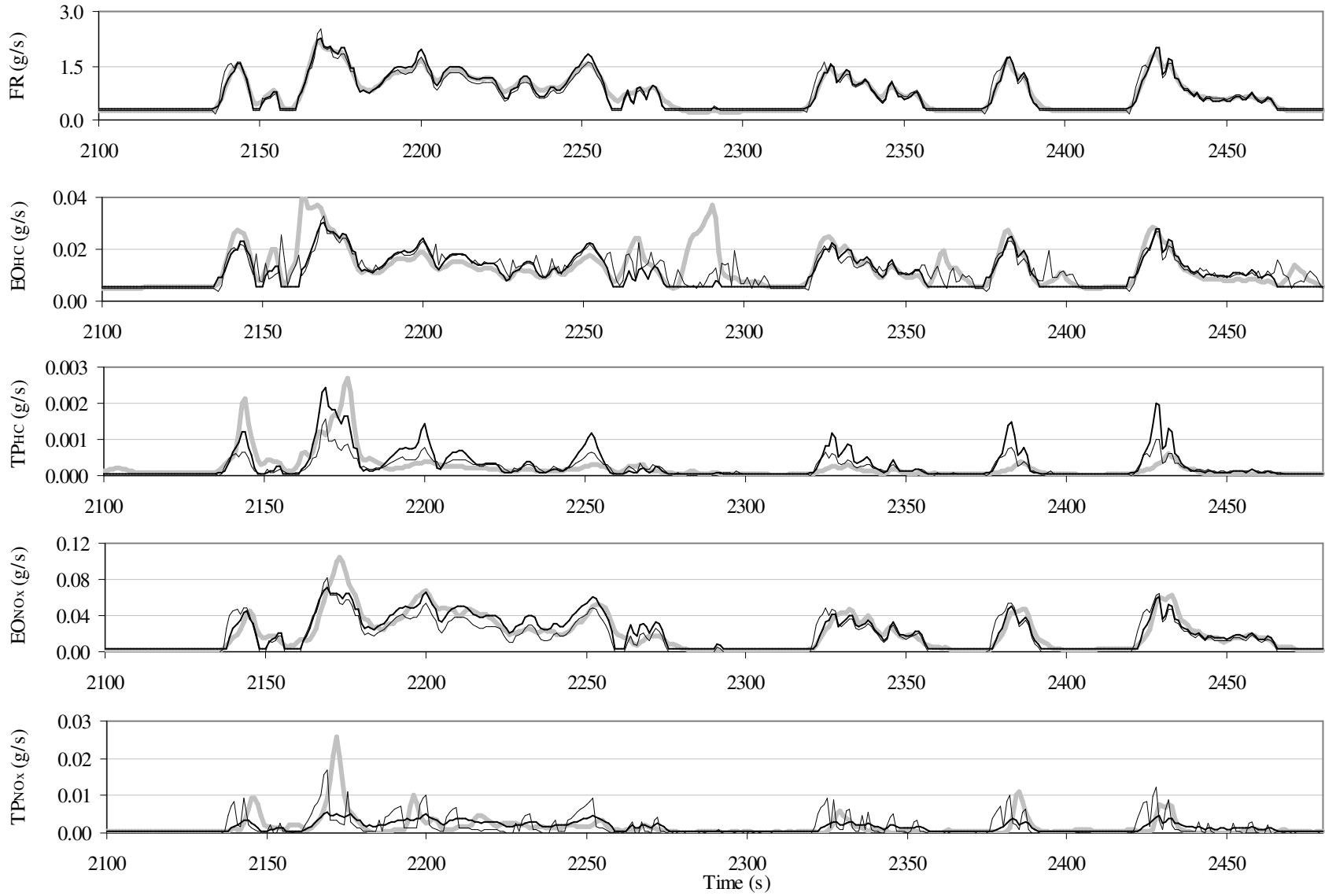


Figure 4-15: **Category 9 - FTP bag 3.** Second-by-second fuel rate (FR) and engine-out (EO) and tailpipe (TP) emission rates of HC and NOx. Thick light line: measurements; dark line: EMIT predictions; thin line: CMEM predictions.

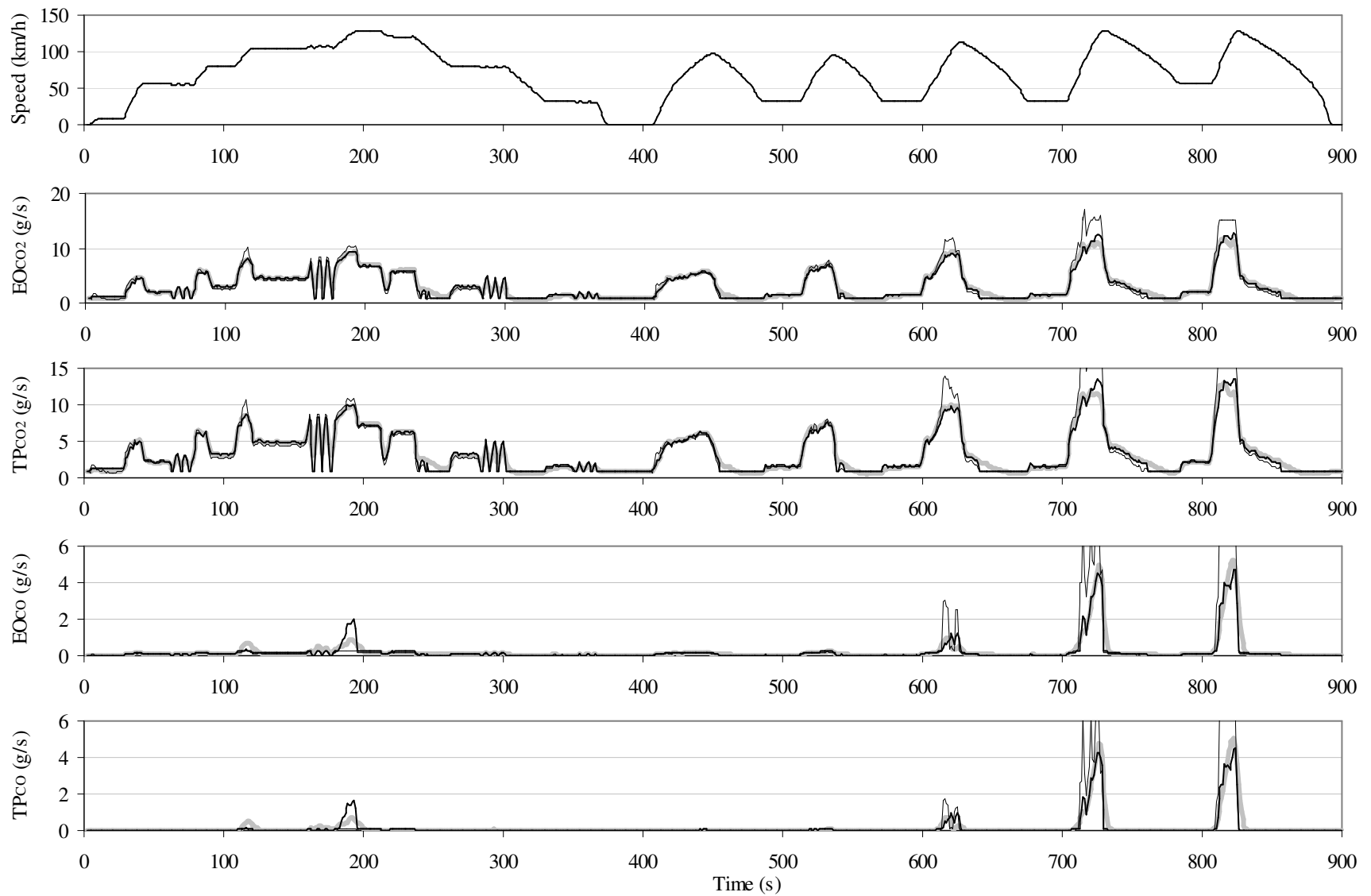


Figure 4-16: **Category 9 – MEC01**. Second-by-second engine-out (EO) and tailpipe (TP) emission rates of CO₂ and CO. Thick light line: measurements; dark line: EMIT predictions; thin line: CMEM predictions. The top plot represents the speed trace.

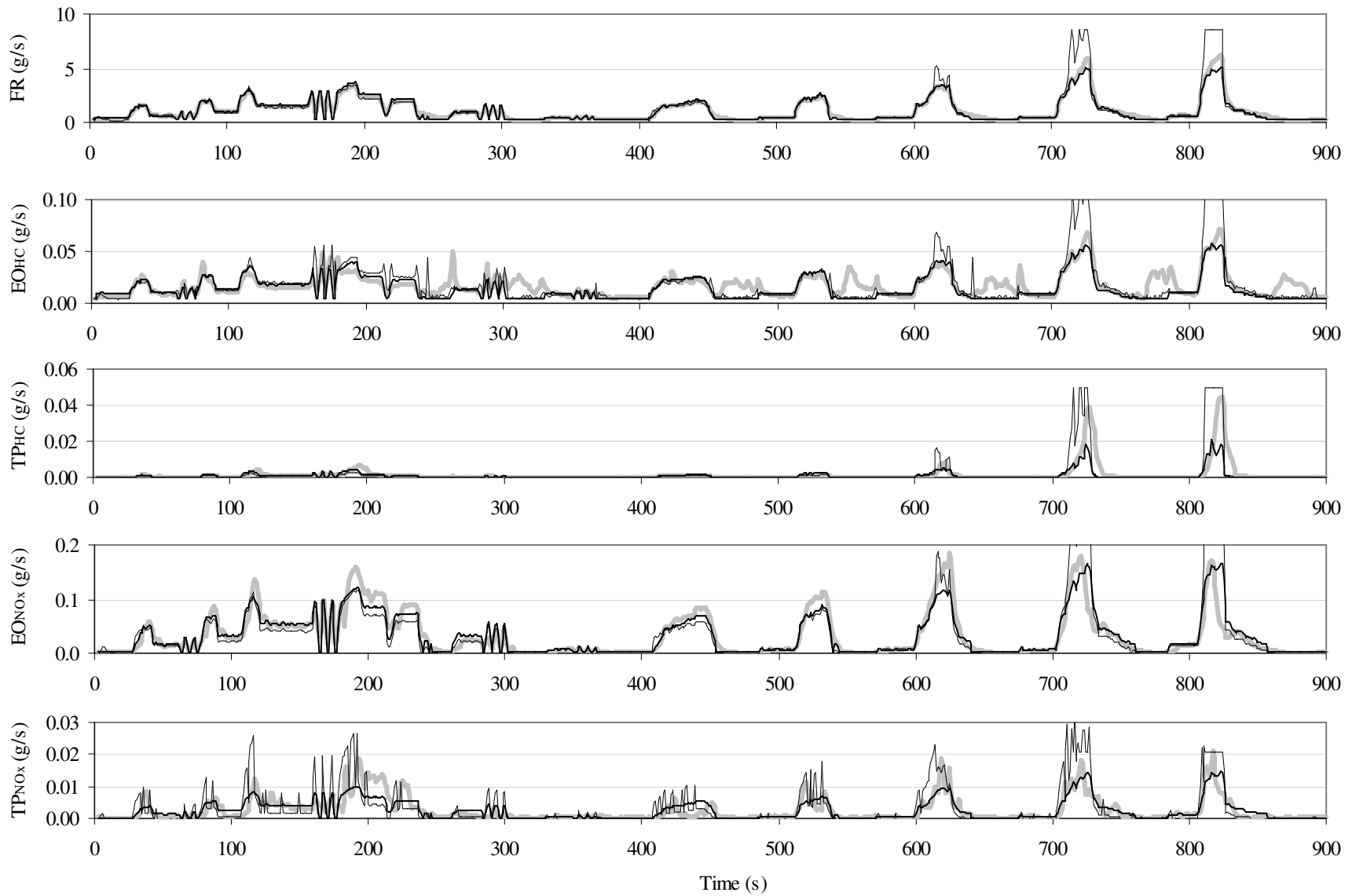


Figure 4-17: **Category 9 – MEC01.** Second-by-second fuel rate (FR) and engine-out (EO) and tailpipe (TP) emission rates of HC and NOx. Thick light line: measurements; dark line: EMIT predictions; thin line: CMEM predictions.

The estimated fuel consumption and CO_2 match the measurements satisfactorily (0.0% error and $R^2 > 0.97$).

For CO , the model fits the measurements quite well (R^2 between 0.84 and 0.90), with the exception of some FTP bag 3 peaks (Figures 4-8 and 4-14) and some MEC01 peaks (Figures 4-10 and 4-16), resulting in a percentage error equal to or less than -3.5% in engine-out and -8.3% in tailpipe.

For HC , the model has a less desirable performance (R^2 between 0.53 and 0.63). For engine-out, as expected, the principal problem is represented by the enleanment puffs, which are not modeled, resulting in an underestimation of approximately -12% . For tailpipe, there is a tendency to overestimate the low emissions and underestimate the highest MEC01 peaks (Figures 4-11 and 4-17). The resulting percentage error (-12.1% for category 7 and -23.6% for category 9) is due not to enleanment puffs (which are not present in the measured tailpipe emissions), but to the underestimation of the MEC01 peaks. Probably the model is not able to capture the decreased catalyst efficiency during these enrichment events.

For NO_x , engine-out emissions fit well, while the fit for tailpipe emissions is lower (R^2 drops from 0.86 to 0.79 for category 7 and from 0.87 to 0.67 for category 9), due to the scattered behavior of CPF_{NOx} , which is highly sensitive to the variability of air-to-fuel ratio. In particular, as in the case of CO , there is underestimation of some FTP bag 3 peaks (Figures 4-9 and 4-15) and of the MEC01 highest speed peak (Figures 4-11 and 4-17). However, the percentage error is very small (less than 2% in absolute value).

Figures 4-18 through 4-21 depict, for all the data used for the calibration of the model for category 9, (a) the predicted tailpipe emission rates plotted versus the measured tailpipe emission rates, (b) the residuals plotted versus the measured tailpipe emission rates, (c) the residuals plotted versus speed, and (d) the residuals plotted versus acceleration. As exemplified in Figures 4-18a, 4-19a, 4-20a, and 4-21a the predicted emission rates as a function of the measured emission rates can show horizontal trends (which correspond to linear trends in Figures 4-18b, 4-19b, 4-20b, and 4-21b). This is probably due to two factors. First, when $P_{tract} = 0$, the model estimates a constant low value (see Equations 4.7b, 4.8b, and 4.9c), while the real data obviously are not exactly constant. Second, it is likely that in the model one or more explanatory variables are missing. This would explain why the model predicts values less variable than the measurements. We verified that, despite such problems, the residuals are largely distributed in a limited range around the zero. Figures 4-18c, 4-18d, 4-19c, 4-19d, 4-20c, 4-20d, 4-21c and 4-21d show that in general there is no significant dependence of the residuals on speed and acceleration.

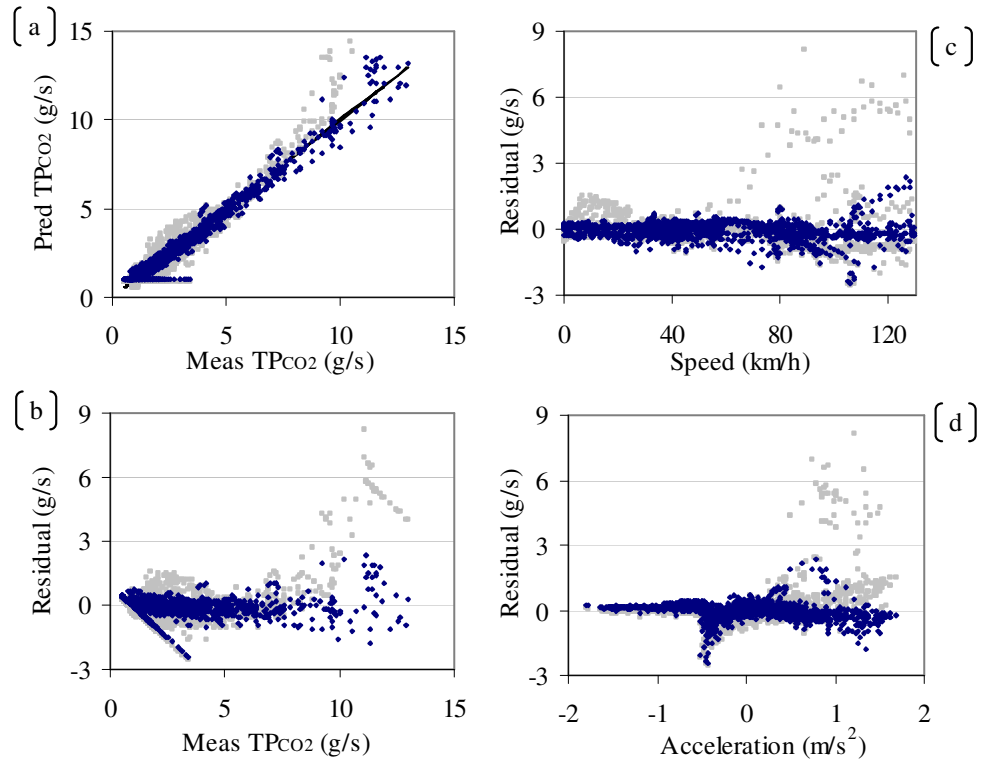


Figure 4-18: Category 9 – Tailpipe CO₂ predicted vs. measured emission rates (a), residuals vs. measured emission rates (b), vs. speed (c), and vs. acceleration (d). In dark EMIT; in gray CMEM.

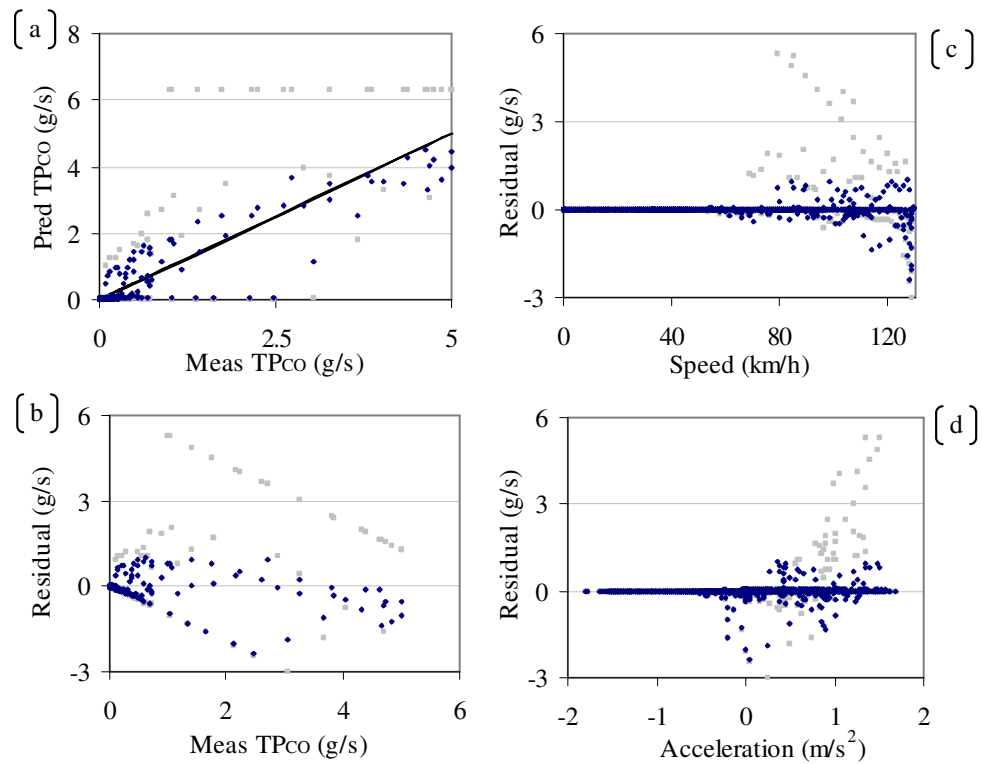


Figure 4-19: Category 9 – Tailpipe CO predicted vs. measured emission rates (a), residuals vs. measured emission rates (b), vs. speed (c), and vs. acceleration (d). In dark EMIT; in gray CMEM.

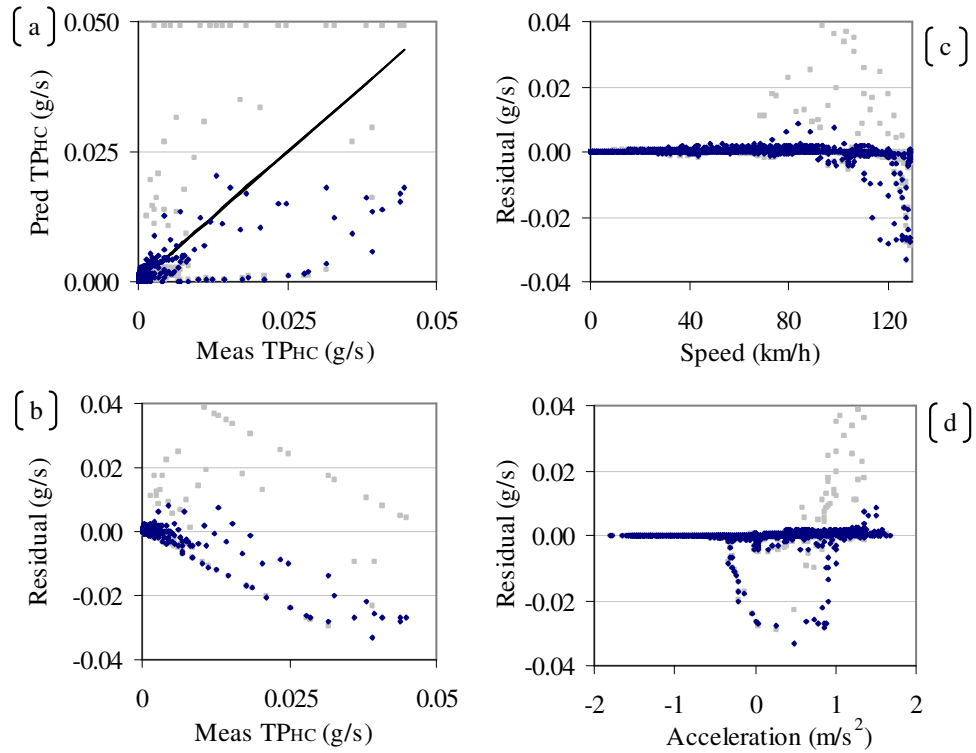


Figure 4-20: Category 9 – Tailpipe HC predicted vs. measured emission rates (a), residuals vs. measured emission rates (b), vs. speed (c), and vs. acceleration (d). In dark EMIT; in gray CMEM.

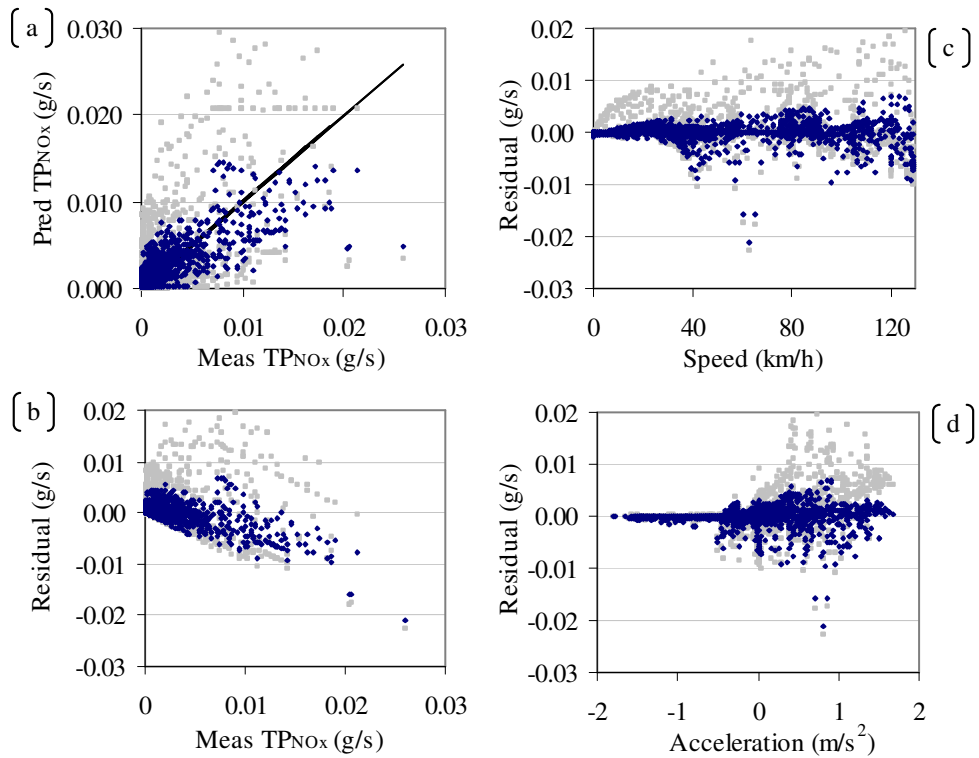


Figure 4-21: Category 9 – Tailpipe NO_x predicted vs. measured emission rates (a), residuals vs. measured emission rates (b), vs. speed (c), and vs. acceleration (d). In dark EMIT; in gray CMEM.

4.5 Model Validation

The validation of the calibrated model is carried out on the composite US06 data, to test the capability of EMIT to predict emissions and fuel consumption from input data different from those used in calibration. The US06 cycle is a difficult test cycle for model predictions (Barth et al., 2000). The results, as shown in Tables 4.13-4.16, are, as expected, poorer than those obtained on the calibration data, but in general quite satisfactory.

Table 4.13: Category 7 – Validation statistics for the engine-out module.

	CO ₂	CO	HC	NO _x	FR
Measured average rate (g/s)	3.87	0.315	0.0243	0.0444	1.40
Average error (g/s)	0.000785	-0.0516	-0.00455	-0.00111	0.0494
Relative average error (%)	0.0	-16.4	-18.7	-2.5	3.5
ρ	0.98	0.68	0.50	0.91	0.97
R ²	0.96	0.46	0.25	0.83	0.94

Table 4.14: Category 7 – Validation statistics for the tailpipe module.

	CO ₂	CO	HC	NO _x
Measured average rate (g/s)	4.37	0.154	0.00119	0.00427
Average error (g/s)	-0.113	-0.0256	0.000993	0.000846
Relative average error (%)	-2.6	-16.7	83.4	19.8
ρ	0.98	0.60	0.47	0.79
R ²	0.96	0.36	0.22	0.63

Table 4.15: Category 9 – Validation statistics for the engine-out module.

	CO ₂	CO	HC	NO _x	FR
Measured average rate (g/s)	3.89	0.197	0.0220	0.0447	1.34
Average error (g/s)	-0.211	-0.00428	-0.00491	-0.000156	0.0713
Relative average error (%)	-0.5	-2.2	-22.3	-0.4	5.3
ρ	0.98	0.71	0.47	0.91	0.97
R ²	0.95	0.50	0.22	0.83	0.95

Table 4.16: Category 9 – Validation statistics for the tailpipe module.

	CO ₂	CO	HC	NO _x
Measured average rate (g/s)	4.26	0.0786	0.000778	0.00347
Average error (g/s)	-0.0932	0.00513	0.000206	-0.000105
Relative average error (%)	-2.2	6.5	26.5	-3.0
ρ	0.98	0.66	0.57	0.73
R ²	0.95	0.43	0.32	0.53

Figures 4-22 through 4-25 show how the EMIT outputs fit the measured second-by-second emission (or fuel consumption) rates. The EMIT outputs are comparable with those obtained with CMEM for the same vehicle categories.

Fuel consumption and CO_2 are estimated within 5.3% and -2.6% respectively, with a very high R^2 (~0.95).

For CO , both engine-out and tailpipe modules overestimate some medium peaks and underestimate some high peaks (Figures 4-22 and 4-24). R^2 is between 0.36 and 0.50, and the percentage error is less than -17% for category 7 and less than 7% for category 9.

The HC model has the poorest performance (R^2 between 0.22 and 0.32). In engine-out the principal problem is related to enleanment puffs that, however, disappear in the measured tailpipe emissions. Tailpipe emissions are largely overestimated in category 7 (83.4%), while in category 9 there is a tendency towards underestimation of the high values and overestimation of the low values.

For NO_x , engine-out emissions are well predicted, while the fit for tailpipe emissions is lower (R^2 drops from 0.83 to 0.63 for category 7 and from 0.83 to 0.53 for category 9), due to the scattered behavior of CPF_{NOx} . The tailpipe percentage error is 19.8% for category 7 and -3.0% for category 9.

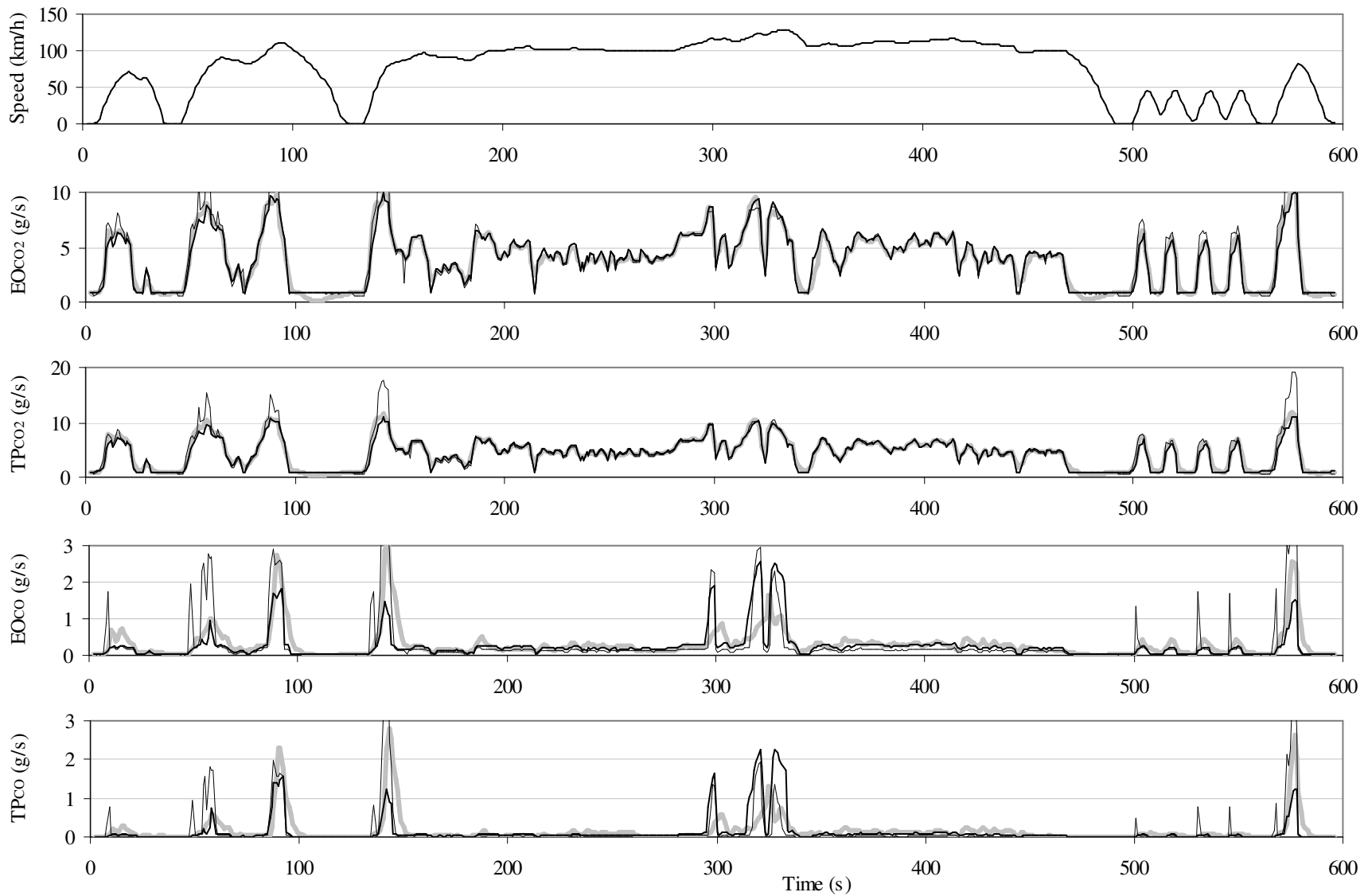


Figure 4-22: **Category 7 – US06**. Second-by-second engine-out (EO) and tailpipe (TP) emission rates of CO₂ and CO. Thick light line: measurements; dark line: EMIT predictions; thin line: CMEM predictions. The top plot represents the speed trace.

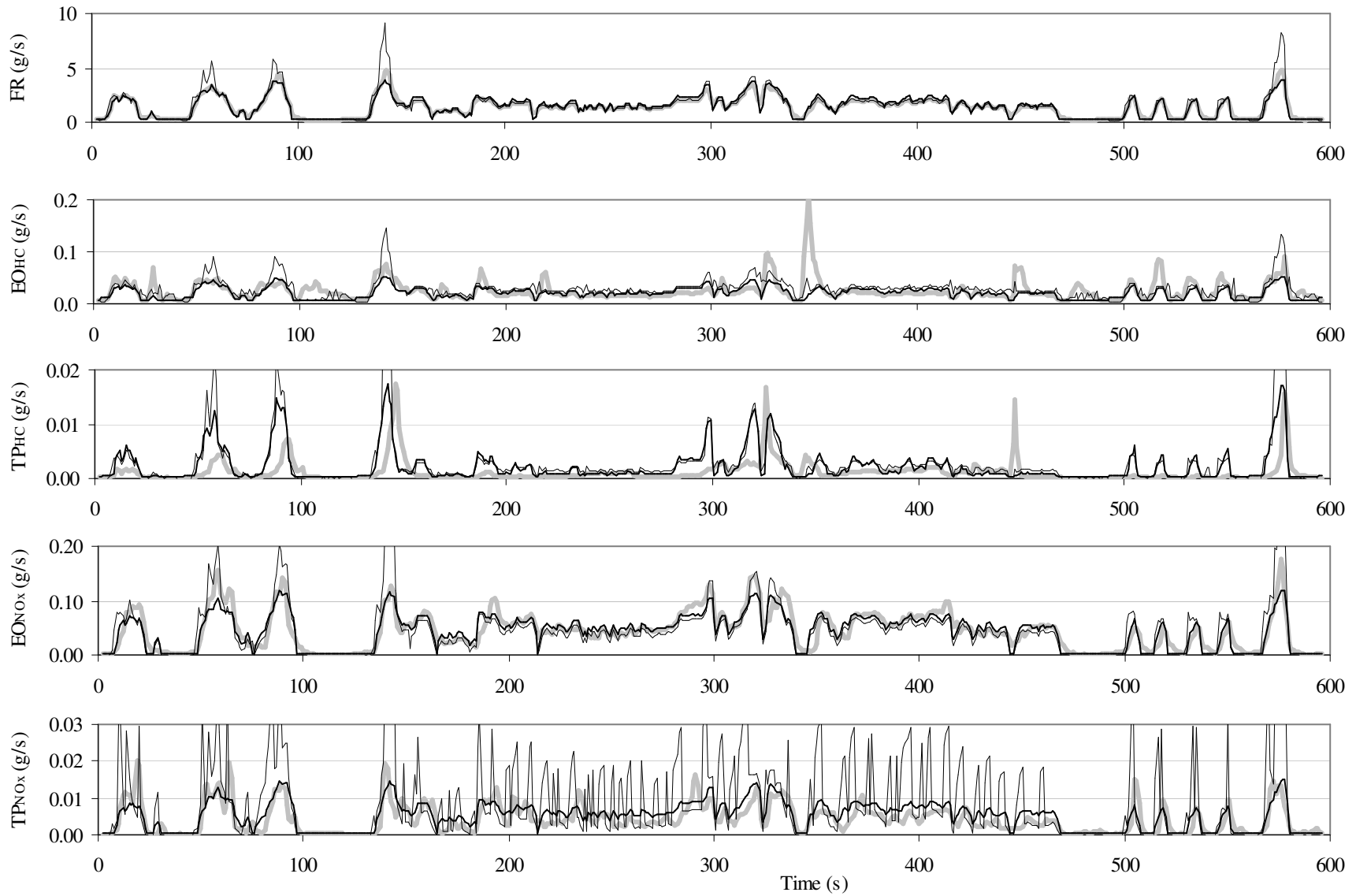


Figure 4-23: **Category 7 – US06**. Second-by-second fuel rate (FR) and engine-out (EO) and tailpipe (TP) emission rates of HC and NOx. Thick light line: measurements; dark line: EMIT predictions; thin line: CMEM predictions.

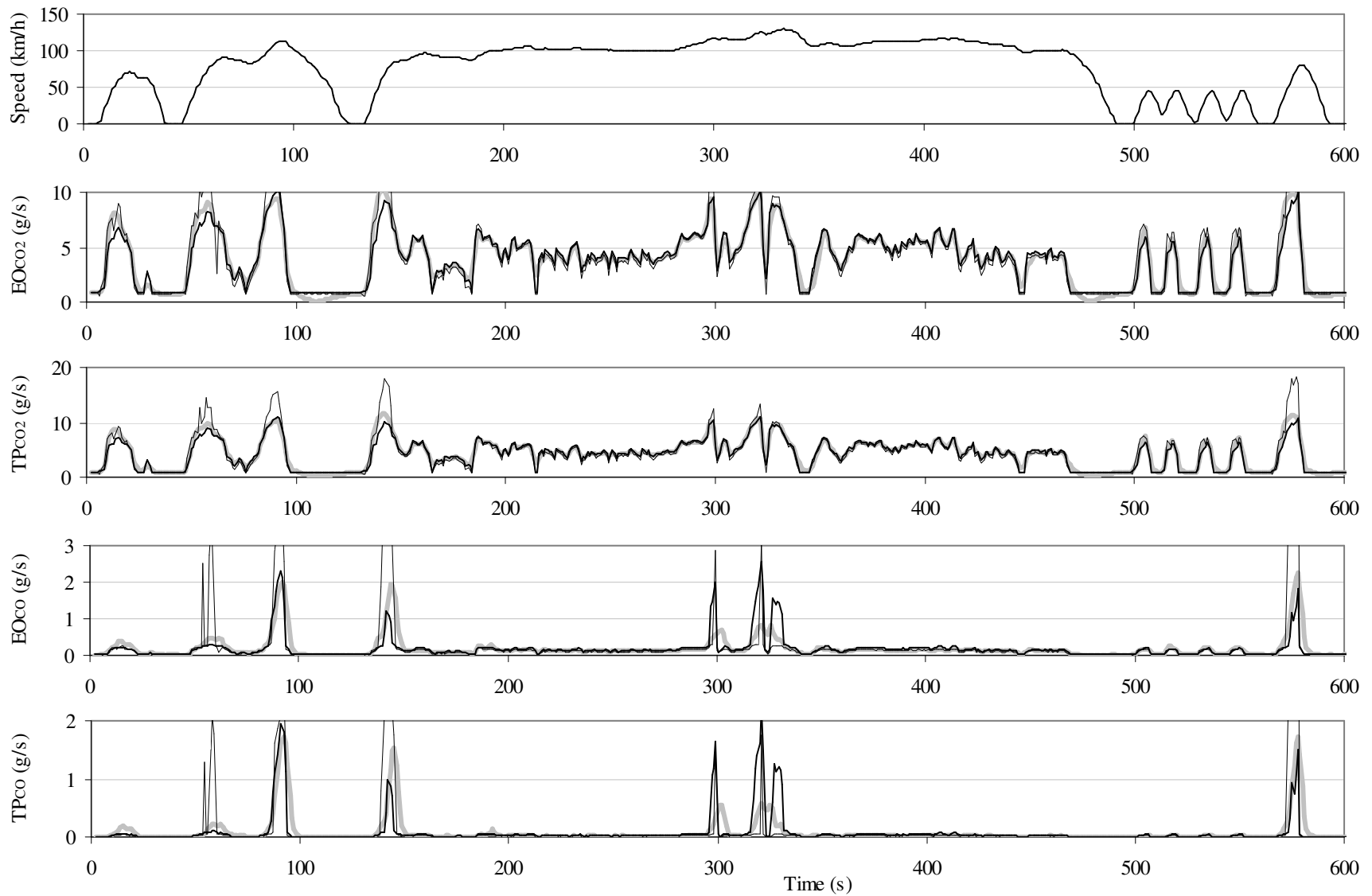


Figure 4-24: **Category 9 – US06**. Second-by-second engine-out (EO) and tailpipe (TP) emission rates of CO₂ and CO. Thick light line: measurements; dark line: EMIT predictions; thin line: CMEM predictions. The top plot represents the speed trace.

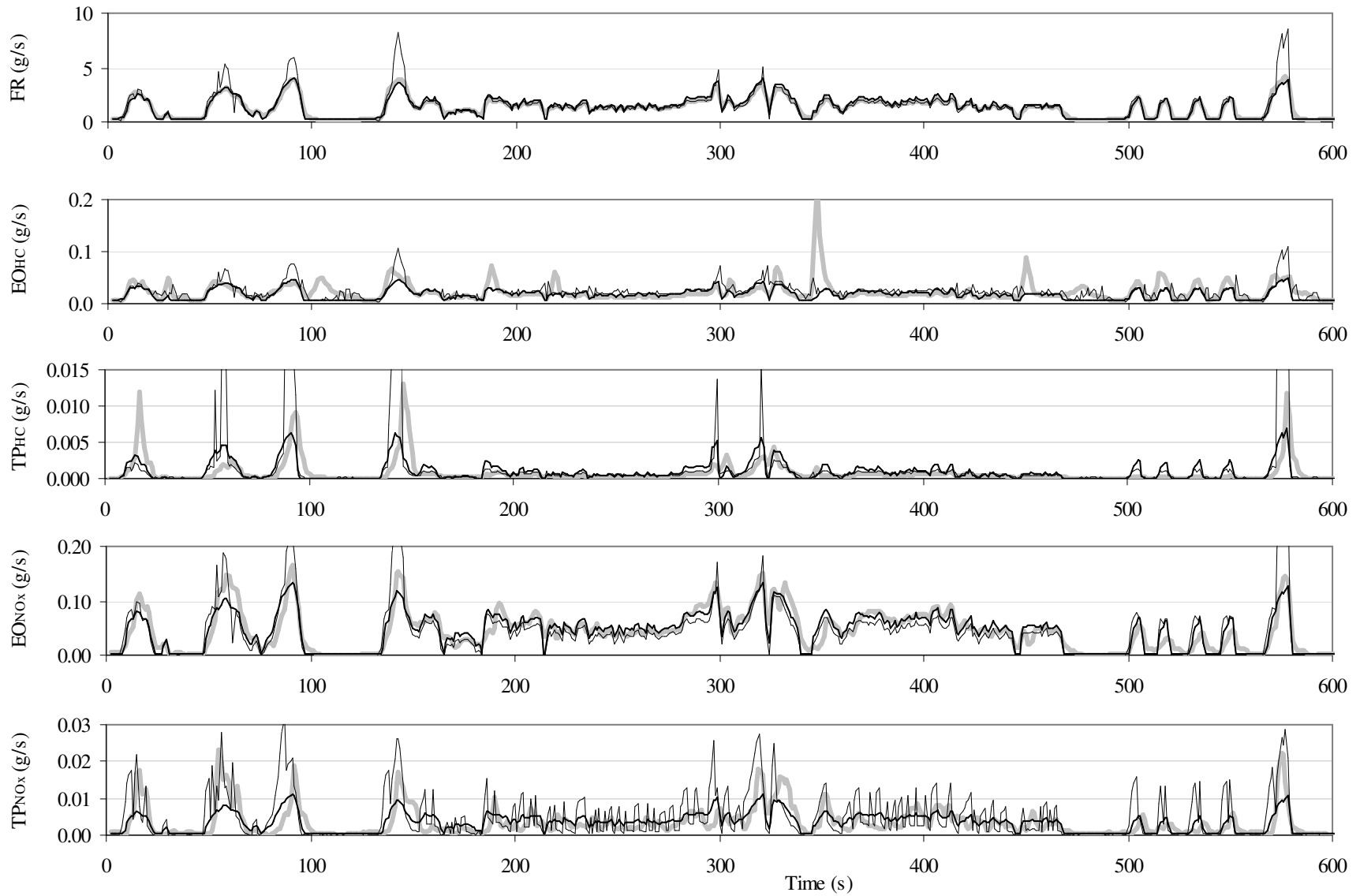


Figure 4-25: **Category 9 – US06.** Second-by-second fuel rate (FR) and engine-out (EO) and tailpipe (TP) emission rates of HC and NO_x. Thick light line: measurements; dark line: EMIT predictions; thin line: CMEM predictions.

4.6 Conclusions

In this chapter, we presented EMIT, a dynamic model of emissions (CO_2 , CO , HC , and NO_x) and fuel consumption for light-duty vehicles. The model was derived from the regression-based and the load-based emissions modeling approaches (presented respectively in Sections 3.1.3.2 and 3.1.3.3), and effectively combines some of their respective advantages. EMIT was calibrated and validated for two vehicle categories.

The results for the two categories calibrated indicate that the model gives reasonable results compared to actual measurements as well to results obtained with CMEM, a state-of-the-art load-based emission model. In particular, the model gives results with good accuracy for fuel consumption and carbon dioxide, reasonable accuracy for carbon monoxide and nitrogen oxides, and less desirable accuracy for hydrocarbons.

The structure and the calibration of EMIT are simpler compared with load-based models. While load-based models involve a multi-step calibration process of many parameters, and the prior knowledge of several readily available specific vehicle parameters, the approach presented in this chapter collapses the calibration into few linear regressions for each pollutant. Compared to a multi-step calibration, here the parameters directly optimize the fit to the emissions, avoiding error accumulations. Furthermore, due to its relative simplicity, the computational time required to run the model is expected to be less compared to load-based models.

Questions for future research related to EMIT are the following:

1. The tailpipe module for HC , which currently gives the least satisfactory results, needs to be improved.
2. The model needs to be calibrated for the other categories present in the NCHRP vehicle emissions database. Moreover, in order to represent the actual emissions sources present on roadways, other databases should be acquired and used for the model calibration, including data on heavy trucks, buses, more recent vehicles than those represented in the NCHRP database, and on-road measurements.
3. The model can be extended to other emission species, such as particulate matter and air toxics, when data are available.
4. Least square regression benefits from calibration data with extreme values. Therefore, it is recommendable to calibrate EMIT using, in addition to the data presently used, also data from aggressive cycles, like the US06. This is not currently possible, since US06

data are not available for many vehicles from the NCHRP vehicle emissions database (see Appendix A).

5. EMIT has been developed and calibrated for hot-stabilized conditions with zero road grade, and without accessory usage. The model does not represent history effects, such as cold-start emissions and hydrocarbon enrichment puffs. Future research should address how to overcome these limitations, in order to provide greater generality to the model. In the following, we suggest some easily realizable modifications to the model to include road grade, cold starts and hydrocarbon enrichment puffs, while how to make the model take account of accessory usage appears to be a more challenging question.

- Road grade ϑ can be easily introduced adding a variable a_g to the vehicle acceleration a in Equations 4.7, 4.8, 4.9, and 4.11. The variable a_g is the component of the gravitational acceleration g (9.81 m/s^2) along the road surface ($a_g = g \cdot \sin \vartheta$).
- In order to model cold-start emissions, two approaches could be pursued. The first approach would consist in simply recalibrating the model using cold-start (e.g. FTP bag 1) data. In this case, EMIT would be composed of two sub-models, one for cold-start and one for hot-stabilized conditions. The second approach would be more general, allowing for intermediate soak times and gradual passage from cold to hot conditions. In this case, it would be necessary to introduce in the model history variables, such as soak time, time elapsed since the beginning of the trip, and possibly cumulative fuel consumption.
- Hydrocarbons puffs, as stated in Section 4.3.1, do not significantly affect tailpipe emissions in normal emitting vehicles. On the other hand, they can constitute a significant portion of the total tailpipe emissions in high emitters. In order to model hydrocarbons puffs in EMIT, it would be necessary to introduce in the model history variables, such as the duration of deceleration since its inception up to the current time.

We note that the introduction of history effects in the emission model should be complemented with an investigation of how the integration with non-microscopic traffic models would be affected by this enhancement.

Chapter 5

Integration of Dynamic Emission Models and Dynamic Traffic Models

As stated in Chapter 3, we are interested in investigating the integration of dynamic emission models with non-microscopic dynamic traffic models. These traffic models do not calculate vehicle accelerations directly, as microscopic models do. However, since they possess better computational speeds and are relatively easier to calibrate, they are more suitable for large-scale applications. To the best of our knowledge, only few papers in the literature address the integration with non-microscopic traffic models (see Section 3.2). The approach described in this chapter is different from the approaches described in the literature. While those approaches are valuable for particular applications, they are not general to allow for the integration of dynamic emission models with any non-microscopic dynamic traffic model.

In this chapter, we propose a probabilistic approach for the integration of dynamic emission models and non-microscopic dynamic traffic models. The proposed approach requires the calculation of expected emission and fuel consumption rates by combining a dynamic emission model with a probabilistic model of accelerations. The latter model is a function of speed and road type. We implement this approach by combining the dynamic emission model EMIT, presented in Chapter 4, and a probabilistic acceleration model, developed by Abou Zeid et al. (2002). The resulting expected emission rates can then be used with any mesoscopic or macroscopic traffic model.

This chapter is organized as follows. In Section 5.1, we introduce the probabilistic approach for the integration of dynamic emission models with non-microscopic dynamic traffic models. In Section 5.2 we summarize the probabilistic acceleration model used in

our implementation. In Section 5.3 we use EMIT and the above acceleration model to derive expected emission and fuel consumption rates.

5.1 A Probabilistic Approach

We investigate the integration between dynamic emission models and non-microscopic dynamic traffic models. The latter models can be classified into those that represent the traffic in individual vehicles (mesoscopic models), and those that represent the traffic as a real number (macroscopic models). There is a variety of each of these two classes of models. Mesoscopic models can calculate the speeds of each vehicle at each time step, or the travel times of each vehicle to traverse each link on its path. Macroscopic models calculate the time-dependent flows entering each link and their average link travel times. All non-microscopic traffic models do not represent explicitly vehicle accelerations. Dynamic emission models, on the other hand, require second-by-second vehicle speed and acceleration. We consider only emission models that do not require as input the values of variables at past times (relative to the current time) (i.e. we consider only models that predict emission and fuel consumption rates at time t based on the speeds and accelerations at time t). The integration of dynamic emission models and dynamic traffic models consists of linking the traffic model's output with the emission model's input.

We propose a probabilistic approach for this integration, which can be adopted in applications where non-microscopic models are typically used, such as the analysis of large-scale networks and the solution of non-operational (such as planning) application problems.

Regardless the particular type of non-microscopic traffic model, it is always possible to obtain the time-dependent link travel time experienced by the traffic flow on each link. In order to obtain the time-dependent speeds for each vehicle, as required by the emission model, we make the following assumptions. Let j denote a generic vehicle, l denote a generic link, t_e denote entrance time in a link, tt denote travel time, and L denote the link length.

- In mesoscopic models, we assume that each vehicle j , which enters link l at time $t_{j,l}^e$ and traverses link l in a travel time equal to $tt_{j,l}$, travels at a speed approximately equal to $v_{j,l} = L/tt_{j,l}$ during its entire traversal of link l (i.e. from time $t_{j,l}^e$ to time $t_{j,l}^e + tt_{j,l}$).
- In macroscopic models, we assume that all vehicles that enter link l at time t_l^e , which have an average link travel time tt_l , travel at a speed approximately equal to $v_l = L/tt_l$ during their entire traversal of link l (i.e. from time t_l^e to time $t_l^e + tt_l$).

Although the speed is assumed to be approximately constant along each link for each vehicle (mesoscopic models) or group of vehicles (macroscopic models), we need to model the accelerations to feed the emission model. We propose to model accelerations as random variables distributed according to some known distribution, for a given speed range and for given values of other parameters, such as road type, vehicle category, and driver characteristics (e.g. aggressiveness, age, gender, etc.). The probabilistic acceleration model that we use is described in Section 5.2.

The accelerations estimated with this approach do not attempt to capture the vehicle dynamics (as they do in microscopic traffic models), but are random variables determined empirically. As a consequence, emission and fuel consumption rates calculated for a generic vehicle by the emission model are random variables. We propose (see Figure 5-1) to calculate the expected emission and fuel consumption rates for a generic vehicle, for given speed ranges and for the values of the other parameters used in the acceleration model, such as road type, vehicle category, and driver characteristics. The calculated expected emission rates are applied to the traffic flow, given the values of vehicle speed and of the other parameters. Once the emissions are calculated for all vehicles at each time instant, they are aggregated in time and/or space (i.e. whole network or sub-networks). It is possible to extend this method to calculate other moments of the emission distribution, such as the variance, in addition to the expected value.

The expected values of emission and fuel consumption rates can be calculated in advance (off-line), and their use is computationally equivalent to the use of emission maps. Therefore, the integrated model constituted by a non-microscopic traffic model and the expected emission and fuel consumption rates would run fast, allowing the simulation of many alternative policies and scenarios in a reasonable time.

With respect to the domain of applicability of the above approach, it is important to specify the following. The emission and fuel consumption rates calculated with this approach cannot represent accurately second-by-second emission and fuel consumption rates of individual vehicles. The combined model has to be used not with respect to single vehicles, but with respect to a large number of events (simulated observations) where vehicles have homogeneous characteristics (i.e. with the same speed range and the same value of the other parameters considered in the acceleration model). Therefore, the applicability of the approach is limited to cases when the number of homogeneous events is large enough over space at a given time, and/or over time on a given link or set of links. This is usually

verified if emissions are aggregated in a large network, or over a long period of time¹⁰ (as in the case of planning applications). The proposed approach is then not applicable to problems that involve the modeling of hot spots or high temporal resolution phenomena.

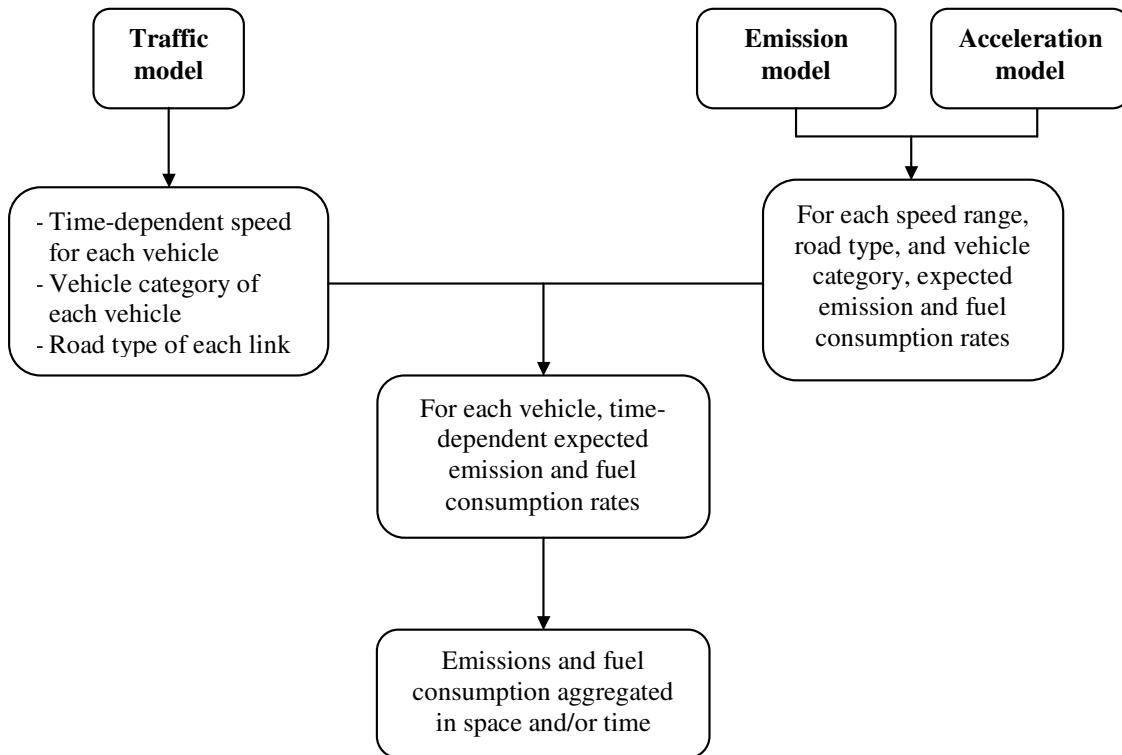


Figure 5-1: Probabilistic approach for the integration between dynamic emission models and non-microscopic dynamic traffic models.

Note: road type is an example of the other possible parameters used in the acceleration model, in addition to speed range.

5.2 Probabilistic Acceleration Model

Because of power and traction limitations of vehicles, the potential for accelerating decreases as speed increases. Decelerations are also limited by traction and braking factors. As these limitations impose bounds on accelerations/decelerations, they are usually not sufficient to describe the dynamics of vehicles.

¹⁰ Given the above assumptions on the speeds, even a single vehicle on a single link produces a large number of homogeneous events. For example, a vehicle traveling on a 1 km link with a speed of 50 km/h produces 70 events, one for each second of the traversal time.

Studies in the literature show that acceleration patterns might be dependent on speed range (Williams et al., 1999), road type, vehicle category, and driving characteristics (Hallmark et al., 2002; Fancher et al., 1998). One possible method to model the acceleration consists in using a probabilistic distribution as a function of the speed and other parameters. The approach presented in Williams et al. (1999) comes close to achieving this goal, but lacks generality and specific statistics.

In this section we present and implement a model recently developed in Abou Zeid et al. (2002), which we use in Section 5.3 to develop the expected emission rates. First we present the model formulation. Then we describe the data used for the model development. Finally, we report the results.

5.2.1 Model Formulation

In Abou Zeid et al. (2002), acceleration is modeled as a random variable, for a given speed range and road type. Although the calibrated parameters and the functional forms used in this model might be specific of the data used, the same methodology can be adopted to develop other acceleration probability distributions. For example, the same methodology can be applied taking into account other parameters, in addition to road type, such as vehicle category and driver characteristics.

The probabilistic modeling of acceleration distributions was conducted as follows. For each road type and speed range (intervals of 10 km/h), a probability distribution was calibrated on the acceleration frequency obtained from the data. Because acceleration and deceleration may have different behaviors, different probability distributions were calibrated. The calibrated distributions are two half-normal distributions, expressed by the following equations:

$$f_{r,v}^{-}(a) = \frac{2}{\sqrt{2\pi}\sigma_{r,v}^{-}} e^{-\frac{1}{2}\left(\frac{a}{\sigma_{r,v}^{-}}\right)^2} \quad \text{given } a \leq 0 \quad (5.1a)$$

$$f_{r,v}^{+}(a) = \frac{2}{\sqrt{2\pi}\sigma_{r,v}^{+}} e^{-\frac{1}{2}\left(\frac{a}{\sigma_{r,v}^{+}}\right)^2} \quad \text{given } a > 0 \quad (5.1b)$$

where $f_{r,v}^{-}(a)$ and $f_{r,v}^{+}(a)$ are respectively the density functions of the deceleration and acceleration distributions. In Equation 5.1, r denotes the road type, v denotes the speed range, a denotes the acceleration, and $\sigma_{r,v}^{-}$, and $\sigma_{r,v}^{+}$ are the standard deviations of the distributions of a , given $a \leq 0$ and $a > 0$ respectively.

In order to consider only physically feasible accelerations, the two half-normal distributions (5.1a) and (5.1b) are truncated at a_v^- and a_v^+ respectively. a_v^- and a_v^+ represent the extreme values of deceleration and acceleration, which in general, for a given vehicle category, depend on speed. The two truncated half-normal distributions are then normalized in the intervals $(a_v^-, 0)$ and $(0, a_v^+)$, which is done by dividing $f_{r,v}^-(a)$ and $f_{r,v}^+(a)$ by $\int_{a_v^-}^0 f_{r,v}^-(a) da$ and by $\int_0^{a_v^+} f_{r,v}^+(a) da$ respectively.

The complete distribution of the accelerations/decelerations, denoted by $f_{r,v}^*(a)$, is obtained as follows. The truncated and normalized distributions are weighted respectively with the probability of instances when $a \leq 0$, denoted by $P_{r,v}^-$, and the probability of instances when $a > 0$, denoted by $P_{r,v}^+$. $f_{r,v}^*(a)$ is then given by:

$$f_{r,v}^*(a) = \begin{cases} P_{r,v}^- \cdot \frac{f_{r,v}^-(a)}{\int_{a_v^-}^0 f_{r,v}^-(a) da} & \text{for } a \leq 0 \\ P_{r,v}^+ \cdot \frac{f_{r,v}^+(a)}{\int_0^{a_v^+} f_{r,v}^+(a) da} & \text{for } a > 0 \end{cases} \quad (5.2)$$

5.2.2 Data

The data used for the model development was collected by the University of Michigan Transportation Research Institute, as part of an Intelligent Cruise Control (ICC) study (Fancher et al., 1998). The intelligent cruise control was not functional during the first week of the study. The model of acceleration is built on this real-world driving portion of the data. 108 randomly chosen drivers participated in the study, driving in counties of South Eastern Michigan that include major metropolitan areas as well as rural areas.

The number of trips conducted by every driver varied between 20 and 60, where most trip durations were less than 30 minutes. The road links were classified in the study in several road types: interstate highway, state highway, arterial, collector, light duty, high-speed ramp, low-speed ramp, alley or unpaved, and unknown. The drivers were classified in five categories, according to their driving behavior: ultraconservative, planner, flow conformist, hunter/tailgater, and extremist. The same type of vehicle was used by all drivers: an instrumented 1996 Chrysler Concorde. Therefore, the parameters of the distributions are specific to this type of vehicle and the model of acceleration correspond to this vehicle type only.

In the development of the model of acceleration, a sub-sample of 18 drivers, representing all five driving behaviors, was considered. With respect to road type, the

following four road types have been considered: interstate highways, state highways, arterials, and collectors. These categories contain most of the observations. Furthermore, for practical purposes, these road types cover most road types in the transportation networks considered in planning applications (except for on-ramps and off-ramps).

5.2.3 Results

Table 5.1 reports the standard deviations calibrated, as described in Abou Zeid et al. (2002), for every road type and speed range. Table 5.2 reports the respective number of observations. Figures 5-3 and 5-4 represent the values of Table 5.1 separately for accelerations and decelerations. The following observations can be made:

- As the speed increases, the variance of the acceleration and deceleration distributions decreases. The only exception is the increase of the standard deviation from the 0–10 km/h to the 11–20 km/h speed range. This behavior is probably due to the common “lurch”¹¹ that follows a light change, or to the stop-and-go traffic, or to the automatic transmission “creep”¹² that accompanies very slow traffic.
- The data show that, in the specific data used for the model calibration, road type has little effect on acceleration and deceleration variation. While it is expected that stop and go conditions, characteristic of collectors and arterials, might lead to higher acceleration and deceleration values, the results actually indicate that highways have similar acceleration/deceleration standard deviations as those of arterials and collectors, and in some cases have even higher variations. This observation is consistent with other results in the literature (LeBlanc et al., 1995).

¹¹ “Lurch” is a sudden positive variation in acceleration.

¹² “Creep” is a very slow motion of the vehicle, usually at a constant speed. This occurs because auto transmissions are in gear (even at stop) and do not go into neutral unless forced.

Table 5.1: Standard deviation of acceleration and deceleration as a function of speed range and road type.

Speed range (km/h)	Acceleration				Deceleration			
	Interstate highway	State highway	Arterial	Collector	Interstate highway	State highway	Arterial	Collector
0 – 10	0.971	1.004	0.972	0.914	1.119	1.020	1.176	1.089
11 – 20	1.451	1.331	1.514	1.416	1.294	1.145	1.322	1.302
21 – 30	1.325	1.261	1.334	1.165	1.108	1.000	1.128	1.067
31 – 40	1.070	0.994	1.131	0.943	1.107	1.052	1.208	1.001
41 – 50	0.904	0.757	0.897	0.739	0.884	0.805	0.801	0.686
51 – 60	0.696	0.625	0.638	0.541	0.660	0.563	0.484	0.470
61 – 70	0.569	0.559	0.516	0.473	0.515	0.452	0.378	0.383
71 – 80	0.462	0.450	0.480	0.418	0.433	0.340	0.386	0.306
81 – 90	0.427	0.413	0.400	0.375	0.374	0.308	0.346	0.277
91 – 100	0.368	0.407	0.395		0.232		0.261	
101 – 110	0.351				0.228			
111 – 120	0.353				0.180			

Table 5.2: Number of observations of acceleration and deceleration for every speed range and road type.

Speed range (km/h)	Acceleration				Deceleration			
	Interstate highway	State highway	Arterial	Collector	Interstate highway	State highway	Arterial	Collector
0 – 10	319	356	1130	346	475	571	1775	578
11 – 20	277	333	927	299	365	429	1353	438
21 – 30	404	432	1476	618	502	551	1800	792
31 – 40	364	358	1200	578	437	430	1305	810
41 – 50	531	509	1870	920	582	751	2546	1759
51 – 60	609	524	2408	1147	840	934	4588	2519
61 – 70	514	430	1764	1080	913	870	3573	2216
71 – 80	479	475	815	638	961	1178	1313	1530
81 – 90	488	198	301	178	1025	360	452	401
91 – 100	854	18	68		3673		117	
101 – 110	636				2192			
111 – 120	122				604			

To truncate and weight the half-normal distributions, a_v^- , a_v^+ , $P_{r,v}^-$, and $P_{r,v}^+$ are estimated. The extreme values of deceleration and acceleration are respectively: $a_v^- = -5 \text{ m/s}^2$ and $a_v^+ = 5 \text{ m/s}^2$ for speed ranges from 0-10 to 71-80 km/h, $a_v^- = -2.5 \text{ m/s}^2$ and $a_v^+ = 2.5 \text{ m/s}^2$ for speed range 81-90 km/h, $a_v^- = -1 \text{ m/s}^2$ and $a_v^+ = 1 \text{ m/s}^2$ for speed range 91-100 km/h, $a_v^- = -0.75 \text{ m/s}^2$ and $a_v^+ = 0.75 \text{ m/s}^2$ for speed range 101-110 km/h, and $a_v^- = -0.5 \text{ m/s}^2$ and $a_v^+ = 0.5 \text{ m/s}^2$ for speed range 111-120 km/h. These values are approximately the maximum values of deceleration and acceleration present in the database for each speed range. $P_{r,v}^-$ and $P_{r,v}^+$ are estimated for each road type and speed range with the sample relative frequency respectively of $a \leq 0$ and $a > 0$ from the database.

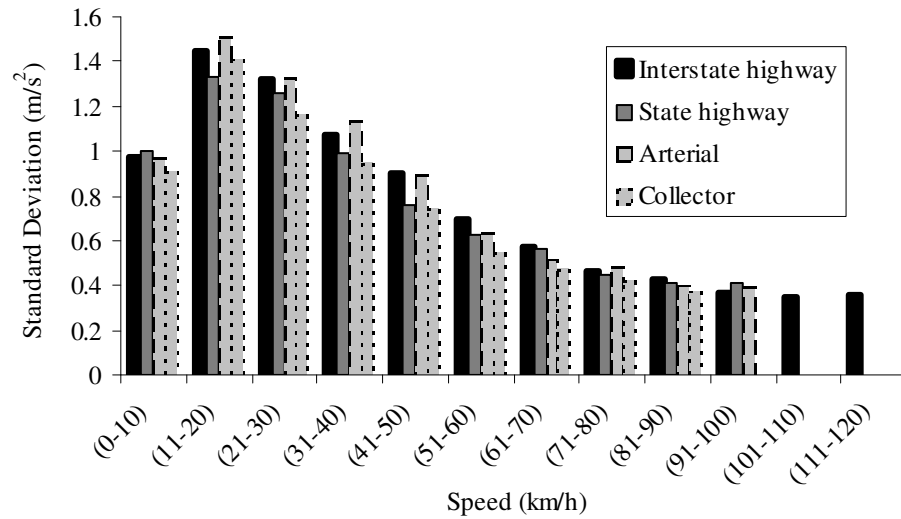


Figure 5-3: Standard deviations of the acceleration distributions for every speed range and road type (from Abou Zeid et al., 2002).

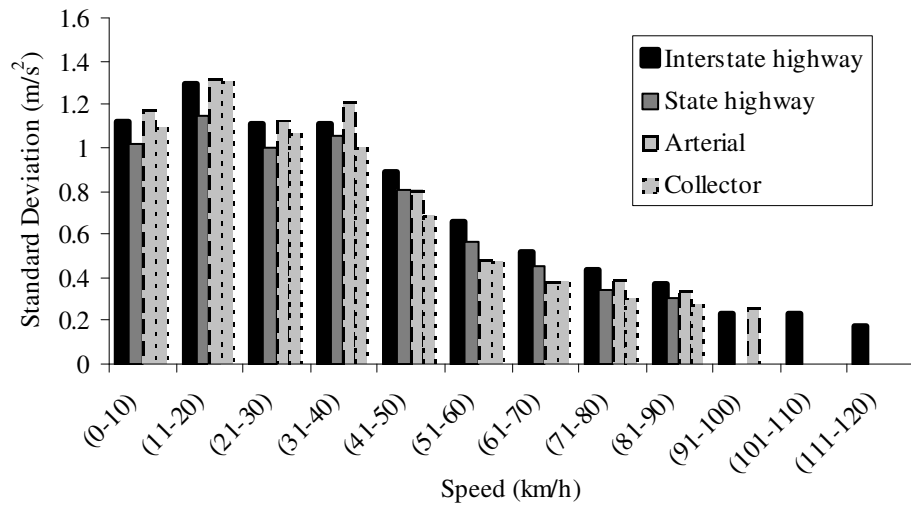


Figure 5-4: Standard deviations of the deceleration distributions for every speed range and road type (from Abou Zeid et al., 2002).

The error analysis conducted in Abou Zeid et al. (2002) confirms the hypothesis that the accelerations and decelerations are distributed as in Equation 5.2. As an example, Figure 5-5 compares, for the road type arterial and for the speed range 0-10 km/h , the cumulative relative frequency from the data and the cumulative probability from the calibrated model of positive accelerations. Figures for medium and high speeds and other road types would indicate slightly different results.

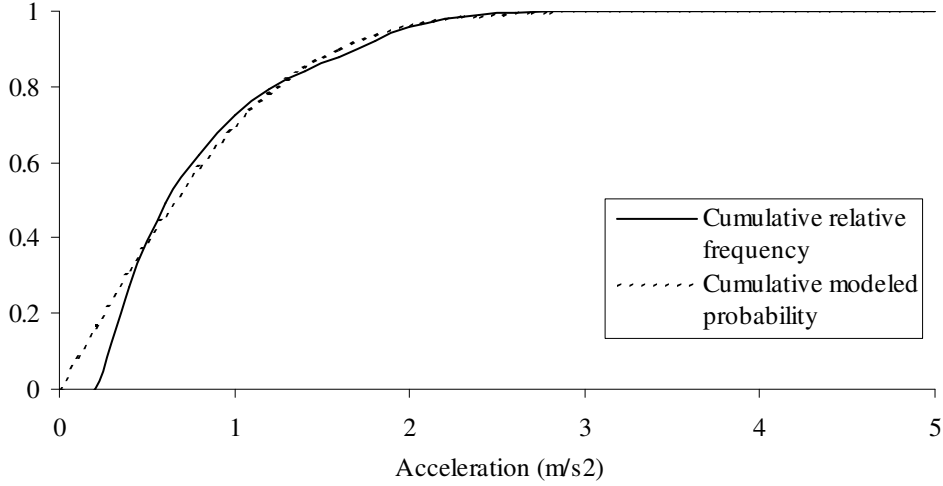


Figure 5-5: Cumulative relative frequency and cumulative modeled probability of accelerations for the road type arterial and speed range (0-10) km/h (from Abou Zeid et al., 2002).

5.3 Expected Emission Rates for a Given Speed and Road Type

Now we describe how speed and road type dependent expected emission rates are generated applying EMIT to the above acceleration model.

For a given emission species i and vehicle category c , let $e_{i,c}(v, a)$ denote the emission rate as a function of vehicle speed v and acceleration a . $e_{i,c}(v, a)$ is calculated by using EMIT.

Let $\bar{e}_{i,c,r,v}$ denote the expected emission rate for species i , vehicle category c , road type r and speed range v . By definition $\bar{e}_{i,c,r,v}$ is:

$$\bar{e}_{i,c,r,v} = E_{a \in [a_1, a_2]} [e_{i,c}(v, a)] = \int_{a_1}^{a_2} e_{i,c}(v, a) \cdot f_{r,v}^*(a) da \quad (5.3)$$

To calculate $\bar{e}_{i,c,r,v}$, the variable a is discretized in the interval $[a_1, a_2]$, and Equation 5.3 becomes:

$$\bar{e}_{i,c,r,v} = \sum_{a \in S_a} e_{i,c}(v, a) \cdot \pi_{r,v}(a) \quad (5.4)$$

where:

$S_a = \{a_1 + h/2, a_1 + 3h/2, \dots, a_2 - 3h/2, a_2 - h/2\}$ is the discretization interval. We adopt $h = 0.1 \text{ m/s}^2$.

$\pi_{r,v}(a) = \int_{a-h/2}^{a+h/2} f_{r,v}^*(x) dx$ is the probability that the realization of the random variable

acceleration \bar{a} is in the interval $(a - h/2, a + h/2)$.

Figures 5-6 and 5-7 depict $\bar{e}_{i,c,r,v}$ for the road types arterial and highway, both for vehicle category 9 (which is defined in Section 4.2.3). As expected, $\bar{e}_{i,c,r,v}$ is in general increasing with the vehicle speed. In fact, the higher the speed, the higher the fuel consumption rate, and the higher the emission rates, which have a positive correlation with fuel rate (see Equation 4.6). For CO , there is a rapid increase in the expected emission rate for high values of speed, due to enrichment conditions.

$\bar{e}_{i,c,r,v}$ can be used to estimate the emissions generated by a traffic flow, as described in Section 5.1.

We observe that as speed increases, emission rates increase, but travel time decreases. We are then interested in analyzing which of the two effects prevails in a hypothetical trip traveled at speed v . Therefore, we also calculate the expected emission rates per km traveled, dividing the expected emission rates $\bar{e}_{i,c,r,v}$ by the speed v . The results for the road types arterial and highway are depicted in Figures 5-6 and 5-7. We note that $\bar{e}_{i,c,r,v}$ presents a relative minimum between 50 and 70 km/h, which in general corresponds to an absolute minimum in the expected emission rates per km traveled.

The expected emission rates per km traveled of CO , HC , and NO_x are also compared with the corresponding emission rates from MOBILE6. These are obtained using the MOBILE6 Tier 1 hot-stabilized basic emission rates (BERs) and the facility-specific speed correction factors developed in EPA (2001a) (see Section 3.1.2).

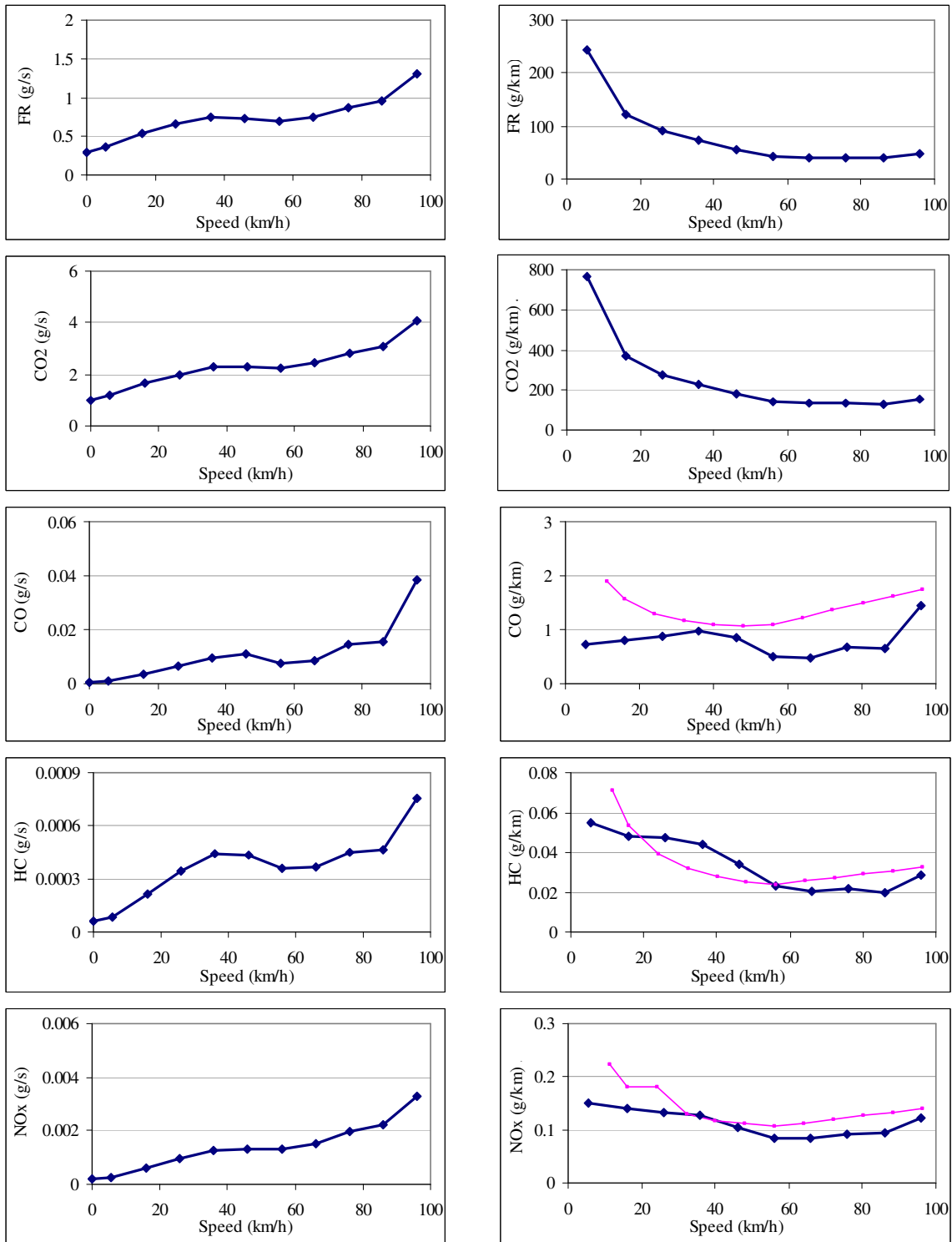


Figure 5-6: Expected emission rates in g/s (on the left) and in g/km (on the right) for road type arterial and vehicle category 9. The expected emission rates in g/km of CO, HC, and NO_x are compared with the facility-specific emission rates from MOBILE6 (thin line).

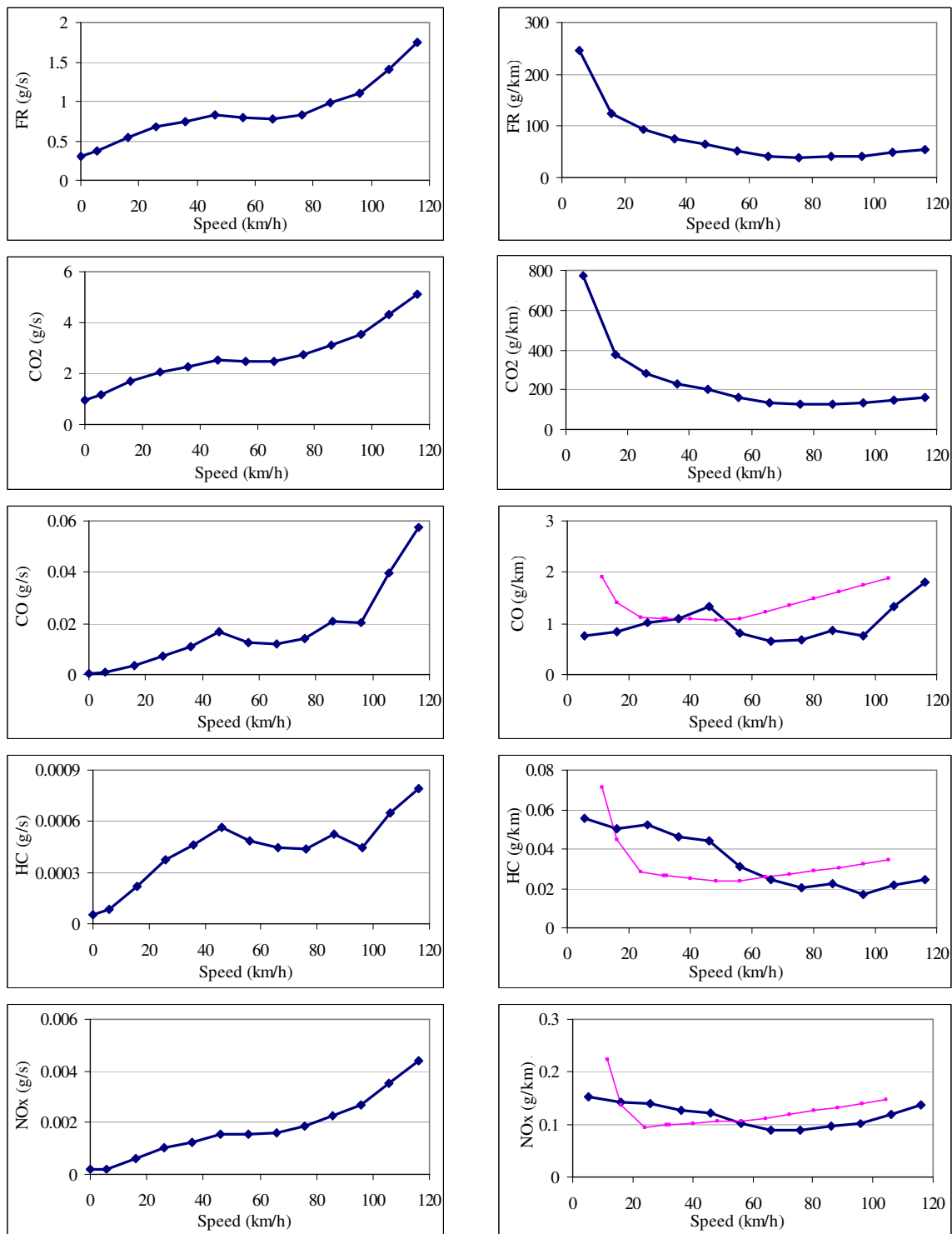


Figure 5-7: Expected emission rates in g/s (on the left) and in g/km (on the right) for road type highway and vehicle category 9. The expected emission rates in g/km of CO, HC, and NO_x are compared with the facility-specific emission rates from MOBILE6 (thin line).

Chapter 6

A Case Study of Traffic Flow Emissions and Fuel Consumption on a Small Network

In this chapter, we present a realization of the approach described in Chapter 5 to integrate dynamic emission models and non-microscopic dynamic traffic models. A set of modeling tools is used to predict the emissions generated and the fuel consumed in a hypothetical case study involving a small traffic network. An objective of this chapter is to test the potential of the methodology proposed in this thesis to predict the effects of congestion and emissions management policies. This is shown by considering various scenarios of traffic conditions and management strategies. The scenarios include situations with and without a traffic incident, and with and without Intelligent Transportation Systems (ITS) measures to alleviate congestion and its effects.

This chapter is organized as follows. Section 6.1 describes the modeling tools. Section 6.2 describes the case study data. Section 6.3 analyzes the results.

6.1 The Modeling Tools

Given a time-dependent O-D demand on a network, we want to estimate the total emissions and fuel consumption aggregated in space and/or time, as discussed in Section 5.1 of this thesis. This section describes the set of modeling tools used.

Figure 6-1 represents the types of modeling tools used, which are:

1. a mesoscopic dynamic traffic model;
2. an expected emission rates component;
3. an integration component.

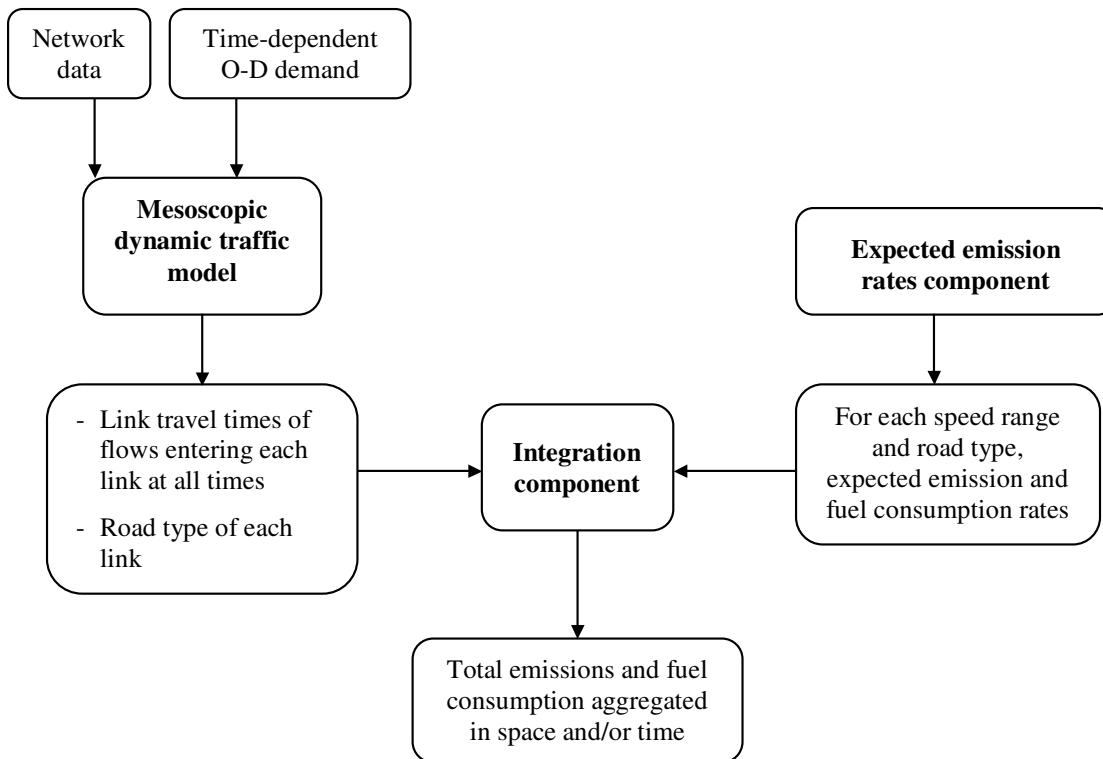


Figure 6-1: Set of models used for the prediction of fuel consumption and emissions on a traffic network.

6.1.1 Mesoscopic Traffic Model

The traffic model used is a simple simulator, designed, and implemented in C++, by Bottom (2000). The model represents links as deterministic first-in-first-out (FIFO) single-server queues with given exit (service) rate and storage capacities. The model represents the traffic in individual vehicles but does not attempt to accurately represent vehicle trajectories and dynamics within a link. A description of the model can be found in Bottom (2000). In this section we provide only the characteristics needed for the discussion related to the case study of this thesis.

The model can represent two types of route guidance: (a) an ubiquitous (available at any node and at all times) route guidance available to a subset of equipped vehicles (possibly all vehicles), and (b) a short-range guidance, available on specific links, which can be accessed by any vehicles in the link. Short time guidance is intended to represent technologies such as variable message signs (VMS).

Therefore, from a route guidance standpoint, traffic can be classified in two information classes: vehicles equipped with route guidance provision, and unequipped vehicles. Equipped vehicles know at each node of their trip the fastest path to their destination, based on consistent anticipated travel times. Unequipped vehicles base their path choice decisions on background travel times, unless they arrive on a link where a VMS is available, at which time they receive the latest estimates of consistent anticipated travel times. They reconsider their current path, and possibly proceed to a different new path. All drivers are assumed to fully comply with the indication provided by the route guidance.

The main inputs to the model are the traffic network configuration and the time-dependent origin-destination (O-D) travel demand. The traffic network configuration is defined in terms of geometry, link capacities, free-flow speeds, and presence of VMS. The O-D demand is defined in terms of step-wise demand flow rates (vehicles/hour) for each O-D pair and for each vehicle information class.

The outputs of the model are, at each time instant of the simulation (i.e. at each second), the number of vehicles entering each link and their respective travel time to traverse that link.

Since this traffic model currently does not allow representing multiple vehicle categories from an emission standpoint, the vehicle fleet is assumed to be composed by just one vehicle category (vehicle category 9, which is defined in Section 4.2.3). Therefore, the effects of multiple vehicle categories simultaneously traveling in the network are not analyzed in this case study.

6.1.2 Expected Emission Rates Component

This tool is described in Section 5.3 of this thesis. It uses a probabilistic model of acceleration and a dynamic emission model.

The probabilistic acceleration model used is described in Section 5.2. Its inputs are the link road types and vehicle speed ranges. Its outputs are the probabilistic distributions of accelerations for each road type and speed range.

The emission and fuel consumption model used is EMIT, which is described in Chapter 4. Its inputs are second-by-second speed and acceleration and vehicle category (though in our case study the vehicle fleet is assumed to be composed by just category 9 vehicles). The outputs of the emission model are second-by-second fuel consumption and emission rates of CO_2 , CO , HC , and NO_x .

This component calculates the expected emission and fuel consumption rates for each speed range. This is obtained by combining EMIT and the probabilistic acceleration model. The results for arterials and interstate highways are shown in Figures 5-6 and 5-7.

The expected emission and fuel consumption rates can be calculated in advance (off-line), and then used as an input to the integration component. For the calculation we used a spreadsheet.

6.1.3 Integration Component

This component links the outputs of the traffic model and the expected emission rates component to calculate the total emissions generated and fuel consumed by the traffic flow. The component, which we coded in C++, performs the following three steps in order:

Step 1 – The first step is to calculate at each second the number of vehicles traveling on each link, and their speeds. This information is obtained from the output of the traffic model (number of vehicles entering each link at each second, and their travel times to exit the link), assuming that each vehicle j travels at a speed approximately equal to $v_{j,l} = L_l / tt_{j,l}$ during its entire traversal of link l (see Section 5.1). Figure 6-2 illustrates this calculation with an example. The top table represents the output of the traffic model, while the bottom table represents the output of Step 1. At a given time t , it is possible to have, on the same link, vehicles that entered at different times, and traveling at different speeds. To represent this, we replicate the information related to each group of vehicles entering a link at a given entrance time t^e for each time t between their entrance time and their exit time. For example, in Figure 6-2, the 2 vehicles entering link 1 (1 km long) at time 1 have a travel time equal to 40 seconds. We want to represent that, from second 1 up to second 40, on link 1 there are 2 vehicles traveling at a speed equal to $1\text{km}/40\text{s}=90\text{km/h}$. Therefore, in the output table, we replicate the record containing the number of vehicles (2) and their speed (90) for all times from 1 to 40. Doing the same for all entrance times, we will obtain, for each time, the information (number, speed) of all the groups of vehicles traveling on each link.

Step 2 – Given the vehicle speeds calculated in Step 1, the integration component multiplies, at each time t , the number of vehicles traveling on link l (of road type r) at speed $v_{j,l}$ by the expected emission rates for speed $v_{j,l}$ and road type r .

Step 3 – Finally, the integration component aggregates the results over time, summing travel times, emissions, and fuel consumption over the vehicles traveling on each link, and then over all network links.

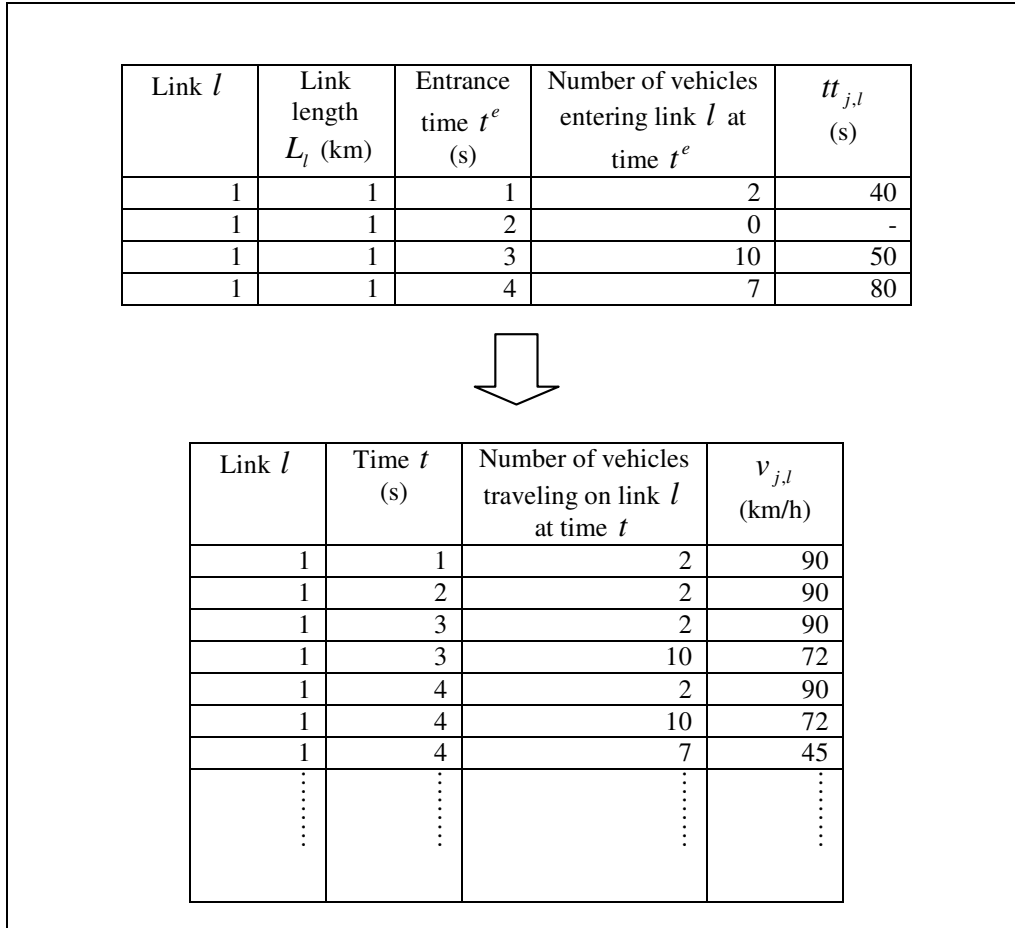


Figure 6-2: Example of calculation of the number of vehicles traveling on each link at each time step and their speeds.

These steps are designed in a general way, that can be easily extended to cases when the spatial and temporal distributions of the emissions along the links are considered. If, as in this case study, the final outputs are the total emissions aggregated over time, similar calculations can be done in other simpler ways.

6.1.4 Scheme of Input and Output Data

This section summarizes the input and output data involved in a run of the tools. In order to estimate the effects on travel times, emissions, and fuel consumption, of a scenario of traffic conditions and management strategies, it is necessary to run the traffic model and the

integration component. The expected emission rates are generated in advance, since they do not depend on the specific case study, and then used as input data to the integration component. Figure 6-3 shows the input data to and output data from the traffic model and the integration component.

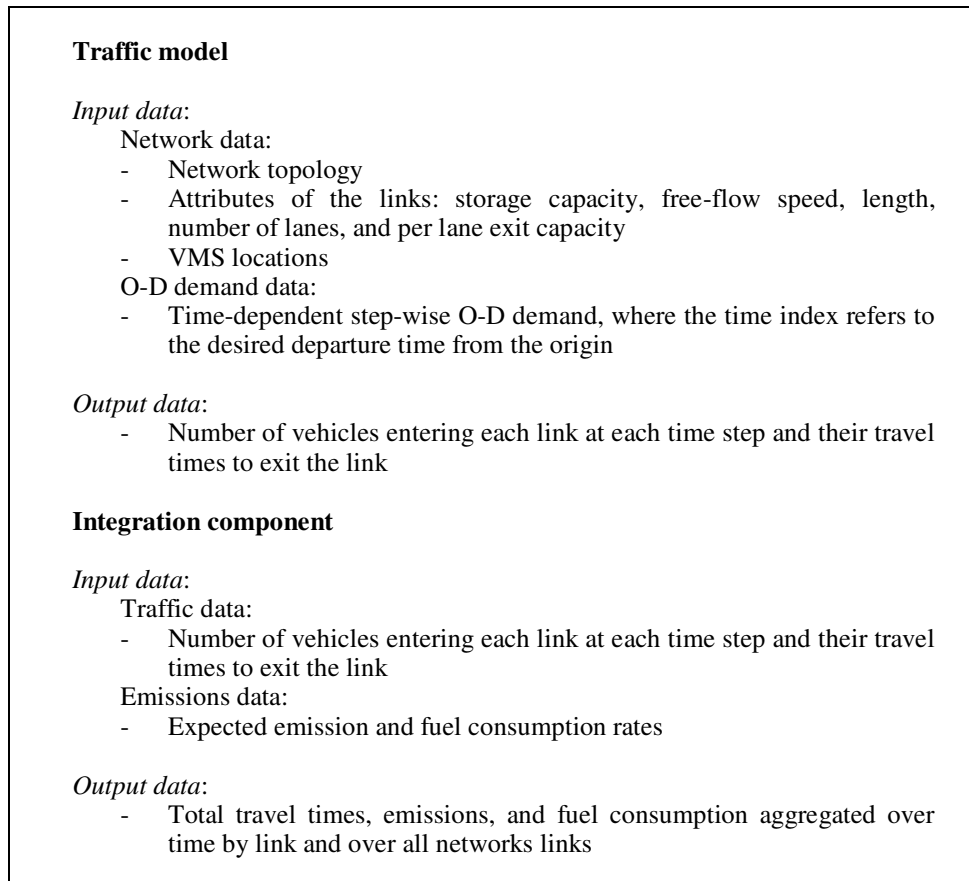


Figure 6-3: Input and output data of the traffic model and the integration component. The expected emission rates component is not represented because it is run in advance and it does not depend on the specific case study.

6.2 The Case Study Data

In this section we describe the network, the time-dependent O-D demand, and the scenarios that characterize the case study.

Figure 6-4 depicts the network used. The network contains 14 links and 9 nodes. All links are 1 km long except links 2 and 9, which are 1.5 km long. Vehicles are assumed to be 7.5 m long, thus the link storage capacity is about 133 vehicles for 1 km long links, and 200 vehicles for 1.5 km long links. The free-flow speeds of all links are equal to 100 km/h. Except for the centroid connectors (link 0 and 7), all links have a flow (and hence exit)

capacity, in normal conditions, equal to 3,600 vehicles/hour. The centroid connectors are considered to have length 0 and infinite storage capacity. All links are assumed to be arterials.

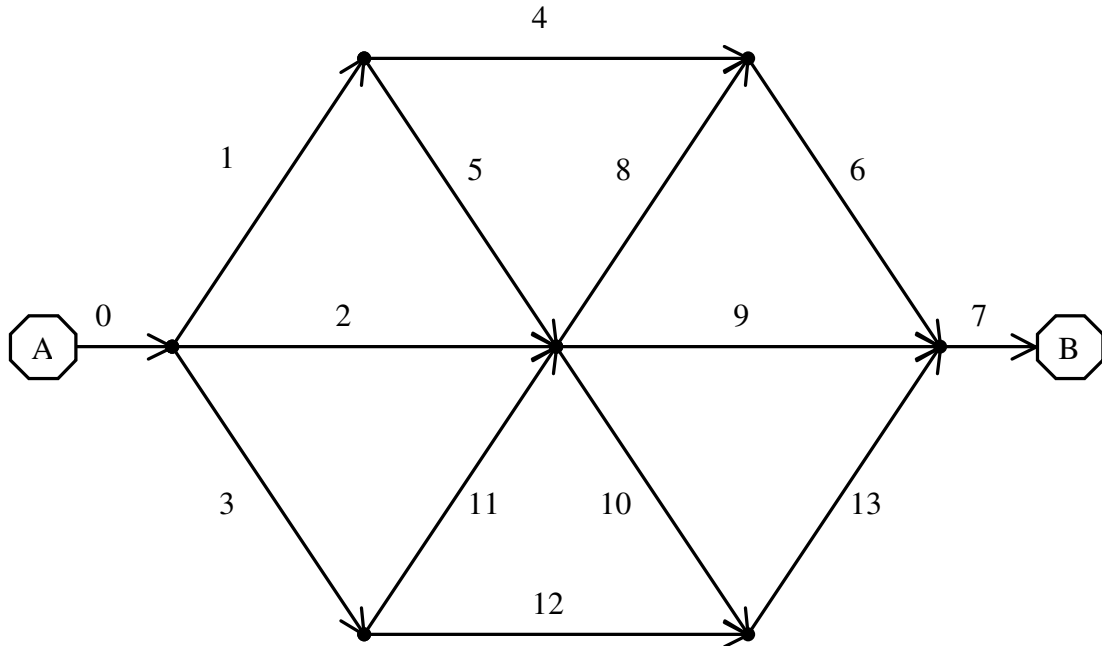


Figure 6-4: Network configuration of the case study.

The demand is present only from node A to node B (centroids). This O-D pair is connected by the following 11 paths: two 3 km long paths (1-4-6, 2-9, and 3-12-13), four 3.5 km long paths (1-5-9, 2-8-6, 2-10-13, and 3-11-9), and four 4 km long paths (1-5-8-6, 1-5-10-13, 3-11-10-13, and 3-11-8-6).

The O-D demand rate is equal to 10,800 veh/h, and its duration is equal to 20 minutes. The simulation ends when all vehicles have left the network. For simplicity, we assume that all vehicles belong to vehicle category 9 (defined in Section 4.2.3). Since the network is constituted of arterials, the expected emission rates shown in Figure 5-6 are used.

The system of models, presented in Section 6.1, is run for five scenarios. We investigate the change in total travel times, fuel consumption, and emissions due to an unplanned road blockage in the network. The blockage is simulated by reducing the capacity of the link where the blockage occurs throughout the entire simulation period. This might be thought of as an unplanned road blockage due to an incident that occurs during the night before the trip (when the network is empty), and about which trip makers only become aware through VMS or if their vehicle is equipped with route guidance provision. Unless they arrive on a

link where a VMS is available, unequipped vehicles base their path choice decisions on background travel times. The background travel times are those experienced in the same network given the same travel demand, and in absence of incidents, assuming that all users have complete information on the actual travel times.

We want to model also the impact of ITS measures implemented to mitigate the congestion induced by the incident. The ITS measures considered are the VMS and the ubiquitous guidance for a given percentage of vehicles equipped with route guidance provision.

The scenarios considered are the following:

- Scenario 0 – This is the background scenario, without incident, and with route guidance to all vehicles. It simulates a situation where all users have become aware of the fastest path to their destination, because of their experience acquired, for example, from everyday trips on the same network.
- Scenario 1 – This is a scenario with incident on link 6 (modeled by reducing the capacity of link 6 from 3,600 veh/h to 1,800 veh/h), with no VMS, and no vehicles equipped with route guidance provision.
- Scenario 2 – This is a scenario with the same incident on link 6 (modeled by reducing the capacity of link 6 from 3,600 veh/h to 1,800 veh/h), with no VMS, and with 25% vehicles equipped with route guidance provision, and 75% unequipped vehicles.
- Scenario 3 – This is a scenario with the same incident on link 6 (modeled by reducing the capacity of link 6 from 3,600 veh/h to 1,800 veh/h), with a VMS on link 1, and no vehicles equipped with route guidance provision.
- Scenario 4 – This is a scenario with the same incident on link 6 (modeled by reducing the capacity of link 6 from 3,600 veh/h to 1,800 veh/h), with a VMS on link 1, and with 25% vehicles equipped with route guidance provision, and 75% unequipped vehicles.

6.3 Results

Appendix B reports the outputs of the traffic model (time-dependent link volumes and link travel times) for the simulated scenarios. Depending on the scenario, the duration of the simulation varies from 1,344 seconds (scenario 0) to 2,575 seconds (scenario 1).

Appendix C reports, for each link, the results for all scenarios aggregated over time on each link. The measures reported are total fuel consumption, total tailpipe emissions of CO_2 , CO , HC , and NO_x , total travel time, and total number of vehicles. These results are useful in the case the analyst is interested in looking at the individual links. For example,

these results can be used to analyze the effects of the scenarios on single links in the proximity of particularly sensitive facilities (e.g. an hospital or a school).

Table 6.1 and Figure 6-5 report, for all scenarios, the results aggregated on all network links and over time. The measures reported are: total fuel consumption, total tailpipe emissions of CO_2 , CO , HC , and NO_x , and total travel time. In Figure 6-5, as well in Appendix C, the measures are represented with different units, in order to visualize them all in the same plot across the various scenarios.

First, we analyze the variations in total travel time across the scenarios.

Scenario 0 represents (as shown in Figure B-1) a user optimum situation¹³. In this scenario, the O-D demand is up to the capacity of the network. A relatively small increase of the O-D demand or a reduction of the network capacity would increase significantly the travel times.

The comparison between scenario 0 and scenario 1 shows that in case of incident, when the users are not aware of it, the congestion increases dramatically (the total travel time triplicates).

In scenarios 2, 3, and 4, the effects of the incident are alleviated as a result of the route guidance. The total travel times are reduced by approximately 40% in all scenarios, compared with scenario 1.

The total travel times of these three scenarios are very similar (the maximum difference is approximately 1.5%). The different levels of information to the users provided by the ubiquitous route guidance and/or VMS do not correspond to significantly different total travel times. Reasons for this can be the following:

- The users' optimal route choice does not necessarily correspond to system optimal criteria. Route guidance optimizes the path choice based on the user optimum, while total travel time is minimized if the optimization is based on system optimum.
- The effectiveness of the VMS is strictly related to its location. In this case study, the VMS is very effective because is located on the first link of the most traveled path that contains the link where the incident occurs.

Now we analyze the variations in terms of total fuel consumption and total emissions across the scenarios.

¹³ Since the traffic model assumes some stochasticity in the users' path choice, also the longer paths are used by a small number of users.

The total fuel consumption and the total emissions of CO_2 follow the trend of the total travel time. For these species, scenario 0 and scenario 1 present respectively the lowest and the highest values, while scenarios 2, 3, and 4 present intermediate values. For CO , the total emissions in scenarios 0 and 1 are comparable, while scenarios 2, 3 and 4 produce lower emissions. The higher total emissions of scenario 0, compared with scenarios 2, 3, and 4, are probably due to the tradeoff between the values of the expected emission rates and the total travel times, during which the vehicles generate the emissions. In scenario 0, the vehicles spend less time in the network, because there is no congestion. However, their speeds are significantly greater, and the values of the expected emission rates, which increase significantly at high speeds (see Figure 5-6), make higher the total emissions.

For HC and NO_x , the total emissions in scenarios 0, 2, 3, and 4 are comparable. Slightly higher HC and NO_x emissions are predicted for scenario 1. A reason for the low sensitivity of the total emissions of these species can be found in the low sensitivity to speed of their expected emission rates per km (see Figure 5-6).

Table 6.1: Total fuel consumption, tailpipe emissions, and travel time (tt) aggregated on all network links and over time for every scenario modeled.

scenario	fuel (g)	CO ₂ (g)	CO (g)	HC (g)	NO _x (g)	tt (s)
0	543,024	1,697,068	14,059	297	1,307	484,209
1	928,030	2,889,707	14,568	402	1,530	1,531,216
2	679,980	2,130,719	10,835	347	1,276	901,880
3	687,733	2,146,816	10,895	362	1,303	886,212
4	675,462	2,119,650	10,041	352	1,270	902,277

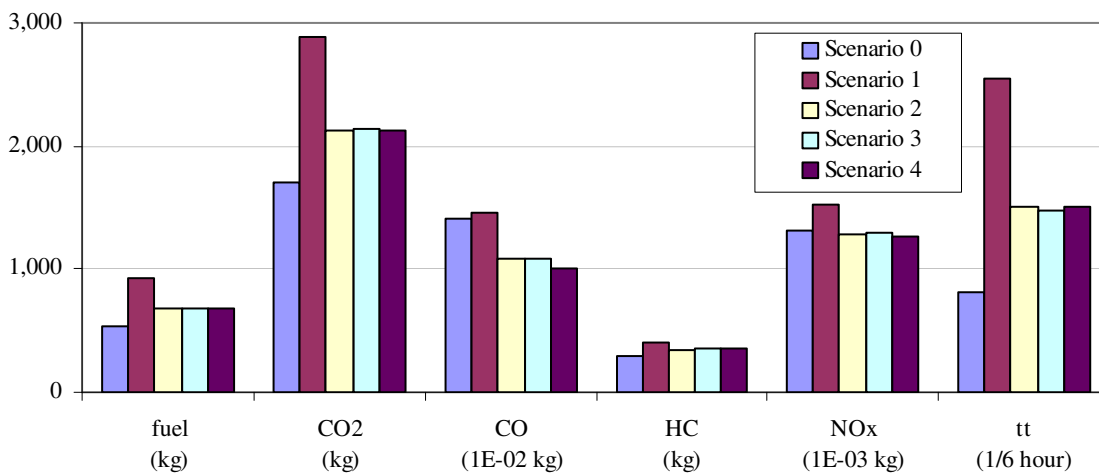


Figure 6-5: Total fuel consumption, tailpipe emissions and travel time (tt) aggregated on all network links and over time for every scenario modeled.

Chapter 7

Conclusions and Directions for Future Research

In this chapter, we summarize the main contributions and results of this thesis, and we identify limitations that can be addressed in future research and other research areas that have not been explored in this thesis.

In the first main part of this thesis, we developed and implemented EMIT, a dynamic model of emissions (CO_2 , CO , HC , and NO_x) and fuel consumption for light-duty vehicles. The model is derived from two emissions modeling approaches (regression-based and load-based), and effectively combines some of their respective advantages. EMIT has been calibrated and validated for two vehicle categories. The model runs fast and is relatively simple to calibrate. The results for the two categories calibrated indicate that the model gives reasonable results compared to actual measurements as well to results obtained with CMEM, a state-of-the-art load-based emission model. In particular, the estimation capabilities of the model are highest for fuel consumption and carbon dioxide, good for carbon monoxide and nitrogen oxides, and less desirable for hydrocarbons.

Several questions for future research related on EMIT are the following:

1. EMIT has been developed and calibrated for hot-stabilized conditions with zero road grade, and without accessory usage. The model does not represent history effects, such as cold-start emissions and hydrocarbon enleanment puffs. Future research should address how to overcome these limitations, in order to provide greater generality to the model. In the conclusions of Chapter 4 of this thesis (Section 4.6) we propose modifications to the model to include road grade, cold starts and hydrocarbon enleanment puffs. These potential modifications can be realized relatively easily. How

to make the model take account of accessory usage appears, however, to be a more challenging question.

2. The introduction of history effects in the emission model should be complemented with an investigation of how the integration with non-microscopic traffic models would be affected by this enhancement.
3. EMIT needs to be calibrated for the other categories present in the NCHRP vehicle emissions database. Moreover, in order to represent the actual emissions sources present on roadways, other databases should be acquired and used for the model calibration, including data on heavy trucks, buses, more recent vehicles than those represented in the NCHRP database, and on-road measurements.
4. The model can be extended to other emission species, such as particulate matter and air toxics, when data are available.

In the second main part of this thesis, we proposed an approach to integrate dynamic emission models with non-microscopic dynamic traffic models. The latter models do not estimate vehicle acceleration. The proposed approach requires the calculation of expected emission and fuel consumption rates. These are obtained by combining a dynamic emission model with a probabilistic acceleration model. The approach does not model trajectories of single vehicles. Therefore, the applicability of this approach is limited to large spatial scales, which arise for instance in transportation planning applications. The calculation of the expected emission and fuel consumption rates was implemented using EMIT and an experimental probabilistic acceleration model. In the latter model, acceleration is modeled as a random variable, for a given vehicle speed range and road type.

Future research should address the dependence of acceleration on other parameters, such as driver characteristics and vehicle category. In particular, driver behavior data should be investigated because they can have important impact on emissions. This would require the acquisition of additional appropriate data.

In the third part of this thesis, using the above approach, we combined the developed emission model and a mesoscopic dynamic traffic model to assess the impact of dynamic traffic management strategies on travel times, emissions, and fuel consumption. This was done on a small hypothetical case study and using route guidance as a traffic management technology.

Future applications of the combined set of models could cover more realistic and large networks, and consider a variety of policies, particularly policies with enforcement

mechanisms (such as congestion pricing and signal control) and emissions as primary control objective.

The effects of route guidance in the various scenarios were assessed from the point of view of total emissions (CO_2 , CO , HC , and NO_x) and total fuel consumption aggregated over the whole analysis period. These assessment criteria are only one of many other possible criteria. For instance, total waiting time in queues could be considered, in addition to the total travel time. The temporal and spatial dimensions may also be significant. In fact, effects on human health are related with the concentration of the pollutants in the air, that depends on the distribution over time and space of the emissions. Moreover, using data on land use and demographic density, it would be interesting to evaluate the degree of exposure of the population to the emissions for a given traffic management strategy.

Other areas that this thesis did not explore, but that are worth the investigation are:

1. Compare the proposed approach to integrate dynamic emission models and non-microscopic traffic models, to other approaches in the literature.
2. Develop other integrated models based on EMIT, but using other traffic models, including microscopic models and mesoscopic models that represent the variation of the speed within a link. An interesting aspect of this research direction would be the comparison of the computational efforts and the numerical accuracy of results obtained by each type of model.
3. Investigate the problem of fleet composition from an emission standpoint. Traffic models either do not represent vehicle categories, such as the mesoscopic model that we used in this thesis, or classify vehicles in coarse categories (i.e. small cars, large cars, trucks, buses). On the other hand, emission models generally need more accurate information on the vehicles, such as mileage, power/weight ratio, and model year. Most importantly, it is relevant to quantify the population of high emitters. Therefore, it is important to include more precise fleet information in traffic models or to develop statistical mapping systems between the traffic-relevant categories and the emission-relevant categories. This is an important aspect in order to estimate real-world emissions.
4. Build a comprehensive suite of analysis and modeling tools that includes a variety of types of traffic as well emission models. The suite can be a fundamental component of decision support systems for the generation, assessment and optimization of policies to alleviate congestion and the environmental impacts of road traffic. The modeling tools could be used in an integrated fashion. For example, mesoscopic models could be used

to analyze a large network, while microscopic models could be used to generate more detailed information on single intersections considered individually.

References

- Abou Zeid M., I. Chabini I., E.K. Nam, and A. Capiello (2002). Probabilistic modeling of acceleration in traffic networks as a function of speed and road type. Accepted for publication at the IEEE 5th International Conference on Intelligent Transportation Systems, Singapore, September.
- Ahn K., H. Rakha, A. Trani, and M. Van Aerde (2002). Estimating vehicle fuel consumption and emissions based on instantaneous speed and acceleration levels, *ASCE Journal of Transportation Engineering*, volume 128, issue 2, pp. 182-190.
- An F., M. Barth, G. Scora, and M. Ross (1998). Modeling enleanment emissions for light-duty vehicles. *Transportation Research Record* 1641.
- Bachman, W., W. Sarasua, S. Hallmark, and R. Guensler (2000). Modeling regional mobile source emissions in a geographic information system framework. *Transportation Research C*, volume 8, pp. 205-229.
- Barratt R. (2001). *Atmospheric dispersion modelling: an introduction to practical applications*. Earthscan Publications, London, United Kingdom.
- Barth M. (1998). Integrating a modal emission model into various transportation modeling frameworks, in *Transportation planning and air quality III – Emerging strategies and working solutions*. American Society of Civil Engineers, Reston, Virginia.
- Barth M., F. An, T. Younglove, G. Scora, C. Levine, M. Ross, and T. Wenzel (1999a). *Comprehensive Modal Emission Model (CMEM), version 2.0 User's Guide*. University of California, Riverside, California.
- Barth M., F. An, T. Younglove, G. Scora, C. Levine, M. Ross, and T. Wenzel (2000). *Development of a comprehensive modal emissions model*. Final report. National Cooperative Highway Research Program Project 25-11.
- Barth M., G. Scora, and T. Younglove (1999b). Estimating emissions and fuel consumption for different levels of freeway congestion. *Transportation Research Record* 1664, paper 99-1339.
- Ben-Akiva M. and J.L. Bowman (1998). Activity based travel demand model systems, in *Equilibrium and advanced transportation modeling*, eds. P. Marcotte and S. Nguyen, Kluwer Academic Publishers, Boston, Massachusetts.
- Berkowicz R. (1997). Modelling street canyon pollution: model requirements and expectations. *International Journal of Environment and Pollution*, volume 8, no. 3-6, pp. 609-619.
- Bottom J. (2000). *Consistent anticipatory route guidance*. PhD thesis. Massachusetts Institute of Technology, Cambridge, Massachusetts.

- Button K.J. and E.T. Verhoef (1999). *Road pricing, traffic congestion, and the environment: issues of efficiency and social feasibility*. Edwar Elgar Publishing, Northampton, Massachusetts.
- Cappiello A., I. Chabini I., E.K. Nam, M. Abou Zeid, and A. Luè (2002). A statistical model of vehicle emissions and fuel consumption. Accepted for publication at the IEEE 5th International Conference on Intelligent Transportation Systems, Singapore, September.
- CARB (1996). *Methodology for estimating emissions from on-road motor vehicles*, California Air Resources Board. (<http://www.arb.ca.gov/msei/mvei/mvdocs.html>)
- Cascetta E. (2001). *Transportation systems engineering: theory and methods*. Kluwer Academic Publishers, Dordrecht, Boston, Massachusetts.
- Colorni A., Laniado E. and Muratori S. (1999b). Decision support systems for environmental impact assessment of transport infrastructures, *Transportation Research D*, volume 4, no.1, pp. 1-11.
- Degobert P. (1995). *Automobile and pollution*. Editions Technip. Paris, France.
- Dion F., M. Van Aerde, and H. Rakha (1999). Mesoscopic fuel consumption and vehicle emission rate estimation as a function of average speed and number of stops. Proceedings of the 79th Transportation Research Board Annual Meeting, Washington, DC.
- Dowling Associates (2000). *Predicting short-term and long-term air quality effects of traffic-low improvements projects*. Prepared for the National Cooperative Highway Research Program 25-21.
- EPA (1993). *Federal Test Procedure review project: preliminary technical report*. EPA420-R-93-007. United States Environmental Protection Agency.
- EPA (2001a). *Final facility-specific speed correction factors*. EPA420-R-01-060. United States Environmental Protection Agency.
- EPA (2001b). *Inventory of US greenhouse gas emissions and sinks: 1990–1999*. EPA236-R-01-001. United States Environmental Protection Agency.
- EPA (2001c). *National air quality and emission trends report, 1999*. EPA454-R-01-004. United States Environmental Protection Agency.
- EPA (2002). *User's Guide to MOBILE6.0. Mobile Source Emission Factor Model*. EPA420-R-02-001. United States Environmental Protection Agency.
- Fancher P., R. Ervin, J. Sayer, M. Hagan, S. Bogard, Z. Bareket, M. Mefford, and J. Haugen (1998). *Intelligent cruise control field operational test*. Final Report, volume 1, United States Department of Transportation.
- Fellendorf M. (1999). Integrated simulation of traffic demand, traffic flow, traffic emissions and air quality. Proceedings of the 8th International Symposium on Transport and Air Pollution, Graz, Austria.

- Fomunung I., S. Washington, and R. Guensler (1999). A statistical model for estimating oxides of nitrogen emissions from light-duty motor vehicles. *Transportation Research D*, volume 4, no. 5, pp. 333-352.
- Fomunung I., S. Washington, R. Guensler, and W. Bachman (2000). Validation of the MEASURE automobile emissions model: a statistical analysis. *Journal of transportation and statistics*, volume 3, no. 2.
- Gal T., T.J. Stewart, and T. Hanne (1999). *Multicriteria decision making: advances in MCDM models, algorithms, theory, and applications*. Kluwer Academic Publisher, Boston, Massachusetts.
- Goodwin R. (1996). A model of automobiles exhaust emissions during high-power driving episodes and related issues. PhD Thesis, University of Michigan, Ann Arbor, Michigan.
- Guariso G., and H. Werthner (1989). *Environmental decision support systems*. Halsted Press, New York.
- Hallmark S.L., R. Guensler, and I. Fomunung (2002) Characterizing on-road variables that affect passenger vehicle modal operation, *Transportation Research D*, volume 7, pp. 81-98.
- Heywood J. (1988). *Internal combustion engine fundamentals*. McGraw-Hill, New York.
- Hickman J., D. Hassel, R. Joumard, Z. Samaras, and S. Sorenson (1999). *Methodology for calculating transport emissions and energy consumption*. Deliverable 22 for the project MEET, Transport and Road Research Laboratory, Crowthorne, United Kingdom.
- Hunt, P.B., D.I. Robertson, R.D. Bretherton, and R.I. Winton (1991). *SCOOT - a traffic responsive method of co-ordinating signals*. TRRL Laboratory Report 1014, Transport and Road Research Laboratory, Crowthorne, United Kingdom.
- Jimenez J.L., P. McClintock, G.J. McRae, D.D. Nelson, and M.S. Zahniser (1999). Vehicle specific power: a useful parameter for remote sensing and emission studies. Proceedings of the 9th CRC On-Road Vehicle Emissions Workshop, San Diego, California.
- Jost P., D. Hassel, and F.J. Weber (1992). *Emission and fuel consumption modeling based on continuous measurements*. Deliverable N. 7 of the DRIVE Project V1053. TÜV Rheinland, Cologne, Germany.
- Joumard R. (1999). *Methods of estimation of atmospheric emissions from transport: European scientist network and scientific state-of-the-art*. COST 319 Final Report LTE 9901, INRETS, Lyon, France.
- Kosonen I. (1999). *HUTSIM - Urban traffic simulation and control model: principles and applications*. Helsinki University of Technology, Transportation Engineering, Publication 100.
- LeBlanc D.C., F.M. Saunders, M.D. Meyer, and R. Guensler (1995). Driving pattern variability and impacts on vehicle carbon monoxide emissions. *Transportation Research Record* 1472, pp. 45-52.

- Los Alamos National Laboratory (2002). *TRANSIMS: transportation analysis simulation system. Version: TRANSIMS –3.0 Volume Three - Modules*. LA-UR 00-1725. Los Alamos, New Mexico.
- Malcom C., G. Score, and M. Barth (2001). Validating a microscale transportation/emissions model with tunnel study data. Proceedings of the 11th CRC On-Road Vehicle Emissions Workshop, San Diego, California.
- Nam E. K. (1999). *Understanding and modeling NOx emissions from light driving vehicles during hot operation*. PhD thesis. University of Michigan, Ann Arbor, Michigan.
- Nam E. K., H. Brazil, and S. Sutulo (2002). The integration of a fuel rate based modal emissions model (CMEM modified) into the VISSIM microscopic traffic model – inventory comparison with MOBILE6 in Southfield Michigan. Proceedings of the 12th CRC On-Road Vehicle Emissions Workshop, San Diego, California.
- Niittymaki J., M. Granberg, and A. Karpiinen (2001). Development of integrated air pollution modelling systems for urban planning - DIANA project. Proceedings of the 80th Transportation Research Board Annual Meeting, Washington, DC.
- NRC (1991). *Rethinking the ozone problem in urban and regional air pollution*. National Research Council. National Academy Press, Washington, DC.
- NRC (2000). *Modeling mobile-source emissions*. National Research Council Committee to Review EPA's Mobile Source Emissions Factor (MOBILE). National Academy Press, Washington, DC.
- Ntziachristos L. and Z. Samaras (2000). COPERT III Version 2.1: methodology and emission factors. European Topic Centre on Air Emissions, European Environmental Agency.
- Schafer A. (1998). The global demand for motorized mobility. *Transportation Research A*, volume 32, no. 6.
- Schultz D., T. Younglove, and M. Barth (2001). Statistical analysis and model validation of automobile emissions. *Journal of transportation and statistics*, volume 3, no. 2.
- Sierra Research (1997). *Development of speed correction cycles*. Report no. SR97-04-01, document no. M6.SPD.001.
- Sturm P.J., P. Boulter, P. de Haan, R. Joumard, S. Hausberger, J. Hickmann, et al. (1998). *Instantaneous emission data and their use in estimating passenger car emissions*. MEET Deliverable 6, COST 319 Final Report A2, Technische Universitaet Graz, Graz, Austria.
- Sussman J. (2000). *Introduction to transportation systems*. Artech House, Norwood, Massachusetts.
- Teng H., L. Yu, and Y. Qi (2002). Statistical microscale emission models incorporating acceleration and deceleration. Proceedings of the 81st Transportation Research Board Annual Meeting, Washington, DC.
- Thomas M., and M. Ross (1997). Development of second-by-second fuel use and emissions model based on an early 1990s composite car. SAE paper 971010.

- UKDOT (1995). *Design manual for roads and bridges*, Vol.11, Environmental Assessment Section 3. United Kingdom Department of Transport.
- WBCSD (2001). *Mobility 2001 – World mobility at the end of the twentieth century and its sustainability*. Prepared for the Sustainable Mobility Working Group of the World Business Council for Sustainable Development by the Massachusetts Institute of Technology Laboratory for Energy and the Environment and Charles River Associates Inc.
- Wenzel T. and M. Ross (1996). Emissions from modern passenger cars with malfunctioning emissions controls. SAE paper 960067.
- Williams M.D., G. Thayer, M. Barth, and L.L. Smith (1999). *The TRANSIMS approach to emissions estimation*. LA-UR 99-471. Los Alamos National Laboratory, Los Alamos, New Mexico.
- Young Park J., R. Noland, and J. Polak (2001). A microscopic model of air pollutant concentrations: comparison of simulated results with measured and macroscopic estimates. Proceedings of the 80th Transportation Research Board Annual Meeting, Washington, DC.

Appendix A

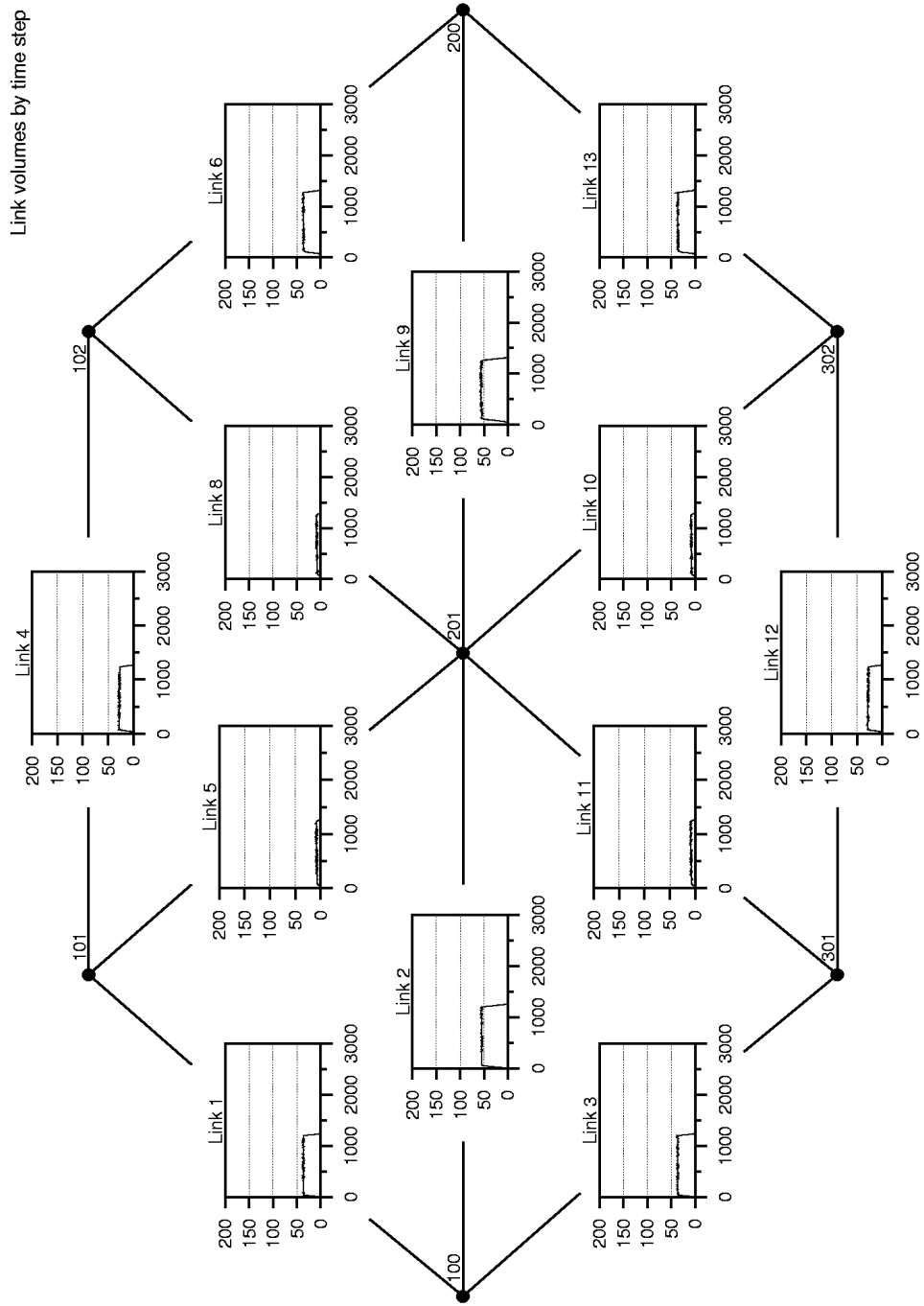
This appendix reports information about the vehicles contained in the NCHRP vehicle emissions database, which is used to calibrate EMIT, as described in Sections 4.2.1 and 4.2.2.

The vehicle classification identified in Barth et al. (2000) was adopted with some minor modification. The classification of individual vehicles was partly revised, with particular attention to high emitters, which we considered misclassified in a number of cases. In this appendix, we present the revised classification. The fields reported are:

- Category – The same 26 categories used in the original database are adopted. We divided the original category 22 (bad catalyst) it into two separate categories (cars and trucks). The definition of the categories is reported in Table 4.1.
- Used for composite vehicle – An ‘x’ indicates that the vehicle is used in our compositing procedure
- Vehicle ID – Vehicle identification number used in the original database
- Model name
- Model year
- Mass (lb)
- Tier – This field indicates the emission standard for which the vehicle is certified (see Section 2.1.2 for the definition of the emission standards).
- Vehicle type – This field indicates if the vehicle is a car or a truck
- State – The origin state of the vehicle
- Odometer – The odometer reading on the test date
- FTP, MEC01, and US06 – Each column indicates if the database contains engine-out (E) and/or tailpipe (T) data, respectively for the driving cycles FTP, MEC01, and US06.

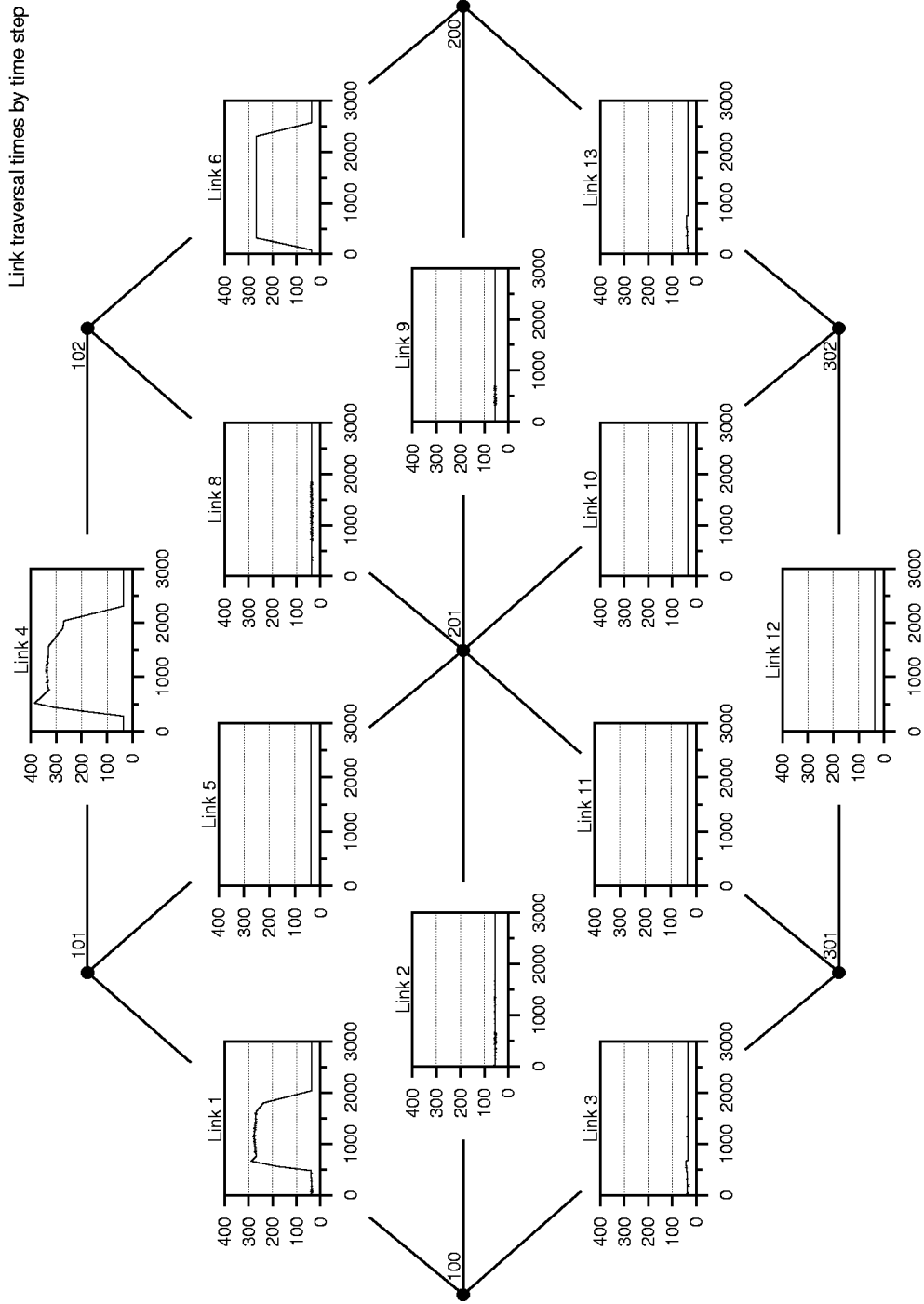
Appendix B

In this appendix, we report the outputs of the traffic model (time-dependent link volumes and link travel times) for the scenarios simulated in the case study of Chapter 6. The description of the traffic model can be found in Section 6.1.1. The description of the scenarios can be found in Section 6.2.



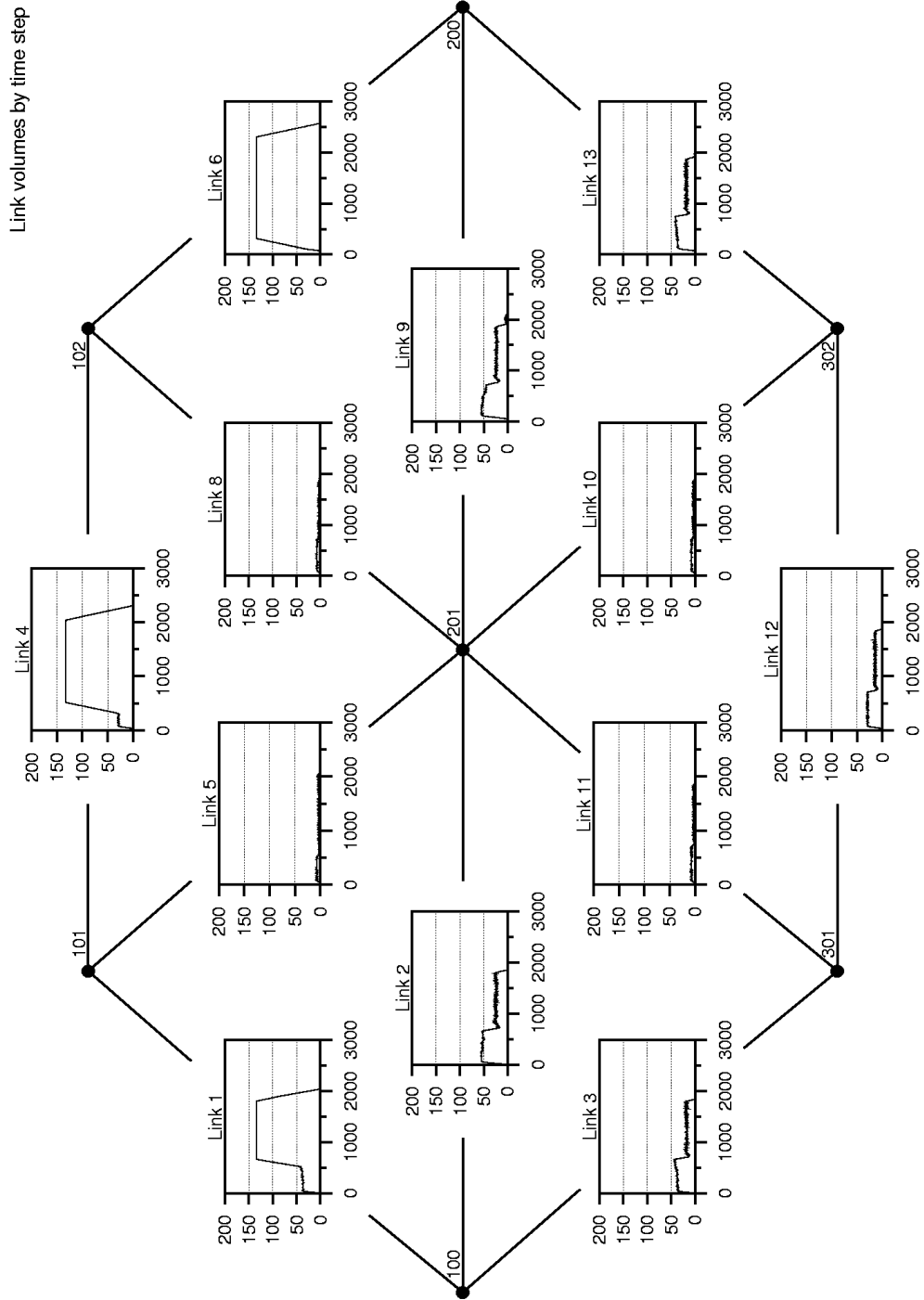
background hr out

Figure B-2: Link volumes for the scenario 0.



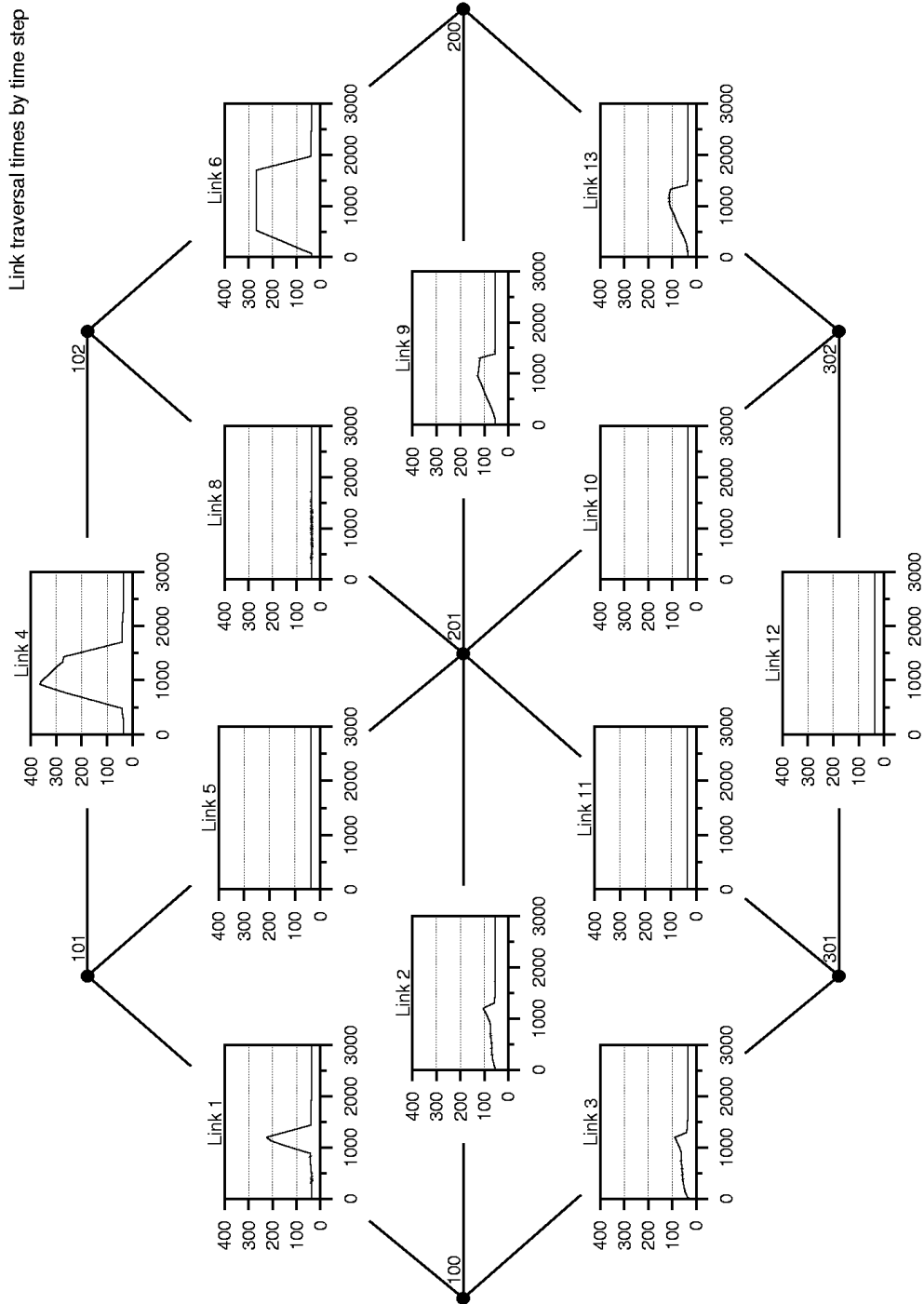
inproWMSnorriso.fr-in.out

Figure B-3: Link travel times for the scenario 1.



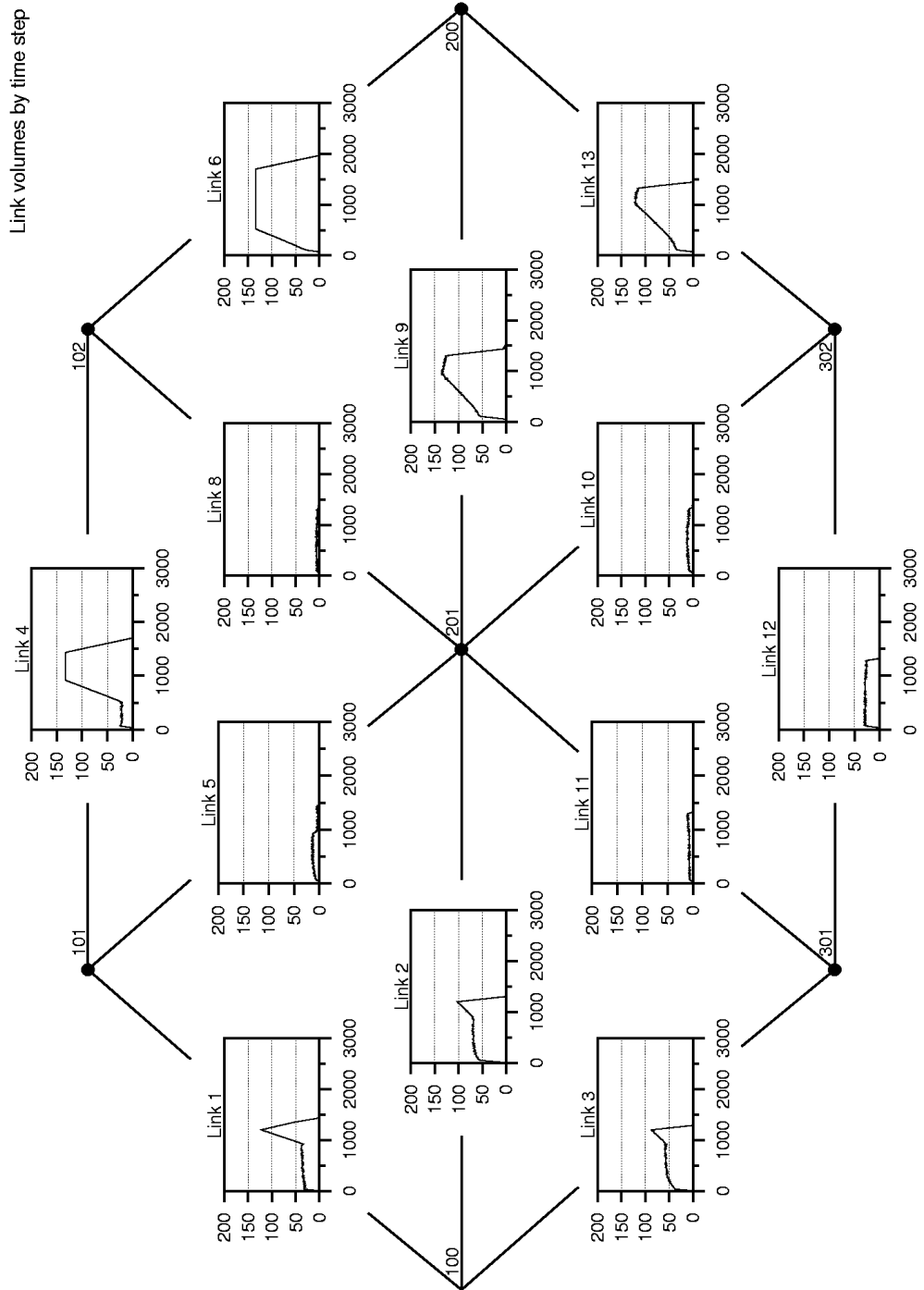
macroVMScreenInfo_M1.out

Figure B-4: Link volumes for scenario 1.



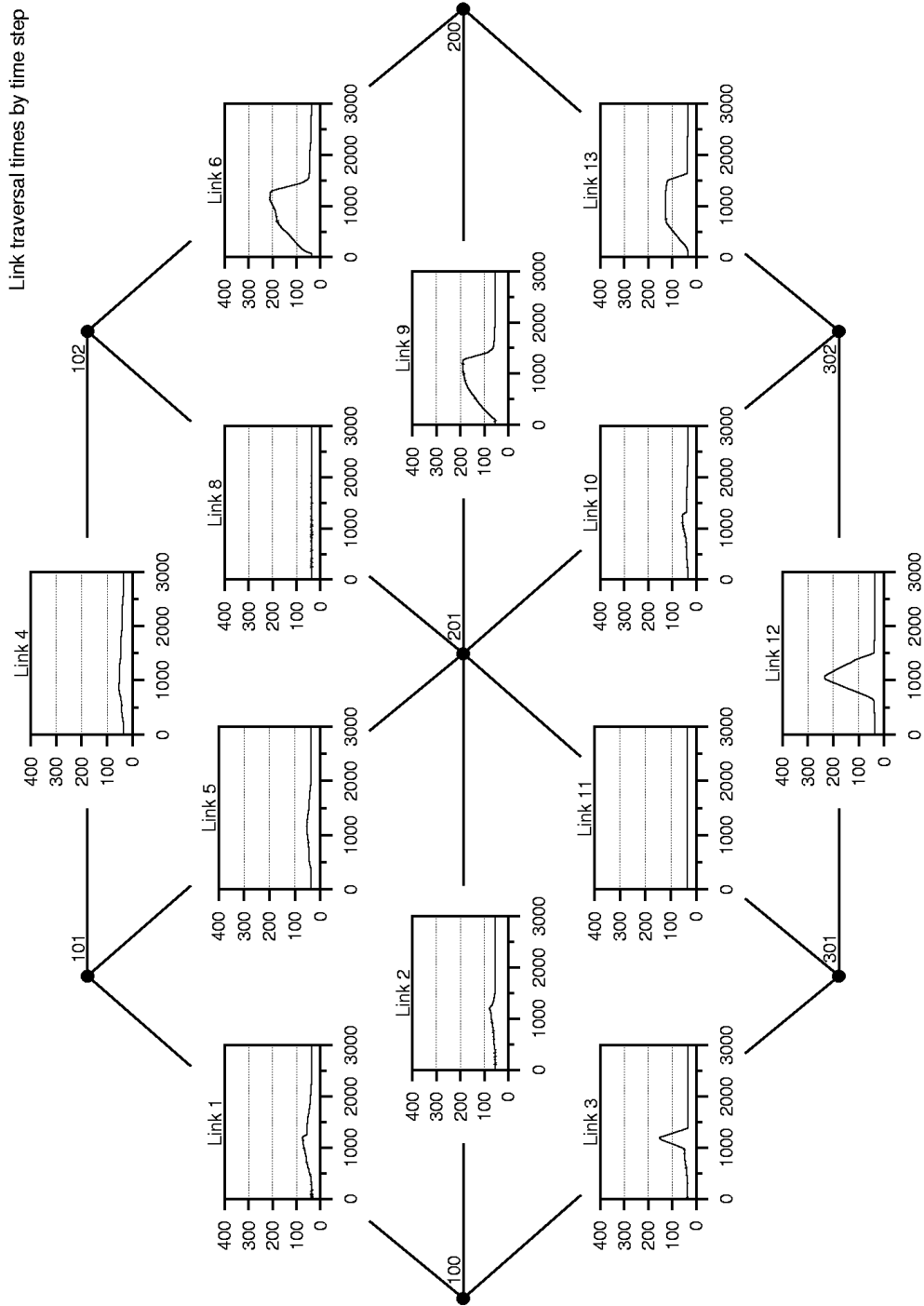
inroWMS25Info.jfr.in.out

Figure B-5: Link travel times for scenario 2.



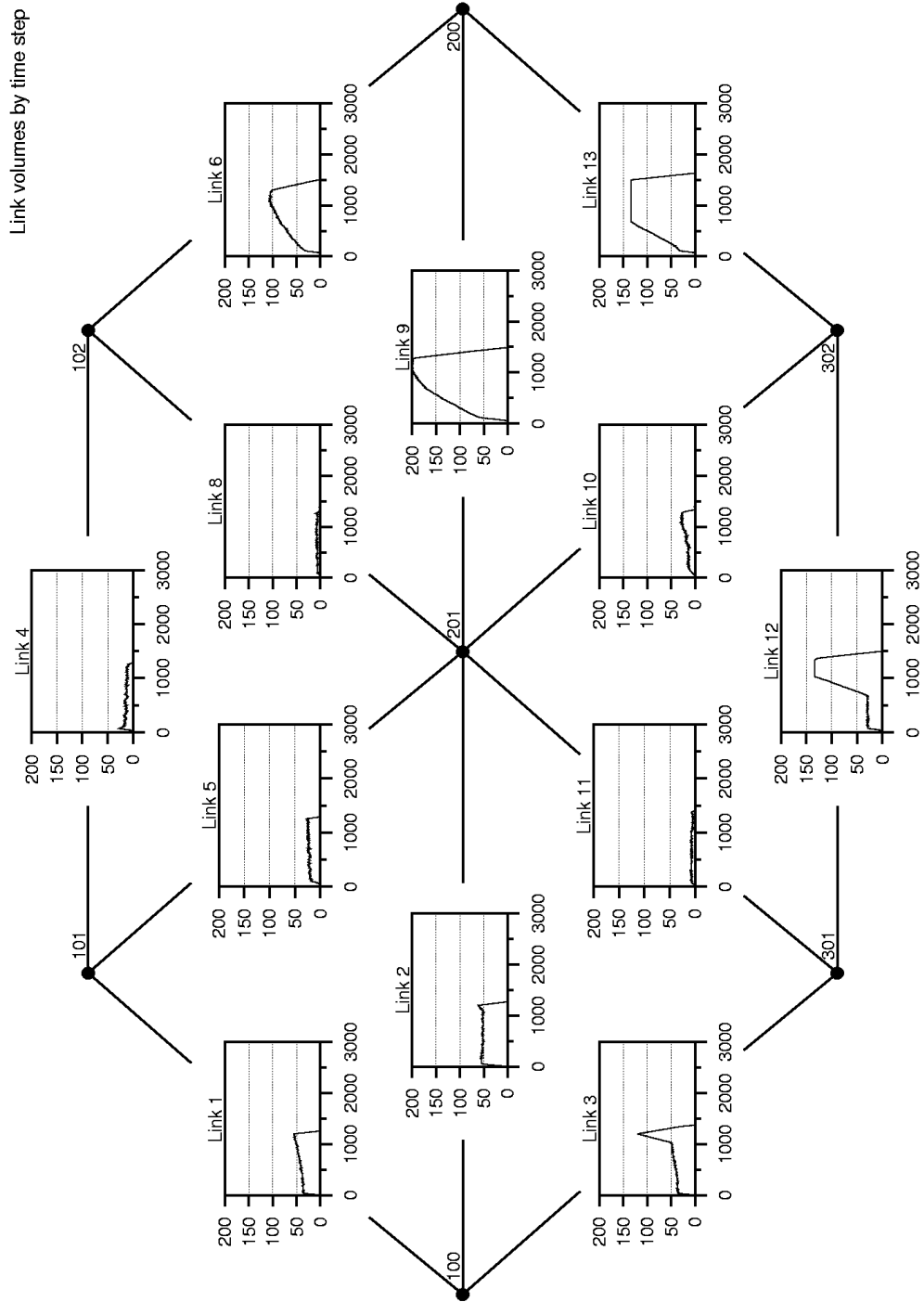
macroVMS25inf0_M1.out

Figure B-6: Link volumes for scenario 2.



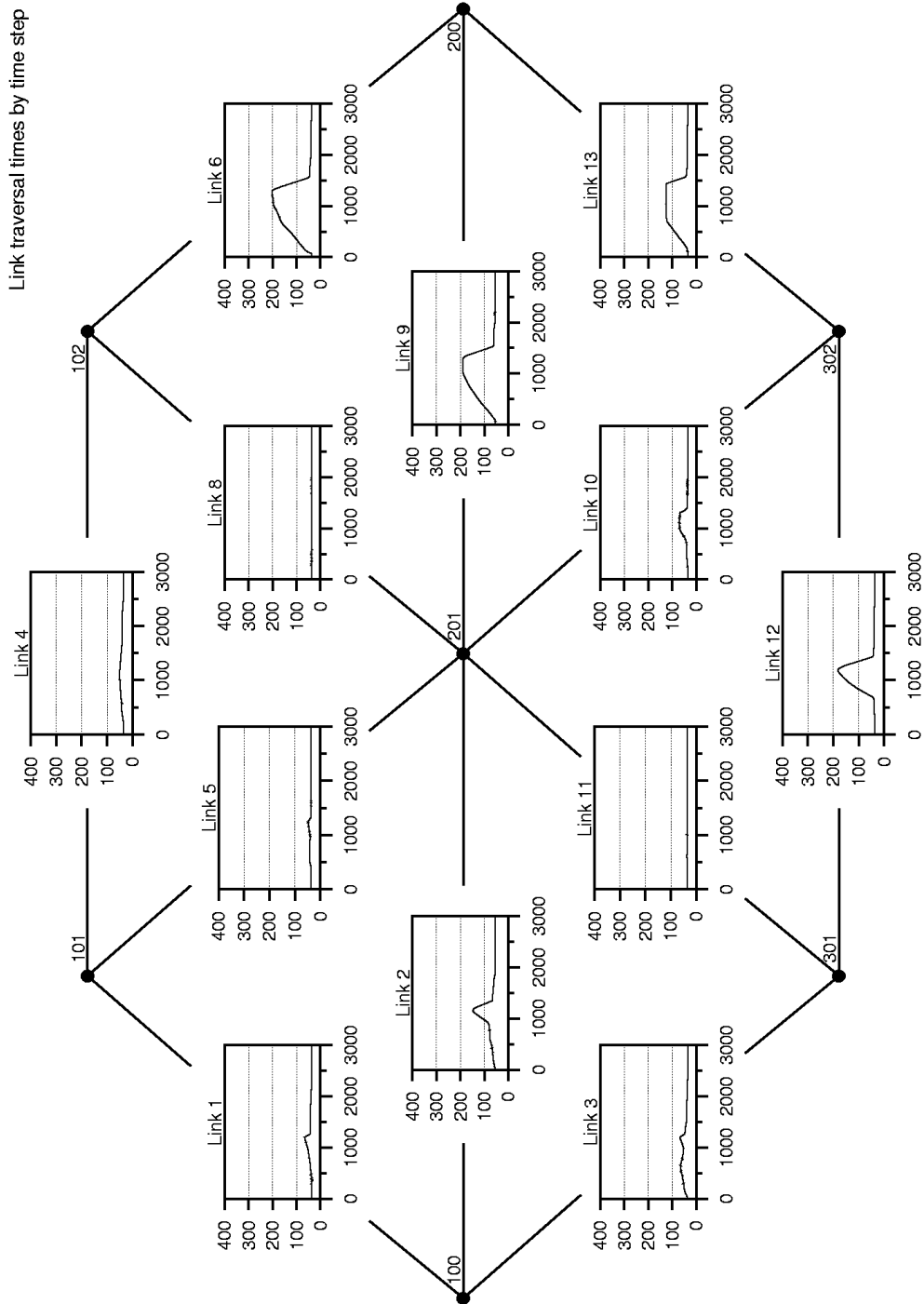
inc\WIS\reports\lfr-in-out

Figure B-7: Link travel times for scenario 3.



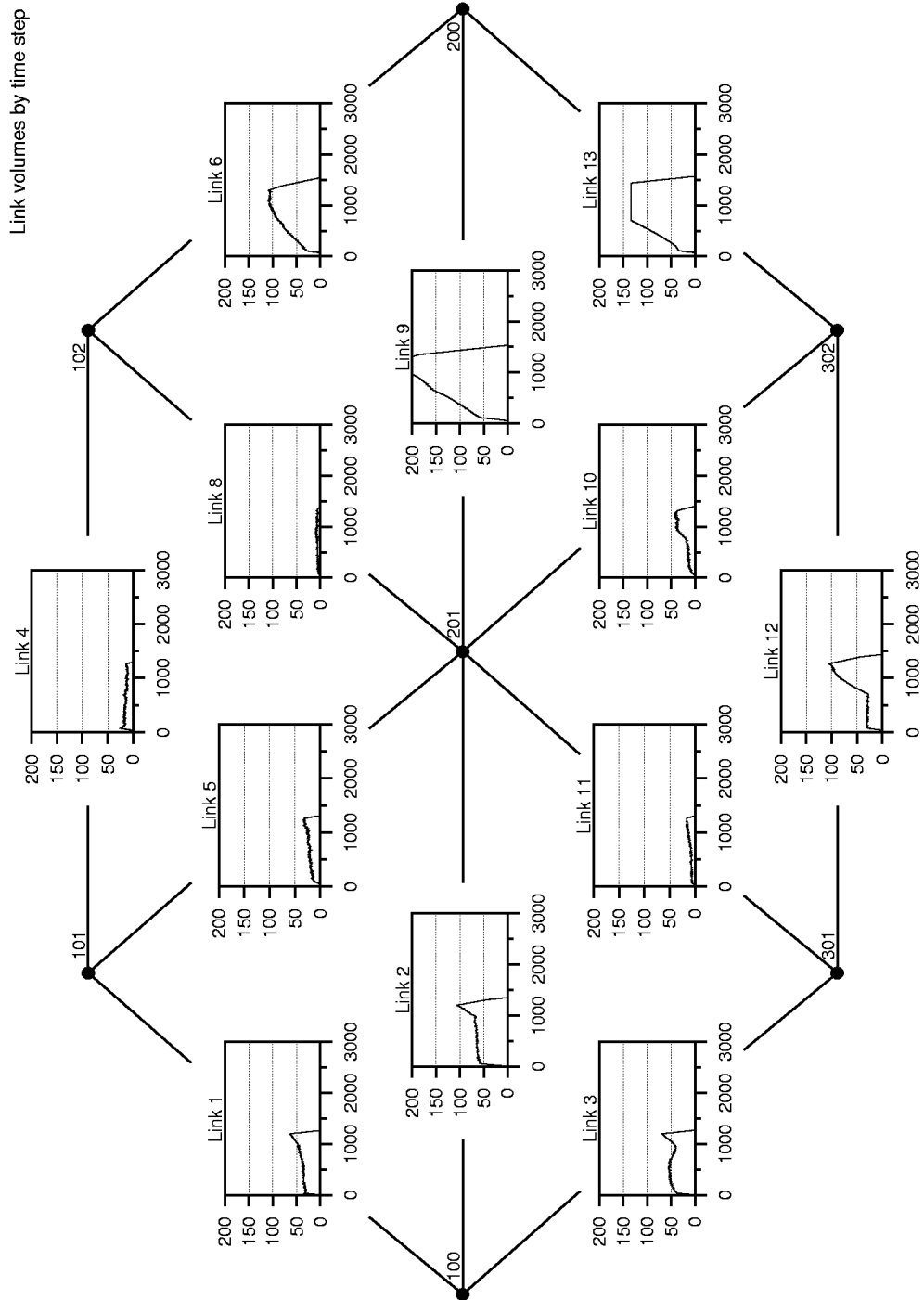
incWScreenInfo_M1.out

Figure B-8: Link volumes for scenario 3.



inc\MS25\info_ltr-in.out

Figure B-9: Link travel times for scenario 4.



inc\MSZ52\info_M1.out

Figure B-10: Link volumes for scenario 4.

Appendix C

In this appendix, we report, for the scenarios simulated in the case study of Chapter 6, the results for each link, aggregated over time. The measures reported in Figures C-1 through C-5 are total fuel consumption, total tailpipe emissions of CO_2 , CO , HC , and NO_x , total travel time, and total number of vehicles. These results are useful in the case the analyst is interested in looking at the effects of the scenarios on single links.

The description of the case study and the scenarios can be found in Section 6.2.

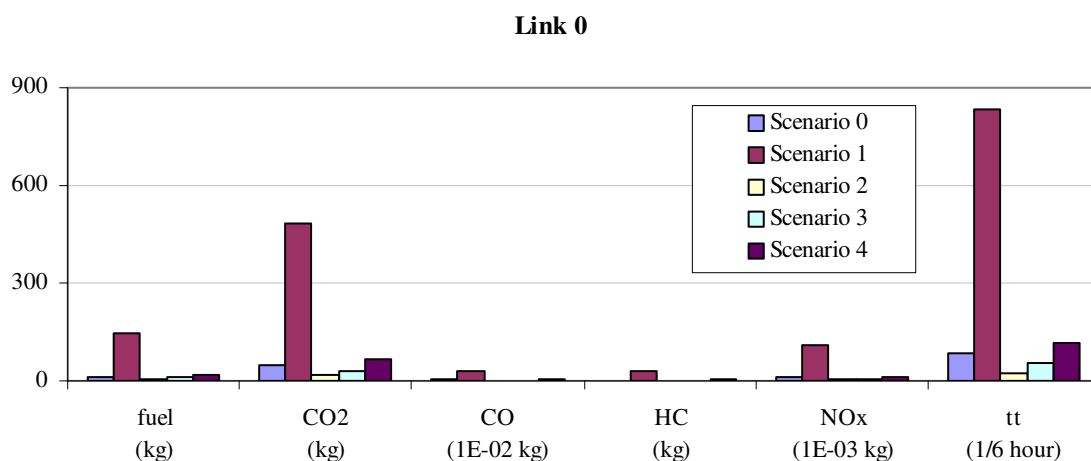


Figure C-1: Total fuel consumption, tailpipe emissions, and travel time (tt) on link 0 for every scenario modeled.

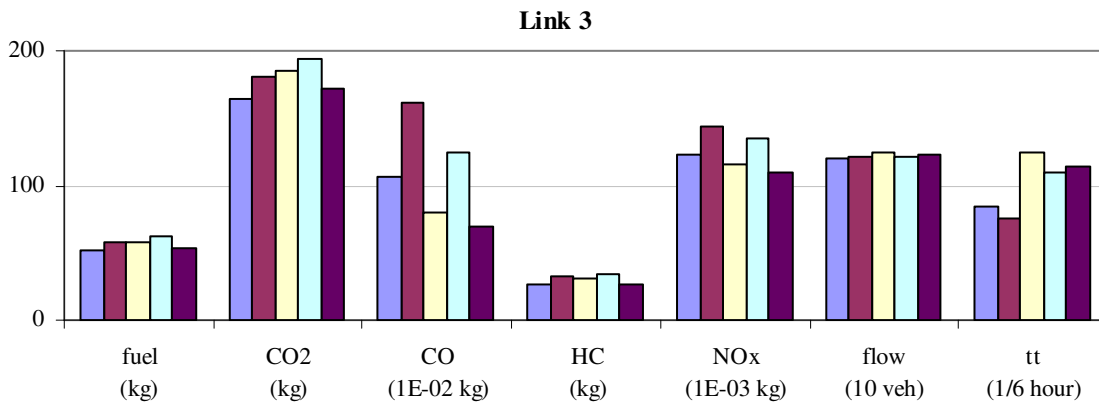
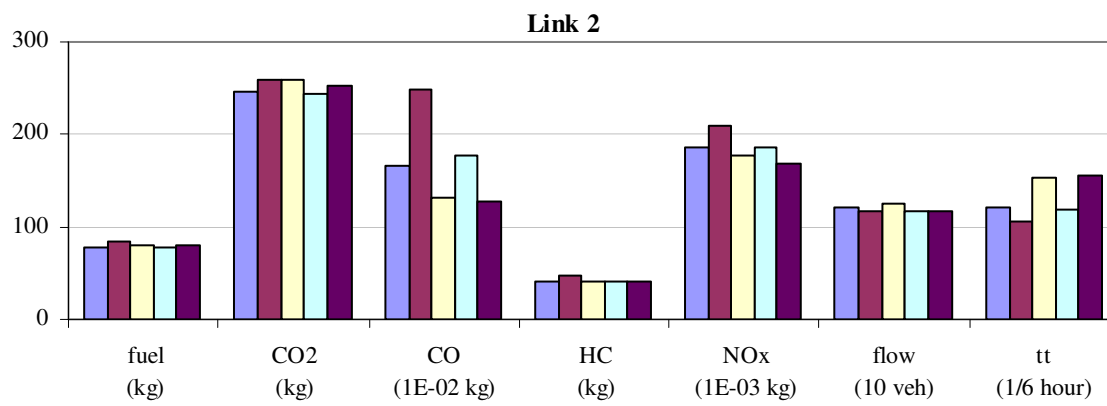
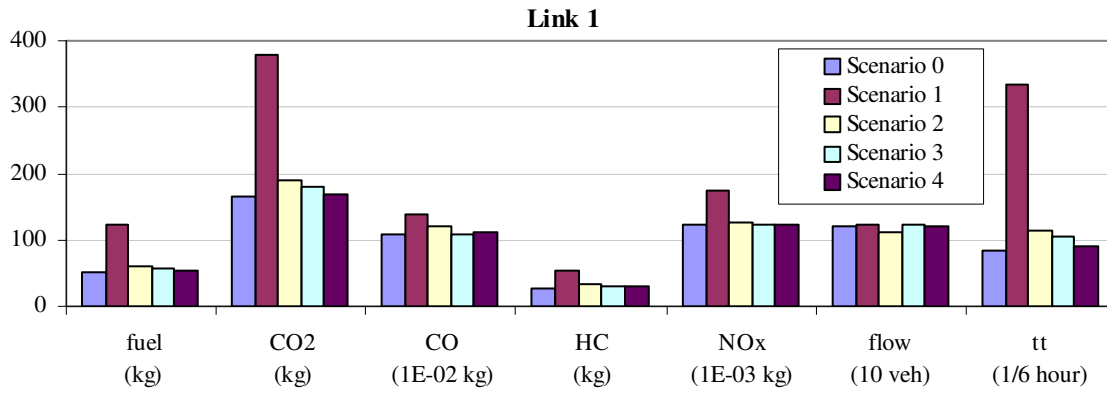


Figure C-2: Total fuel consumption, tailpipe emissions, flow, and travel time (tt) on links 1, 2, and 3 for every scenario modeled.

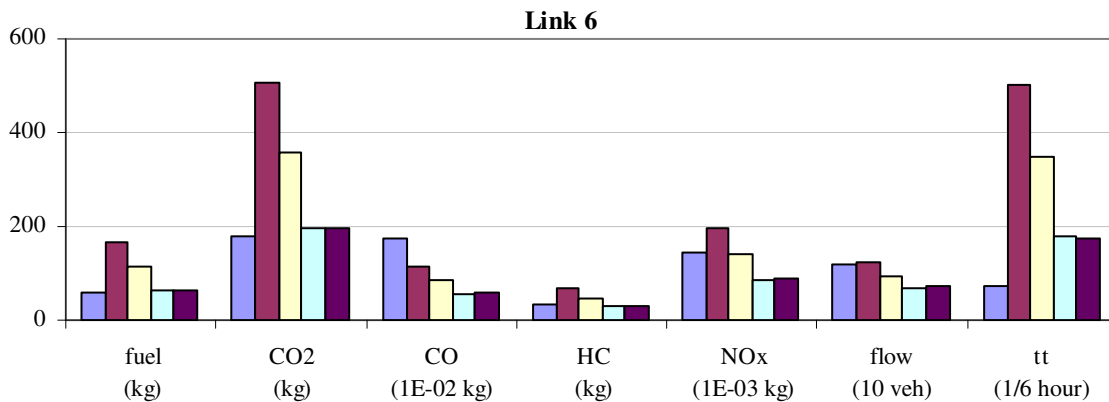
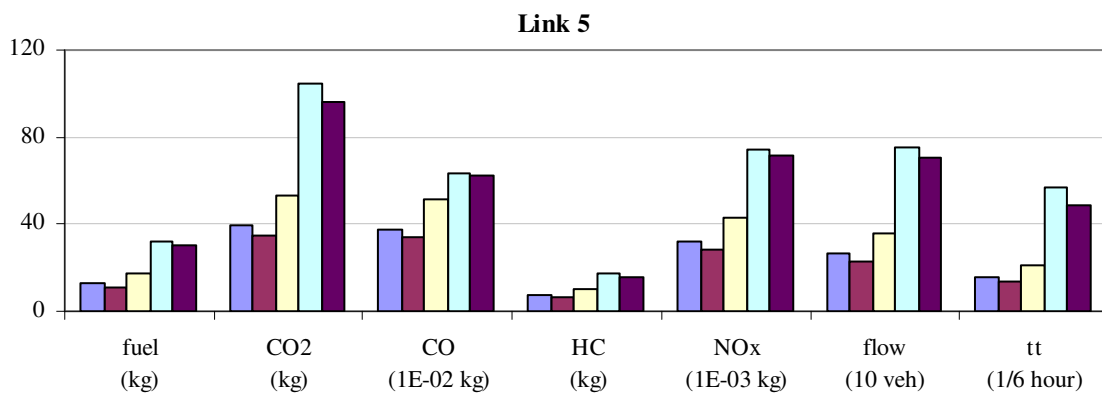
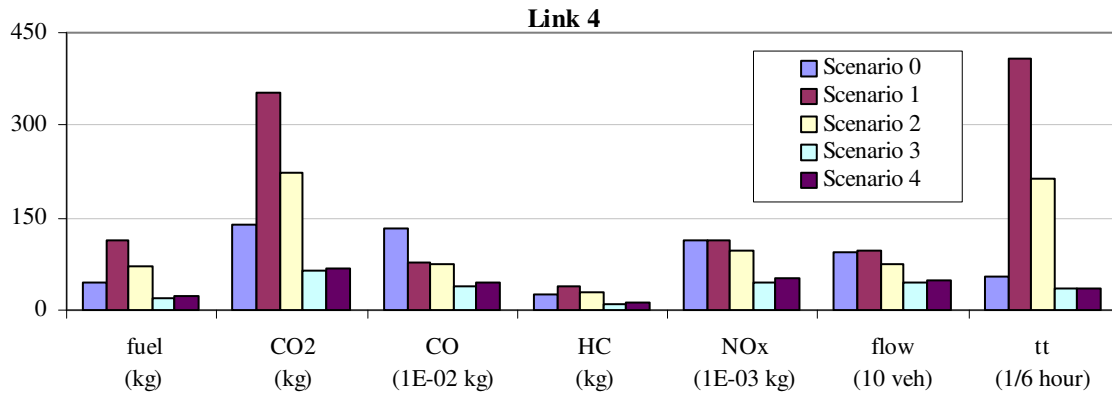


Figure C-3: Total fuel consumption, tailpipe emissions, flow, and travel time (tt) on links 4, 5, and 6 for every scenario modeled.

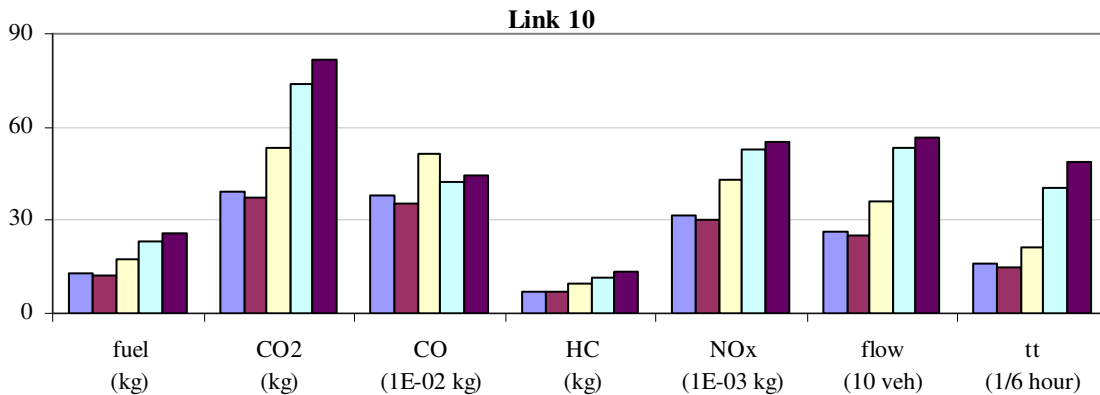
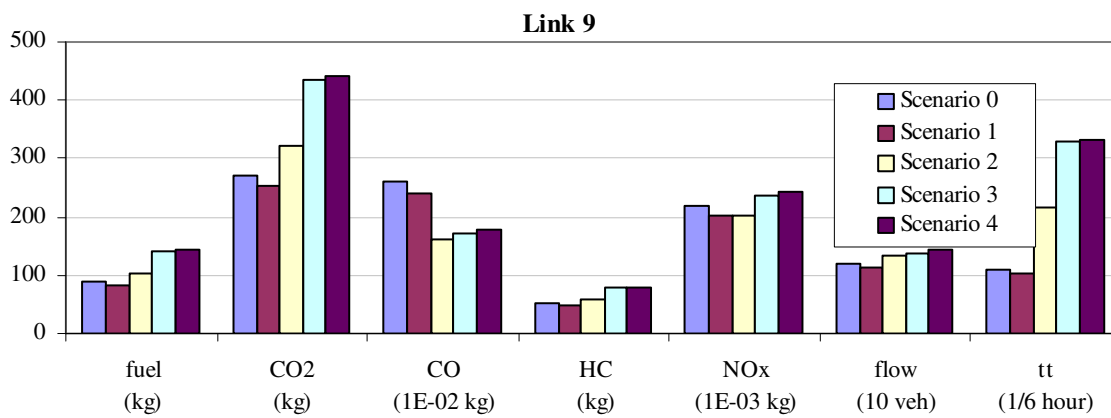
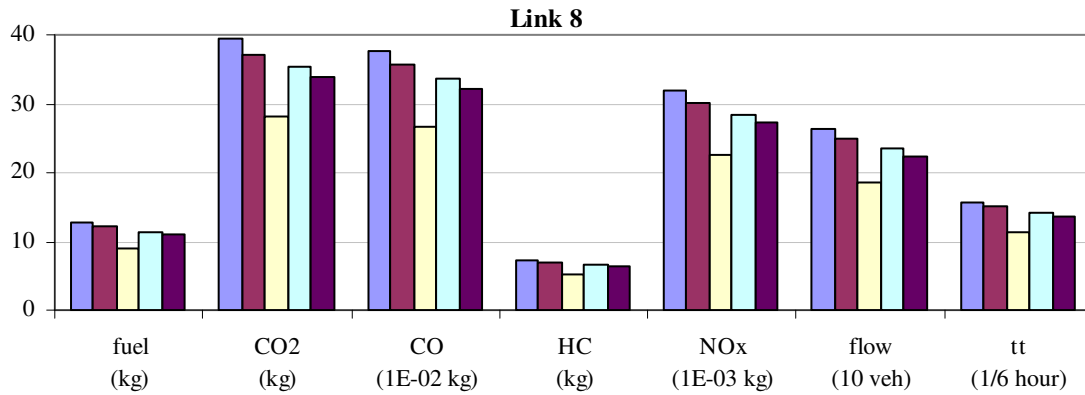


Figure C-4: Total fuel consumption, tailpipe emissions, flow, and travel time (tt) on links 8, 9, and 10 for every scenario modeled.

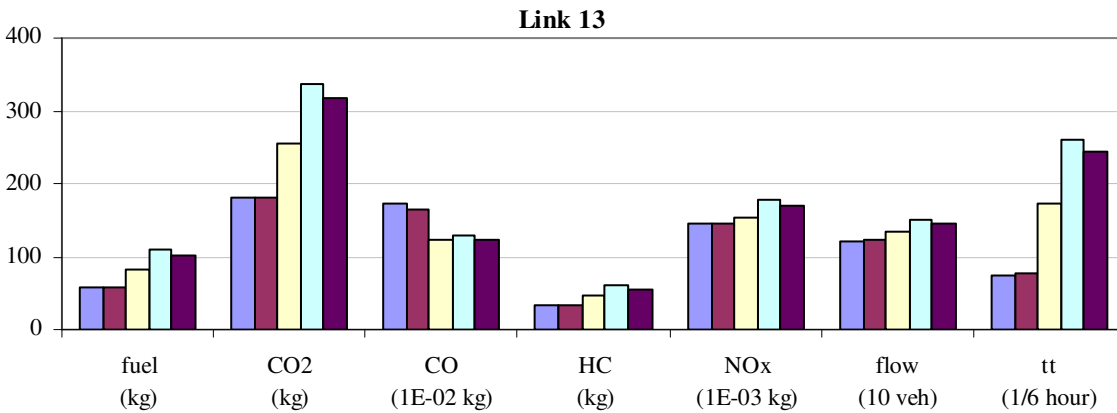
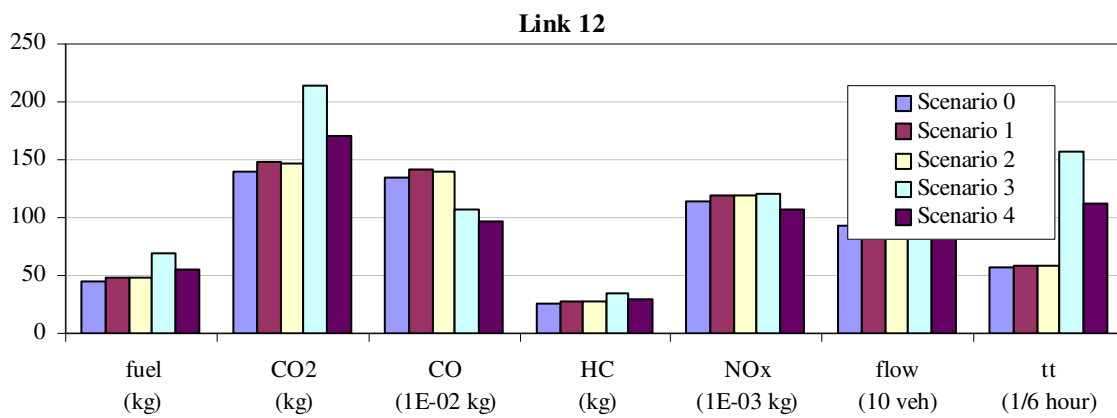
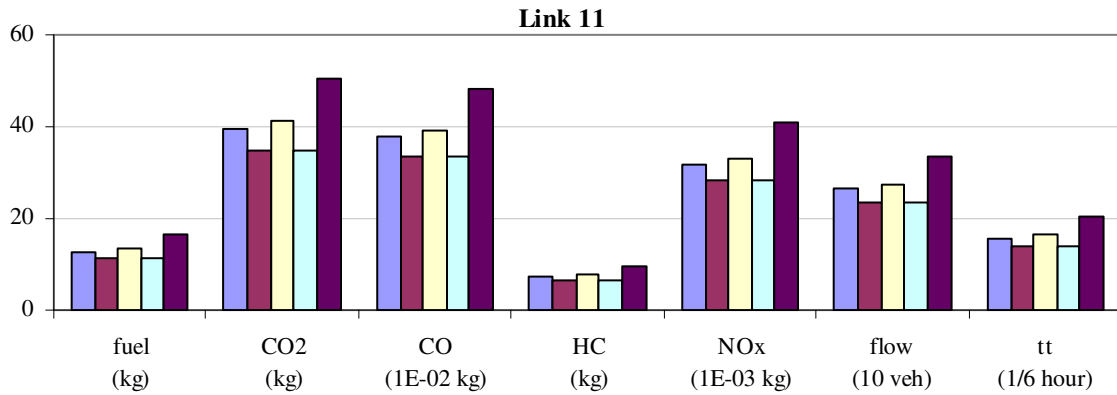


Figure C-5: Total fuel consumption, tailpipe emissions, flow, and travel time (tt) on links 11, 12, and 13 for every scenario modeled.